APPLICATIONS OF DISTRIBUTIONALLY ROBUST OPTIMIZATION IN OPERATION OF POWER SYSTEMS

LU XI

PhD

The Hong Kong Polytechnic University

2020

The Hong Kong Polytechnic University

Department of Electrical Engineering

Applications of Distributionally Robust Optimization in Operation of Power Systems

LU XI

A thesis submitted in partial fulfillment of the requirements for the degree of Doctor of Philosophy

May 2020

CERTIFICATE OF ORIGINALITY

I hereby declare that this thesis is my own work and that, to the best of my knowledge and belief, it reproduces no material previously published or written, nor material that has been accepted for the award of any other degree or diploma, except where due acknowledgement has been made in the text.

_____(Signed)

_____LU Xi_____(Name of student)

Abstract

As power systems evolve, their components with uncertainties keep expanding. For example, renewable energy sources (RESs) including wind turbines and solar panels are growing to phase fossil fuels out. RESs are usually influenced by weather and therefore have unpredictable outputs. Besides, increasing penetration of electric vehicles (EVs) bring highly uncertain loads because they are influenced by human behaviours and the transportation system. With greater uncertainties, the operation of power systems becomes more challenging. As many operation tasks of power systems highly depend on optimization, it is crucial to have efficient approaches to solve optimization problems involving uncertainties.

Stochastic optimization (SO) and robust optimization (RO) have been often used to solve optimization problems with uncertainties. SO assumes that the uncertainty follows a certain probabilistic distribution or uses discrete distributions based on selected scenarios to approximate the uncertainty distribution. As information about uncertainties is limited, there is ambiguity in the uncertainty distribution. SO ignores such ambiguity and thus often has inferior performance. Different from SO, RO constrains uncertainties within certain sets and focuses on the worst case in the considered sets. As the worst case rarely happens, over-conservative results are often obtained when RO is used to evaluate the economic efficiency of system operation. Without the drawbacks of SO and RO, a more recently developed approach named distributionally robust optimization (DRO) is becoming popular. In this thesis, potentials of DRO in economic dispatch are further exploited beyond the state-of-art literature and DRO is applied to facilitate balance responsible distribution systems (BRDSs) and balance responsible distribution companies (BR-DISCOs) to utilize the flexibility of electric vehicle aggregators (EVAs) for the first time.

In works on economic dispatch using DRO, statistical moments are often adopted

by DRO to depict the uncertainty distribution. As statistical moments are derived from limited samples of uncertainties, they may deviate from the actual moments. Instead of being ignored as in previous works, such deviations are considered by the DRO technique adopted here. Besides, because the output of RESs cannot be negative nor exceed the installed capacity, the uncertainty in RES outputs is always bounded. In this regard, ellipsoidal support sets are used to limit the range of possible uncertainty realizations under DRO. Moreover, as the proposed multi-period model is carried out as a rolling-plan, modelling of the first period is more important than that of the other periods. Therefore, a two-stage framework is employed here to model the first period without approximation. While for the other periods, segregated linear decision rule approximation is applied. With such structure, a proper trade-off between modelling accuracy and computational tractability is achieved by the proposed model. Furthermore, within the framework of DRO, RO is integrated to enhance the system security. A Constraint Generation algorithm is proposed to solve the proposed model. Through case studies, it is shown that the proposed model avoids over-conservative solutions and prevents inferior performance under limited uncertainty information through adopting more realistic DRO techniques. Also, the proposed model guarantees economical and secure long-term operation without causing excessive computational burden.

Nowadays, many components of power systems are required to act as balance responsible parties (BRPs). BRPs should contribute to the energy balance of the entire system by maintaining their planned energy portfolio and will be penalized if they fail to do so, which means that BRPs should mitigate their forecast uncertainties. As BRPs, BRDSs with EVAs can utilize the flexibility of EVAs at the expense of disturbing their charging. Without influencing driving activities of EVs in the next day, a model is established here for BRDSs to delay uncertainties through the flexibility of EVAs and thus create opportunities for uncertainties from different times to offset each other. In the established model, linear decision rules approximation is used to reduce the computational complexity, based on which a scheme of uncertainty transferring is

proposed to relieve disturbance to EVAs. DRO is used to evaluate the average performance of the operation plans. As the possibility that uncertainties offset each other depends on uncertainty correlations, temporal and spatial covariances of uncertainties are considered by DRO. Comprehensive case studies are carried out based on charging demands of EVAs simulated from real traffic data. The results show that the adopted DRO technique effectively avoids unnecessary costs. Also, the established model achieves the trade-off between cost savings brought by the flexibility of EVAs and the corresponding payments to EVAs. Overall, the operation costs of BRDSs are reduced with the established model.

The model proposed for BRDSs is extended to be applicable for distribution companies serving as BRPs. Such distribution companies are here referred as BR-DISCOs. Different from BRDSs, BR-DISCOs would purchase energy to deliver to their customers and hence need to consider energy costs as well. Therefore, apart from mitigating uncertainties, the flexibility of EVAs can also be used by BR-DISCOs to shift EVA charging demands to hours with lower energy prices. Because using EVAs to mitigate uncertainties and shifting EVA charging demands would both disturb the charging of EVAs, their interactions need to be properly considered in the extended DRO model. Besides, it is assumed here that the disturbance to EVAs incurred from uncertainty mitigation needs not be fully recovered at the end of the day as long as the capability of EVAs in accepting disturbance is respected. As a result, the involved uncertainties appear to be eliminated as they will become deterministic information in the next day. Unrecovered disturbance to EVAs would influence their charging demands in the next day, but change on the average operation costs in the next day is little as the expectation of considered uncertainties is close to zero. Although recovering the disturbance to EVAs will cause BR-DISCO to deviate from its decided energy portfolio, it may be preferable in the earlier part of the day because otherwise payments to EVAs will keep increasing as time goes. Then, as in the previous model proposed for BRDSs, involved uncertainties can be regarded as being delayed through EVAs. Meanwhile, power losses in the charging and discharging of EVAs are used to reduce

the scale of uncertainties and thus reduce penalties for energy deviations of BR-DISCO. Through case studies, the extended model is verified to be capable to coordinate the uses of EVAs in mitigating uncertainties and shifting their charging demands. It is found that the two forms of uncertainty mitigation, i.e., eliminating uncertainties and delaying uncertainties, could both reduce the operation costs of BR-DISCO and cooperatively achieve the minimum cost under the proposed model.

Acknowledgements

First, I would like to express my gratitude to my chief supervisor, Dr. Kevin K. W. CHAN, for his continuous support and guidance during my PhD study. He is always nice, patient and willing to help. From him, I learnt not only knowledge and research skills but also many good characters.

I would also like to give special thanks to my parents for their support, and my wife for her encouragement and care. They helped me regain my faith and the courage to carry on when I was frustrated.

Moreover, I owe many thanks to Dr. XIA Shiwei and Dr. LUO Xiao. They gave me a lot of valuable advices and help. I still remember that Dr. XIA picked me up when I arrived in Hong Kong for the first time. During the first year of my PhD study, I sat next to Dr. LUO. Every time I felt worried and anxious, I could get comfort and inspiration by seeing Dr. LUO working continuously and peacefully.

Also, I would like to thank all the friends I met in Hong Kong. The joy brought by them makes my days in Hong Kong so wonderful and special.

Last but not least, I would like to thank the University and the Department for providing an excellent environment for studying and conducting research.

Table of Contents

Lists of Figures, Tables and Abbreviations

List of Figures

List of Tables

List of Abbreviations

AVR	Automatic voltage regulator
BRDS	Balance responsible distribution system
BRP	Balance responsible party
BR-DISCO	Balance responsible distribution company
DG	Distributed generator
DISCO	Distribution company
DRO	Distributionally robust optimization
ED	Economic dispatch
ES	Energy storage
EV	Electric vehicle
EVA	Electric vehicle aggregator
h2h	Home-to-home
IO	Interval optimization
LDR	Linear decision rule
MILP	Mixed integer linear program
RES	Renewable energy source
RO	Robust optimization
SLDR	Segregated linear decision rule
SO	Stochastic optimization
SOC	State of charge

Chapter I
Introduction

1.1 Background

Power systems used to highly depend on fossil fuels, including coal, natural gas and oil. As fossil fuels are formed gradually in natural processes that last for millions of years, their current consumption rate is much faster than their generation rate. With limited reserves, they will certainly be exhausted if alternative energy sources are not developed. Besides, fossil fuels release considerable amounts of carbon dioxide when burned. Because of extensive consumption of fossil fuels, the concentration of carbon dioxide in the atmosphere has significantly increased since the beginning of the industrialization, which leads to global warming. Moreover, the burning of fossil fuels releases pollutants such as sulfur dioxide and heavy metals. Because of these drawbacks of fossil fuels, the world has reached a consensus in phasing them out. In 2015, the Group of Seven agreed to stop using fossil fuels by 2100 and keep the increase of the global average temperature from the level before the industrialization within 2 degrees Celsius. Through the Paris Agreement signed in 2016, more countries joined in this plan.

Different from fossil fuels, renewable energy such as solar and wind energy can replenish itself through natural processes within human timescales and does not have the drawbacks of fossil fuels. Therefore, it is vital in phasing fossil fuels out and is developing rapidly. It is estimated that compared with using fossil fuels, using wind energy of a kWh avoids the release of 600 grams of carbon dioxide [1]. In 2015, wind energy sources with the capacity of 63 GW were installed worldwide. According to the statistics of The World Bank, the share of renewable energy in all energy sources of electricity generation had risen from 17.4% in 2003 to 22.9% in 2015 [2]. The

International Energy Agency predicted in 2014 that the share of solar power could reach 27% by 2050 [3]. Moreover, as technologies and the industry develop, renewable energy is becoming cheaper. The cost of solar energy got lower than grid energy price for the first time in Spain in 2013 [4]. In 2017, National Renewable Energy Laboratory of America estimated that the cost of wind energy could be halved by 2030 [5]. Under such trends, it is certain that the share of renewable energy will keep increasing. However, renewable energy is greatly influenced by external factors such as weather and thus its output is difficult to predict. Although there are various forecasting techniques, the predictability of renewable energy's output is still low for short-term operation [6]. In other words, renewable energy brings uncertainties to the operation of power systems.

Apart from being used in electricity generation, fossil fuels are also vastly consumed by traditional vehicles having internal combustion engines. Because of the promising future of renewable energy, replacing traditional vehicles with electric vehicles (EVs) is a viable way to achieve the phase-out of fossil fuels in transportation. Besides, EVs also have other advantages over traditional vehicles, including little noise pollution and greater starting torque. Also, compared with internal combustion engines, electric motors in EVs are simpler and have higher efficiency in energy conversion. Furthermore, EVs can convert the kinetic energy back to electric energy, which is particularly useful for driving in cities. With these advantages, EVs are growing rapidly. India even plans to sell no traditional vehicles but only EVs by 2030 [7]. J.P. Morgan estimated that the share of EVs and hybrid EVs in all vehicle sales would increase to 30% by 2025 and 60% by 2030 [8]. At the same time, the average price of EVs is decreasing [9, 10], which will further stimulate their growth.

As long as EVs are connected to power systems for a sufficiently long time, their charging rates can be adjusted, and it is even possible to produce vehicle-to-grid power flows. So, EVs can provide flexibility for the operation of power systems. The flexibility of EVs has many potentials such as mitigating uncertainties brought by renewable energy sources (RESs). For the scheduling of EVs' charging, their arrival

and departure time, state of charge (SOC) at arrival and target SOC at departure need to be taken into consideration. However, such information cannot be forecast accurately because of the complexity of the transportation system and the unpredictability of human behaviors [11, 12]. So, similar to RESs, EVs bring uncertainties to the operation of power systems.

As sources of uncertainties used to be limited, many operation problems of power systems depended on deterministic models [13, 14]. But ignoring the significant uncertainties brought by RESs and EVs can now result in severe consequences. For example, energy imbalance can be caused, and thus the deviation of system frequency will happen and stress the synchronous generators. Also, transmission lines may become overloaded. As power systems are very complex, chain reactions can be triggered to cause blackouts of a wide area as well. In distribution networks, the node voltage may vary significantly and exceed the safe range. To avoid these consequences, it is now important to properly take uncertainties into consideration when making operation decisions for power systems.

Optimization is applied in power systems for the first time in 1960s and has become one of the most important approaches [15]. It searches for the best element of a certain set according to certain criterion. The criterion is usually maximizing or minimizing a function. In power system operation, optimization is used to make decisions for various problems such as unit commitment and economic dispatch subject to constraints about system security, economic efficiency and so on. As uncertainties keep increasing in power systems, developing effective approaches to solve optimization problems involving uncertainties becomes crucial.

To alleviate the negative influences on power systems brought by uncertainties, various ways can be adopted. In [16, 17], operating reserves from generators are prepared. It is also possible to curtail excessive renewable energy [18] or initiate load shedding [19]. Besides, the flexibility of EVs may be used as well [20]. With these possible approaches, it is important to know how they could cooperate to achieve the best outcome. On the other hand, new trends in power systems such as the growth of

flexible components and the increase of uncertainties bring new operating mechanisms. For example, some system components are now required to act as balance responsible parties (BRPs). To contribute to the energy balance of the entire system, BRPs should plan their energy portfolio in advance and follow their plans. If they fail to do so, corresponding penalties will be applied [21, 22]. With such mechanism, costs of maintaining the energy balance can be recovered from BRPs, and BRPs are motivated to reduce their energy imbalances. To achieve secure and economical operation under the new operating mechanisms, new models need to be developed.

1.2 Research Motivations

1.2.1 Approaches for solving optimization problems involving uncertainties

To deal with optimization problems with uncertainties, several approaches have often been used. Among them, stochastic optimization (SO) is a major one. One common type of SO is based on scenarios for realizations of uncertainties. For example, for a univariate uncertainty ξ, SO can be based on scenarios like $\xi = -1$, $\xi = 0$ and $\xi = 1$. Generally, constraints of the optimization problem are required to be satisfied for all the selected scenarios and the weighted objective over all the scenarios is optimized under such type of SO, which is equivalent to approximating the probability distribution of the uncertainty by discrete distributions based on the selected scenarios.

In terms of selecting or generating scenarios, various ways have been adopted in literature. In [23], uncertainties in wind power and load demands are assumed to follow zero-mean normal distributions, and Monte Carlo simulation is conducted to generate scenarios, whose weights are set to be equal. [24] assumes that uncertainties in wind power and loads follow truncated normal distributions. The possible range of uncertainties under the assumed distribution is divided into several intervals. Middle points of each interval are chosen as the scenarios. Their weights are set to the probabilities that uncertainty realizations fall into their corresponding intervals. In [25], given the historical data of wind speed, an inverse normal distribution is generated to

fit the distribution of wind speed, based on which an autoregressive model is developed. Scenarios are generated using this autoregressive model and their weights are determined in a way such that certain statistical information of the discrete distribution based on the scenarios matches that of the generated inverse normal distribution as well as possible. In contrast with [25], [26] determines the scenarios and their weights by directly solving an optimization problem that minimizes the difference between the discrete distribution based on the scenarios and the assumed uncertainty distribution in terms of certain statistical information. In [27], scenarios for uncertain market prices are generated by stochastic models in a tree format. Parameters of the stochastic model are fitted according to historical data. In this way, dependency between market prices in different hours is reflected.

Obviously, the uncertainty distribution will be poorly approximated if only a few scenarios are generated or selected, which can lead to sub-optimal results [28]. While if a large number of scenarios are used to guarantee the approximation accuracy, heavy computational burden will be caused [29-33]. So, to achieve the trade-off between accuracy and computational efficiency, scenario reduction techniques are often adopted in literature to select scenarios that are representative. For example, only one of several scenarios that are very close to each other can be kept. Scenario reduction is often achieved by using probability distances, which measure the distances between probability distributions. In literature, different kinds of probability distances have been adopted by different scenario reduction techniques. For example, [34] uses Kantorovich distances and [35] uses Fortet–Mourier metrics. Moreover, different scenario reduction techniques have different focuses and are suitable for different problems [25]. No scenario reduction technique is universally suitable, and choosing a proper one is often troublesome. Besides, scenarios can only be generated based on the available information about the uncertainties. Because such information is always limited, over-fitting can easily be incurred, and the uncertainty distribution will be poorly approximated. As a result, the quality of the obtained solution will be greatly degraded [29, 31, 36].

Another type of SO assumes that the uncertainty follows a certain distribution, and transforms the optimization problem involving uncertainties into deterministic forms analytically. For example, chance constraints are eliminated through analytical transformation in [37] by assuming that the uncertain wind speed follows Weibull distributions and in [38] by assuming that the uncertain wind power follows a new type of probability distributions named versatile distributions. [39] assumes that the load uncertainty follows normal distributions and transforms both chance constraints and expectations of uncertainty-affected terms analytically. But this type of SO meets mathematical intractability easily and thus has limited applications [28, 40]. Also, it is often over-optimistic because of the assumption that the uncertainty follows a specific distribution. To improve this type of SO, some literature attempts to take the ambiguity of the uncertainty distribution into consideration. For example, [41] assumes that uncertainties in renewable power outputs follow normal distributions but allows the mean and variance of each univariate uncertainty to vary within symmetric intervals instead of setting them to fixed values. Apart from assuming that uncertainties follow normal distributions with varying means and variances, [42] incorporates constraints on means and variances of different univariate uncertainties. Despite the efforts of [41, 42] in considering the ambiguity of the uncertainty distribution, assuming that uncertainties follow a specific type of distributions such as normal distributions is still problematic given the limited information about uncertainties.

Interval optimization (IO) is another approach to handle optimization problems involving uncertainties. Different from SO, IO constrains uncertainties within intervals and focuses on the worst realization of uncertainties within the considered intervals [43-45]. Similar to IO, robust optimization (RO) is also worst-case oriented. But under RO, the possible range of uncertainties is constrained by uncertainty sets, which are not restricted to intervals. For example, uncertainty sets can be ellipsoids [46], polyhedrons [47] and union of discrete points [48]. As done in [49], uncertainty sets can also be constructed with cardinality constraints, which limit the number of univariate uncertainties that have non-zero realizations. It is also possible for uncertainty sets to

be based on general norms [50]. RO has relatively little requirement of information about uncertainties compared with SO [51] and has been widely applied [52-54]. However, despite its advantages, RO can often be over-conservative [55, 56]. To alleviate the conservativeness of RO, some literature attempts to utilize more information about uncertainties. In [57], several uncertainty sets are adopted simultaneously to model uncertainties more comprehensively and proper weights are assigned to them. Uncertainty correlation is used to construct uncertainty sets in [58]. In [59], uncertainty sets are segregated into multiple bands and the number of univariate uncertainties that fall into each band is constrained, which eliminates extreme cases that are unlikely to happen in uncertainty sets. Similarly, multi-band uncertainty sets are established in [60]. But different from [59], different weights are assigned to different bands and the asymmetry of the uncertainty can be captured in [60]. However, even with more information utilized, RO is still over-conservative when it is used to optimize the economic efficiency of power system operation because it is worst-case oriented and the worst case rarely happens. Instead of optimizing the economic efficiency under the worst case, it is more reasonable to optimize the average economic efficiency, which is beyond the capability of RO.

In view of the gaps of the SO, IO and RO, a more recently developed approach named distributionally robust optimization (DRO) is adopted in this thesis. DRO depicts uncertainties through their probability distributions. As information about uncertainties is always limited, it is impossible to acquire the exact uncertainty distribution. In other words, there is ambiguity about the uncertainty distribution. Instead of ignoring or partly considering such ambiguity as done by SO, DRO fully takes it into account. The specific practice of DRO is to consider the family of all distributions that match certain information about uncertainties. The set constituted by such family of distributions is called the ambiguity set [61, 62]. To avoid being over-optimistic, DRO focuses on the worst distribution in the ambiguity set, which means that DRO is worst-distribution oriented. So, compared with SO, DRO reduces the possibility of having unexpected outcomes. Compared with RO which is worst-case

oriented, DRO can evaluate the average outcome over all possible uncertainty realizations. More detailed introduction about DRO will be given in Chapter II. Because of its advantages, DRO has been applied in power system operation. But the potentials of DRO and the features of the studied problems have not yet been fully exploited. Also, applications of DRO can be further extended to more operation problems of power systems.

1.2.2 Primitive applications of DRO in literature

The expectation and covariance matrix of uncertainties are often used by DRO to depict uncertainties and are assumed to be exactly known [63-65]. However, the fact is that only their statistical values can be calculated based on historical samples of uncertainties and the statistical values may deviate from the actual values. [63-65] ignore such facts and thus may obtain sub-optimal solutions. If the deviations of the statistical expectation and covariance matrix from the actual ones can be properly considered, DRO will be more robust against the ambiguity of the uncertainty distribution.

Besides, as discussed in Section 1.2.1, RO is worst-case oriented and DRO is worst-distribution oriented. With their orientations, RO can be used to guarantee the security of system operation, and DRO can be used to improve the average economic efficiency or average performance in other aspects such as carbon emissions, which are both important. Therefore, it is meaningful to study how to simultaneously take advantage of DRO and RO. However, in most current works using DRO, there is no such attempt.

Moreover, single-stage models are often established in literature adopting DRO [66-69]. However, in modern power system operation, recourse actions are usually needed to alleviate the negative effects brought by uncertainties. In this regard, single-stage models in [66-69] assume that recourse actions respond affinely to uncertainty realizations, which can be rough and inaccurate. In contrast to single-stage formulations, two-stage ones model recourse actions without approximation [63]. But, for multi-period problems such as economic dispatch (ED), their each period has two stages

under two-stage formulations and there are quite many stages in total. The temporal sequences of the decisions and uncertainty realizations in these stages will incur great computational difficulty. To achieve the trade-off between modelling accuracy and computational tractability, it is desirable to develop new model formulations based on two-stage and single-stage formulations.

1.2.3 Gap of applying DRO to facilitate the operation of balance responsible distribution systems with electric vehicle aggregators

DRO has been applied in various operation problems of power systems, but its applications can still be extended. Nowadays, EVs are becoming increasingly popular and bring uncertainties to power system operation. A salient feature of EVs is that their connection times to power systems are usually longer than the times needed to fulfill their charging requirements. As a result, instead of keeping constant charging rates, adjusting their energy consumption patterns is possible. In other words, EVs are able to provide flexibility, which can be used in mitigating uncertainties. Another trend in power systems is that some distribution systems are required to act as BRPs by maintaining their energy portfolio and will be penalized if they fail to do so. For these balance responsible distribution systems (BRDSs), proper use of the flexibility of EVs is crucial.

The flexibility of EVs has been widely utilized. For example, a receding horizon optimization model is established in [70] to shift charging demands of EVs to off-peak hours. In [71], a scheduling scheme is designed to maintain the voltage profile under high EV penetration. [72] proposes a charging strategy of EVs to regulate fluctuations of wind generation. These works achieve their targets by taking circumstances of specific EVs into consideration. However, it will be very difficult for future system operators to directly manage a large number of EVs because the computation requirement for taking every EV into consideration and the investment requirement for collecting all necessary information will be too demanding [73]. Instead, it is more reasonable to have EVs controlled by electric vehicle aggregators (EVAs), and the

system operator dispatches EVAs rather than EVs. Such hierarchical scheme is used in [73] to improve wind power utilization. In [74], EVAs are dispatched as a whole to maximize the hosting capacity of distribution systems for their charging demands. But the models in [73] and [74] are not designed for BRDSs.

Different from EVs, EVAs can be regarded as loads that are always connected to the system and have time varying charging demands. Because of uncertainties related to EVs, there are uncertainties in charging demands of EVAs. Meanwhile, EVAs provide flexibility for system operation as they represent aggregated EV flexibilities. Apart from EVAs, there are also other flexible components in distribution systems. In [75-77], energy storage (ES) is used. Distributed generators (DGs) are resorted to in [78, 79]. However, models using ES and DGs cannot be directly applied to distribution systems with EVAs because of the following distinct features of EVAs. Firstly, EVAs possess uncertainties in their charging demands, while ES and DGs do not. Secondly, the primary tasks of EVAs are guaranteeing energy requirements of driving activities of EVs, instead of facilitating distribution system operation as ES and DGs. Thirdly, costs of EVAs are incurred when their charging is disturbed, while costs of ES and DGs result from their operation. Apart from ES and DGs, load curtailment is another option and is used in [80-82], which is effective only when demands surpass supplies but not vice versa, while EVAs are applicable for both cases. In view of the particularity of EVAs, new models need to be established to fully exploit their features.

Uncertainties in charging demands of EVAs will influence operation costs of BRDSs. In terms of properly evaluating uncertainty-affected costs and thus facilitating BRDSs to make use of EVA flexibility, DRO is the ideal approach because of its advantages discussed in Section 1.1. In order to fully exploit the potentials of DRO in improving the economic efficiency of BRDSs, proper models should be established and the ambiguity set of DRO should be constructed with appropriate information about uncertainties in consideration of the characteristics of the established model.

1.2.4 Potentials of DRO for balance responsible distribution companies with EVAs

Different from BRDSs discussed in Section 1.2.3, distribution companies need to purchase energy and deliver to their customers within the distribution systems [75, 83]. So, when they are required to be BRPs, they need to pay energy costs as well as penalties for deviations from their planned energy portfolio. Such distribution companies are referred to as balance responsible distribution companies (BR-DISCOs) in this thesis and their operation is worth studying. From the perspective of BR-DISCOs, the flexibility of EVAs can be used to shift EVA charging demands from times with higher energy prices to times with lower energy prices apart from being used to mitigate uncertainties. Using EVAs to mitigate uncertainties can reduce the penalty for energy deviations of BR-DISCOs, while using EVAs to shift their charging demands can reduce energy costs. In other words, both applications of EVAs can bring cost savings for BR-DISCOs. Besides, the two applications both disturb the charging of EVAs and thus are limited by the capability of EVAs to accept disturbance. If EVAs are used to mitigate uncertainties more extensively, they can shift less charging demands and vice versa. So, the two applications of EVAs are correlated and need to be properly coordinated to achieve the optimal outcome for BR-DISCOs.

When EVAs are used to shift charging demands, they can discharge in some hours to have more charging demands shifted. Because of power losses in the discharging of EVAs, the power that the distribution system receives is smaller than that EVAs supply. Similarly, the power that the distribution system supplies is greater than that EVAs receive as a result of power losses in the charging of EVAs. Such phenomenon influences the scale of uncertainties from the perspective of BR-DISCOs. Because of these features of BR-DISCOs, their operation is more complicated than that of BRDSs, and EVAs can play a more important role for BR-DISCOs than for BRDSs. To facilitate BR-DISCOs to fully utilize the flexibility of EVAs, more advanced models need to be developed using DRO.

1.3 Primary Contributions

Firstly, based on the state-of-art applications of DRO in ED in literature, potentials of DRO in ED are further exploited in the established security-constrained multi-period ED model M-SCED. A two-stage framework is adopted to model initial operation plans and recourse actions before and after the uncertainty realization of RES power. For ensuring superior system economic efficiency, DRO is utilized to evaluate the expectations of operation costs affected by RES uncertainties. Practical issues, including boundedness of uncertainties and inaccurate statistical values, are considered in modeling uncertainties in DRO. RO is used to enhance system security through limiting load shedding and is integrated with DRO under the two-stage framework. To achieve computational tractability without substantially degrading the model accuracy, decision variables after the first period in M-SCED are approximated by segregated linear decision rule (SLDR). A Constraint Generation algorithm is proposed to solve this problem with comprehensive case studies illustrating the effectiveness of the proposed M-SCED.

Next, DRO is applied to facilitate the operation of BRDSs with EVAs for the first time. Without influencing driving activities of EVs in the next day, a model is established to make use of EVAs, whose contributions are delaying uncertainties through their flexibility and thus creating opportunities for uncertainties from different hours to offset each other. In this model, a scheme of uncertainty transferring is proposed to relieve disturbance to EVAs and DRO is adopted to evaluate the average performance of the operation plans with temporal and spatial uncertainty correlations considered. Comprehensive case studies are carried out based on charging demands of EVAs simulated from real traffic data to verify the effectiveness of the proposed model.

The model proposed for BRDSs is further developed to facilitate BR-DISCOs to utilize the flexibility of EVAs. Case studies are conducted under various settings. With the proposed model, BR-DISCO uses EVAs to mitigate uncertainties, which is further classified into eliminating uncertainties and delaying uncertainties. Both forms of

uncertainty mitigation reduce average penalties for deviations of BR-DISCO from its planned energy portfolio. Besides, EVA charging demands are shifted to hours with lower energy prices to reduce energy costs of BR-DISCO. Using EVAs to mitigate uncertainties and shifting EVA charging demands are properly coordinated through DRO to achieve the minimum overall operation costs. Moreover, power losses in EVA charging and discharging are utilized to reduce the scale of uncertainties, which decreases penalties for energy deviations of BR-DISCO.

1.4 Thesis Layout

The rest of this thesis consists of five chapters organized as follows.

In Chapter II, ambiguity sets of DRO based on statistical distances and moments are introduced. Further illustration of moments-based ambiguity sets is given. Transformation of worst expectations of uncertainty-affected terms over moments-based ambiguity sets is finally discussed.

In Chapter III, the adopted DRO techniques are first detailed. Next, first-stage and second-stage problems under the two-stage formulation for ED are presented explicitly and are used to construct the multi-period ED model M-SCED. SLDR approximation is applied on decision variables after the first period in M-SCED to achieve mathematical tractability, and the dual problem of the second-stage problem and Farkas Lemma are utilized to transform M-SCED into deterministic forms. A Constraint Generation algorithm is proposed to solve the transformed M-SCED. Superiority of M-SCED is verified through case studies based on the IEEE 118-bus and 30-bus system.

In Chapter IV, settings on distribution system operation are presented and followed by the formulation of the model proposed for BRDSs to use the flexibility of EVAs. Linear decision rule (LDR) approximation and the proposed uncertainty transferring scheme are discussed before the proposed model is transformed into deterministic forms. Charging demands of EVAs are simulated by using real traffic data in Atlanta,

based on which case studies are conducted to show the effectiveness of the proposed model.

In Chapter V, background settings for BR-DISCO and EVAs are given. Applications of EVA flexibility are next discussed. Afterwards, the proposed model is formulated and transformed into deterministic forms. Through comprehensive case studies based on the IEEE 33-node system, it is shown that the proposed model is effective in making use of EVA flexibility to reduce operation costs of BR-DISCO.

Lastly, conclusions and discussions about possible future work are given in Chapter VI.

1.5 List of Publications

1. X. Lu, K. W. Chan, S. Xia, B. Zhou and X. Luo, "Security-Constrained Multiperiod Economic Dispatch With Renewable Energy Utilizing Distributionally Robust Optimization," in IEEE Transactions on Sustainable Energy, vol. 10, no. 2, pp. 768-779, April 2019. DOI: 10.1109/TSTE.2018.2847419
2. X. Lu, K. W. Chan, S. Xia, X. Zhang, G. Wang and F. Li, “A Model to Mitigate Forecast Uncertainties in Distribution Systems Using the Temporal Flexibility of EVAs,” in IEEE Transactions on Power Systems, Vol.35, No.3, pp. 2212-2221, May 2020. DOI: 10.1109/TPWRS.2019.2951108
3. X. Lu, K. W. Chan, S. Xia, M. Shahidehpour, “An Operation Model for Distribution Companies Using the Flexibility of Electric Vehicle Aggregators,” IEEE Transactions on Smart Grid, TSG-00665-2020, 30 Apr 2020, under review.
4. X. Luo, S. Xia, K. W. Chan and X. Lu, "A Hierarchical Scheme for Utilizing Plug-In Electric Vehicle Power to Hedge Against Wind-Induced Unit Ramp Cycling Operations," in IEEE Transactions on Power Systems, vol. 33, no. 1, pp. 55-69, Jan. 2018. DOI: 10.1109/TPWRS.2017.2696540

5. S. Xia, S. Q. Bu, X. Luo, K. W. Chan and X. Lu, "An Autonomous Real-Time Charging Strategy for Plug-In Electric Vehicles to Regulate Frequency of Distribution System with Fluctuating Wind Generation," in IEEE Transactions on Sustainable Energy, vol. 9, no. 2, pp. 511-524, Apr. 2018. DOI: 10.1109/TSTE.2017.2746097
6. X. Gao, K. W. Chan, S. Xia, B. Zhou, X. Lu, and D. Xu, "Risk-constrained offering strategy for a hybrid power plant consisting of wind power producer and electric vehicle aggregator," Energy, vol. 177, pp. 183-191, Jun. 2019. DOI: 10.1016/j.energy.2019.04.048
7. S. Xia, S. Bu, C. Wan, X. Lu, K. W. Chan and B. Zhou, "A Fully Distributed Hierarchical Control Framework for Coordinated Operation of DERs in Active Distribution Power Networks," in IEEE Transactions on Power Systems, vol. 34, no. 6, pp. 5184-5197, Nov. 2019. DOI: 10.1109/TPWRS.2018.2870153
8. B. Zhou, K. Zhang, K. W. Chan, C. Li, X. Lu, S. Bu, X. Gao, “Optimal Coordination of Electric Vehicles for Virtual Power Plants with Dynamic Communication Spectrum Allocation (Early Access)”, IEEE Transactions on Industrial Informatics, 13 Apr 2020. DOI: 10.1109/TII.2020.2986883

Chapter II
Essentials on DRO

2.1 Ambiguity Sets

DRO focuses on the worst distribution within the ambiguity set, which is made up of a family of distributions that satisfy certain requirements. Generally, there are two types of ambiguity sets. One type is based on statistical distances, while the other is based on moments. This thesis adopts the later type, but the former one will also be briefly introduced here for completeness.

Statistical distances measure the distances between probability distributions. With historical samples of uncertainties, the discrete empirical uncertainty distribution based on them can be obtained. The ambiguity set can be constructed by including all distributions that are within certain distances from the empirical distribution. Obviously, as the chosen distance grows, the ambiguity set gets bigger and is more likely to include the actual uncertainty distribution, but the obtained result tends to be more conservative at the same time. So, the proper size of the ambiguity set needs to be decided according to the attitude of decision makers towards risks. The most common statistical distances adopted to construct ambiguity sets include Wasserstein metric [84-86] and Kullback–Leibler divergence [87-89]. Wasserstein metric can be regarded as the minimum transportation cost of moving from one probability distribution to another, and Kullback–Leibler divergence reflects the information lost when one probability distribution is used to approximate another [28]. The computational complexity of DRO using ambiguity sets based on statistical distances often grows rapidly with the increase of utilized historical samples, and further approximations are often needed [85].

Moments are measures for the shape of functions and can be used to depict probability density functions of uncertainties. The n^{th} moment of a continuous

function $f(x)$ about a constant value c is defined as in (2.1), where n can be any non-negative integer. So, there are infinite number of moments and each would reveal different information. When moments are used in statistics, they can be further divided into raw and central moments. Raw moments are about zero, while central moments are about the first raw moments. The n^{th} raw and central moment are defined as in (2.2) and (2.3), respectively. $f(\xi)$ is the probability density function of the random variable ξ, and μ_1^r is the first raw moment, i.e., expectation, of ξ. The explicit expression of μ_1^r is given in (2.4). The second central moment of ξ, i.e., μ_2^{c}, is just its variance and is given in (2.5). μ_2^{c} roughly reflects how far ξ spreads out. Furthermore, moments for multiple random variables are called mixed moments. A typical mixed moment for two random variables is their covariance as shown in (2.6), where μ_{ξ_1} and μ_{ξ_2} are the expectation of ξ_1 and ξ_2, respectively. Covariances measure the variation of two random variables. If the variances of the two random variables are also known, the Pearson correlation coefficient can be calculated as in (2.7), where $\sigma_{\xi_1}^2$ and $\sigma_{\xi_2}^2$ are the variance of ξ_1 and ξ_2, respectively. The Pearson correlation coefficient lies in the interval [-1,1]. If it is positive, the two random variables have greater positive linear correlation as it gets larger. When it equals to 1, total positive linear correlation holds for the two random variables, and the relationship between them can be expressed in the form of affine functions as in (2.8), where a is positive. Similarly, if Pearson correlation coefficient is negative and it gets smaller, the two random variables have greater negative linear correlation. When it equals to -1, total negative linear correlation holds for the two random variables, and the relationship between them can also be expressed in the form of (2.8), but a is now negative. While if the Pearson correlation coefficient equals to 0, the two random variables have no linear correlation.

As uncertainties are random variables, their moments reveal information about their distributions. With historical samples of uncertainties, the statistical values of their moments can be obtained, and moments-based ambiguity sets can be constructed. For illustration purposes, an ambiguity set for a multivariate uncertainty $\boldsymbol{\xi}$ is given in (2.9), where $f_{\boldsymbol{\xi}}$ is the probability distribution of $\boldsymbol{\xi}$, and $\mathrm{N}_{\boldsymbol{\xi}}$ is the dimension of $\boldsymbol{\xi}$. The first

row of (2.9) limits the range of $\boldsymbol{\xi}$ within U, which can be the entire real space or its subsets. The expectation of $\boldsymbol{\xi}$ is constrained through the second and third row of (2.9). As the expectation of $\boldsymbol{\xi}$ is just the vector of first raw moments of all univariate uncertainties in $\boldsymbol{\xi}$, (2.9) is moment-based. It should be emphasized that ambiguity sets are estimates of the uncertainty distribution. The estimating accuracy can be improved by incorporating more information about the uncertainties. For example, the covariance matrix of $\boldsymbol{\xi}$ can also be constrained in (2.9). But including more information in ambiguity sets will generally increase the computational difficulty. So, to construct proper ambiguity sets, accuracy and computational tractability need to be balanced in consideration of the characteristics of the studied problems. In Chapter 3, two different ambiguity sets are adopted for uncertainties in different periods. The ambiguity set for uncertainties in the first period limits uncertainty realizations within an ellipsoidal set and depicts the uncertainty distribution through the statistical expectation and covariance matrix, whose deviations from the actual moments are also considered, while the ambiguity set for other uncertainties bounds the mean of segregated uncertainties within a tractable conic representable set and limits uncertainty realizations within a polyhedral set. In Chapter 4 and 5, another ambiguity set is adopted. It sets the uncertainty expectation and covariance matrix to fixed values and has no limitation on uncertainty realizations.

$$\mu_{\mathrm{n}} = \int_{-\infty}^{\infty} (x - \mathrm{c})^n f(x)\, \mathrm{dx} \tag{2.1}$$

$$\mu_{\mathrm{n}}^{\mathrm{r}} = \int_{-\infty}^{\infty} \xi^n f(\xi)\, \mathrm{d}\xi \tag{2.2}$$

$$\mu_{\mathrm{n}}^{\mathrm{c}} = \int_{-\infty}^{\infty} (\xi - \mu_1^r)^{\mathrm{n}} f(\xi)\, \mathrm{d}\xi \tag{2.3}$$

$$\mu_1^{\mathrm{r}} = \int_{-\infty}^{\infty} \xi f(\xi)\, \mathrm{d}\xi \tag{2.4}$$

$$\mu_2^{\mathrm{c}} = \int_{-\infty}^{\infty} (\xi - \mu_1^r)^2 f(\xi)\, \mathrm{d}\xi \tag{2.5}$$

$$\mathrm{cov}(\xi_1, \xi_2) = \int_{-\infty}^{\infty} \int_{-\infty}^{\infty} (\xi_1 - \mu_{\xi_1})(\xi_2 - \mu_{\xi_2}) f(\xi_1) f(\xi_2)\, \mathrm{d}\xi_1 \mathrm{d}\xi_2 \tag{2.6}$$

$$\frac{\mathrm{cov}(\xi_1, \xi_2)}{\sqrt{\sigma_{\xi_1}^2 \sigma_{\xi_2}^2}} \tag{2.7}$$

$$\xi_1 = a\xi_2 + b \tag{2.8}$$

$$\mathrm{D} = \left\{ f_{\xi} \middle| \begin{matrix} \Pr(\boldsymbol{\xi} \in \mathrm{U}) = 1 \\ \mathrm{E}[\boldsymbol{\xi}] \leq \boldsymbol{\mu}_1 \\ \mathrm{E}[\boldsymbol{\xi}] \geq \boldsymbol{\mu}_2 \end{matrix} \right\} \tag{2.9}$$

2.2 Duality in optimization

DRO using moments-based ambiguity sets highly depends on the duality theory in optimization, which is briefly introduced here before further discussions about DRO. A typical optimization problem is shown in (2.10)-(2.12). "min" in (2.10) stands for "minimize". Similarly, " max " in optimization problems means "maximize". Sometimes, "min" is replaced by "inf", and "max" is replaced by "sup". "inf" and "sup" are short for "infimum" and "supremum", respectively. Compared with "min" and "max", "inf" and "sup" are also applicable to optimization problems that have no minimum or maximum but only the greatest lower or upper bound. In (2.11), "$s.t.$" stands for "subject to", and "∀" means "for all".

The Lagrangian and Lagrange dual function of the optimization problem (2.10)-(2.12) are defined in (2.13) and (2.14), respectively. λ_i is the i^{th} element of the vector $\boldsymbol{\lambda}$. Similarly, ω_j is the j^{th} element of the vector $\boldsymbol{\omega}$. $\mathcal{A}$ in (2.14) is the intersection of the domain of $g_i, \forall i = 1, \dots, m$ and $h_j, \forall j = 1, \dots, n$. With (2.11) and (2.12), (2.15) can be obtained obviously. The "≥" in (2.15) is component-wise. To be more specific, $\boldsymbol{\lambda} \geq \mathbf{0}$ in (2.15) means that every element in the vector $\boldsymbol{\lambda}$ is non-negative. According to (2.15), the Lagrange dual function $k(\boldsymbol{\lambda}, \boldsymbol{\omega})$ is not greater than the optimal value of (2.10)-(2.12) when $\boldsymbol{\lambda} \geq \mathbf{0}$. In other words, the Lagrange dual function provides lower bounds for (2.10)-(2.12). But if the Lagrange dual function takes values of minus

infinity $-\infty$, the lower bound it provided is useless. Without doubt, the greatest or best lower bound is more desirable than $-\infty$. In pursuit of the best lower bound, the Lagrange dual problem is defined as (2.16)-(2.17). In the following parts of the thesis, "Lagrange dual problem" will be replaced by "dual problem" for short. The property that the optimal value of (2.16)-(2.17) is not greater than that of (2.10)-(2.12) is called weak duality. While if the optimal value of (2.16)-(2.17) equals to that of (2.10)-(2.12), it is said that strong duality holds.

$$\min_{\boldsymbol{x}} \ f(\boldsymbol{x}) \tag{2.10}$$

$$s.t. \ g_i(\boldsymbol{x}) \leq 0, \forall i = 1, \dots, m \tag{2.11}$$

$$h_j(\boldsymbol{x}) = 0, \forall j = 1, \dots, n \tag{2.12}$$

$$L(\boldsymbol{x}, \boldsymbol{\lambda}, \boldsymbol{\omega}) = \ f(\boldsymbol{x}) + \sum_{i=1}^{m} \lambda_i \, g_i(\boldsymbol{x}) + \sum_{j=1}^{n} \omega_j \, h_j(\boldsymbol{x}) \tag{2.13}$$

$$k(\boldsymbol{\lambda}, \boldsymbol{\omega}) = \inf_{\boldsymbol{x} \in \mathcal{A}} L(\boldsymbol{x}, \boldsymbol{\lambda}, \boldsymbol{\omega}) = \inf_{\boldsymbol{x} \in \mathcal{A}} \left(f(\boldsymbol{x}) + \sum_{i=1}^{m} \lambda_i \, g_i(\boldsymbol{x}) + \sum_{j=1}^{n} \omega_j \, h_j(\boldsymbol{x}) \right) \tag{2.14}$$

$$L(\boldsymbol{x}, \boldsymbol{\lambda}, \boldsymbol{\omega}) \leq \ f(\boldsymbol{x}), \forall \boldsymbol{\lambda} \geq \mathbf{0} \tag{2.15}$$

$$\sup_{\boldsymbol{\lambda}, \boldsymbol{\omega}} k(\boldsymbol{\lambda}, \boldsymbol{\omega}) \tag{2.16}$$

$$s.t. \ \boldsymbol{\lambda} \geq \mathbf{0} \tag{2.17}$$

For clearer illustration of the duality theory in optimization, dual problems in linear programing are presented here. Linear programming optimizes a linear objective subject to linear constraints. Any linear programs can be put in the form of (2.18)-(2.20), where $\boldsymbol{c}'$ is the transpose of $\boldsymbol{c}$. To be more specific, inequality constraints can be transformed into equality ones by introducing slack variables. Any non-negative variable x_1 can be replaced by a non-positive variable x_2 that satisfies $x_2 = -x_1$. Any variable x that has no sign limitation can be replaced by the difference of two non-positive variables, i.e., $x_1 - x_2$. The Lagrangian of (2.18)-(2.20) is given in (2.21),

where $\mathbf{A}_j$ is the j^{th} row of $\mathbf{A}$. Obviously, $L(\boldsymbol{x}, \boldsymbol{\lambda}, \boldsymbol{\omega})$ will be unbounded if $\mathbf{c} + \boldsymbol{\lambda} + \mathbf{A}'\boldsymbol{\omega} \neq \mathbf{0}$. So, the Lagrange dual function of (2.18)-(2.20) is in the form of (2.22), and the Lagrange dual problem of (2.18)-(2.20) can be given as (2.23)-(2.25), which can be further transformed into (2.26)-(2.27). As discussed earlier, the dual problem (2.26)-(2.27) provides lower bounds for the primal problem (2.18)-(2.20). More particularly, strong duality holds for any feasible linear program [90]. So, the optimal value of a linear program can be obtained by solving its dual problem.

$$\min \mathbf{c}'\boldsymbol{x} \tag{2.18}$$

$$s.t.\ \mathbf{A}\boldsymbol{x} = \mathbf{b} \tag{2.19}$$

$$\boldsymbol{x} \leq \mathbf{0} \tag{2.20}$$

$$L(\boldsymbol{x}, \boldsymbol{\lambda}, \boldsymbol{\omega}) = \mathbf{c}'\boldsymbol{x} + \sum_{i=1}^{m} \lambda_i x_i + \sum_{j=1}^{n} \omega_j \left(\mathbf{A}_j \boldsymbol{x} - \mathrm{b}_j\right) = (\mathbf{c} + \boldsymbol{\lambda} + \mathbf{A}'\boldsymbol{\omega})'\boldsymbol{x} - \mathbf{b}'\boldsymbol{\omega} \tag{2.21}$$

$$k(\boldsymbol{\lambda}, \boldsymbol{\omega}) = \inf_{\boldsymbol{x}} (\mathbf{c} + \boldsymbol{\lambda} + \mathbf{A}'\boldsymbol{\omega})'\boldsymbol{x} - \mathbf{b}'\boldsymbol{\omega} = \begin{cases} -\mathbf{b}'\boldsymbol{\omega}, \text{if } \mathbf{c} + \boldsymbol{\lambda} + \mathbf{A}'\boldsymbol{\omega} = \mathbf{0} \\ -\infty, \text{if } \mathbf{c} + \boldsymbol{\lambda} + \mathbf{A}'\boldsymbol{\omega} \neq \mathbf{0} \end{cases} \tag{2.22}$$

$$\max_{\boldsymbol{\lambda}, \boldsymbol{\omega}} -\mathbf{b}'\boldsymbol{\omega} \tag{2.23}$$

$$s.t.\ \mathbf{c} + \boldsymbol{\lambda} + \mathbf{A}'\boldsymbol{\omega} = \mathbf{0} \tag{2.24}$$

$$\boldsymbol{\lambda} \geq \mathbf{0} \tag{2.25}$$

$$\max_{\boldsymbol{\omega}} -\mathbf{b}'\boldsymbol{\omega} \tag{2.26}$$

$$s.t.\ \mathbf{c} + \mathbf{A}'\boldsymbol{\omega} \leq \mathbf{0} \tag{2.27}$$

2.3 The worst expectation over the ambiguity set

As discussed in Chapter I, DRO focuses on the worst distribution in the ambiguity set. The key of its worst-distribution orientation lies in evaluating the worst expectation of uncertainty-affected terms over the ambiguity set, which is usually achieved by using the duality theory when moments-based ambiguity sets are adopted. Depending on the studied problem, the worst expectation may have the greatest or the lowest value with

respect to the ambiguity set. By assuming that it has the greatest value, an illustration is given here based on the ambiguity set (2.9). The worst expectation of $\Omega(\boldsymbol{\xi})$ over (2.9) is written explicitly as (2.28)-(2.32). In (2.28), the expectation of $\Omega(\boldsymbol{\xi})$ is rewritten as the integration of the product of $\Omega(\boldsymbol{\xi})$ and the probability density function $f(\boldsymbol{\xi})$. $f(\boldsymbol{\xi})$ should be non-negative, which is guaranteed through (2.29). (2.30)-(2.32) are rewritten from (2.9). (2.28)-(2.32) is optimized over $f(\boldsymbol{\xi})$ for all possible realizations of $\boldsymbol{\xi}$, and there will have infinite number of decision variables if $\boldsymbol{\xi}$ is continuous, which would make it difficult to solve. However, by using the duality theory [91, 92], the dual problem of (2.28)-(2.32) can be obtained as (2.33)-(2.36), which has finite decision variables and infinite constraints. The duality between (2.28)-(2.32) and (2.33)-(2.36) can be regarded as the generalization of the duality between optimization problems with finite constraints and finite variables. According to [93], strong duality holds for (2.28)-(2.32) and (2.33)-(2.36). So, instead of solving (2.28)-(2.32), its optimal value can be obtained by solving (2.33)-(2.36).

$$\sup_{f_{\xi}\in \mathrm{D}} \mathrm{E}[\Omega(\boldsymbol{\xi})] = \sup_{f_{\xi}\in \mathrm{D}} \int_{\mathrm{U}} \Omega(\boldsymbol{\xi}) f(\boldsymbol{\xi}) \mathrm{d}\boldsymbol{\xi} \tag{2.28}$$

$$s.t.\ f(\boldsymbol{\xi}) \geq 0, \forall \boldsymbol{\xi} \in \mathrm{U} \tag{2.29}$$

$$\int_{\mathrm{U}} f(\boldsymbol{\xi}) \boldsymbol{d\xi} = 1 \tag{2.30}$$

$$\int_{\mathrm{U}} \boldsymbol{\xi} f(\boldsymbol{\xi}) \boldsymbol{d\xi} \leq \boldsymbol{\mu}_1 : \boldsymbol{w}_1 \tag{2.31}$$

$$\int_{\mathrm{U}} \boldsymbol{\xi} f(\boldsymbol{\xi}) \boldsymbol{d\xi} \geq \boldsymbol{\mu}_2 : \boldsymbol{w}_2 \tag{2.32}$$

$$\inf_{w_0, \boldsymbol{w}_1, \boldsymbol{w}_2} w_0 + \boldsymbol{w}_1{}' \boldsymbol{\mu}_1 + \boldsymbol{w}_2{}' \boldsymbol{\mu}_2 \tag{2.33}$$

$$s.t.\quad w_0 + \boldsymbol{w}_1{}' \boldsymbol{\xi} + \boldsymbol{w}_2{}' \boldsymbol{\xi} \geq \Omega(\boldsymbol{\xi}), \forall \boldsymbol{\xi} \in \mathrm{U} \tag{2.34}$$

$$\boldsymbol{w}_1 \geq \boldsymbol{0} \tag{2.35}$$

$$\boldsymbol{w}_2 \leq \boldsymbol{0} \tag{2.36}$$

2.4 Further transformation

When the uncertainty is continuous, the dual problem of evaluating the worst expectation over the ambiguity set has finite decision variables and infinite constraints. The infinite constraints correspond to all possible realizations of uncertainties, which impedes the dual problem from being solved directly. Therefore, further transformation is needed. Depending on the form of the dual problem, various approaches may be adopted. A possible one is RO, and an illustration is given here by assuming that $\Omega(\boldsymbol{\xi})$ in (2.34) is an affine function of $\boldsymbol{\xi}$ as given in (2.37) and U is a polyhedron as given in (2.38). Then, (2.34) can be rewritten as (2.39). As (2.40)-(2.42) is the dual problem of the optimization problem in the right-hand side of (2.39), (2.34) can be further transformed into (2.43). If there is a $\boldsymbol{y}$ that is feasible for (2.40)-(2.42) and satisfies $w_0 - \mathrm{b} \geq \mathbf{d}'\boldsymbol{y}$, (2.43) is obviously true. So, (2.34) can be finally replaced by (2.44), and uncertainties in the dual problem (2.33)-(2.36) are eliminated. In the following chapters, more details about DRO will be given when it is used.

$$\Omega(\boldsymbol{\xi}) = \mathbf{a}'\boldsymbol{\xi} + \mathrm{b} \tag{2.37}$$

$$\mathrm{U} = \{\boldsymbol{\xi} | \mathbf{A}\boldsymbol{\xi} \leq \mathbf{d}\} \tag{2.38}$$

$$w_0 - \mathrm{b} \geq \max_{\boldsymbol{\xi}:\mathbf{A}\boldsymbol{\xi}\leq\mathbf{d}} (\mathbf{a} - \boldsymbol{w}_1 - \boldsymbol{w}_2)'\boldsymbol{\xi} \tag{2.39}$$

$$\min_{\boldsymbol{y}} \ \mathbf{d}'\boldsymbol{y} \tag{2.40}$$

$$s.t. \ \mathbf{A}'\boldsymbol{y} = \mathbf{a} - \boldsymbol{w}_1 - \boldsymbol{w}_2 \tag{2.41}$$

$$\boldsymbol{y} \geq \mathbf{0} \tag{2.42}$$

$$w_0 - \mathrm{b} \geq \min_{\boldsymbol{y}:\mathbf{A}'\boldsymbol{y}=\mathbf{a}-\boldsymbol{w}_1-\boldsymbol{w}_2,\boldsymbol{y}\geq\mathbf{0}} \mathbf{d}'\boldsymbol{y} \tag{2.43}$$

$$\left\{\begin{array}{c} w_0 - \mathrm{b} \geq \mathbf{d}'\boldsymbol{y} \\ \mathbf{A}'\boldsymbol{y} = \mathbf{a} - \boldsymbol{w}_1 - \boldsymbol{w}_2 \\ \boldsymbol{y} \geq \mathbf{0} \end{array}\right\} \tag{2.44}$$

Chapter III

Security-Constrained Multiperiod Economic Dispatch with Renewable Energy Utilizing Distributionally Robust Optimization

3.1 Introduction

Renewable generation is now taking a larger proportion in power supplies of current power systems. Uncertainties in the forecasted RES power should therefore be carefully handled by system operators; otherwise, secure and economical system operation will be threatened, and power imbalance could be resulted in ED for example. ED is one of the fundamental decision problems in power systems and is often formulated as optimization problems [94], which are now contaminated by uncertainties because of vast allocation of RES.

To achieve effective co-dispatch of energy and reserve under uncertainties brought by RES, a two-stage model was built in [63] using DRO, and is referred as O-DRO here. In O-DRO, the first stage determines initial operation plans with respect to forecasts of RES power with consideration of the second stage, and the second stage determines recourse actions with respect to uncertainty realizations. The second-stage problem minimizes the recourse cost, and the worst expectation of its optimal value is added into the objective of the first-stage problem through DRO techniques, forming the complete two-stage model. With this structure, proper current decisions can be made by accurately considering future recourse actions with respect to uncertainty realizations. [64] presented a similar two-stage model for co-dispatch of hydro, wind and thermal power sources.

Despite the advantages of the models in [63] and [64], the following three concerns, which will be addressed here to establish a more comprehensive ED model, have not

yet been fully considered. Firstly, O-DRO is single-period, and thus coupled ramping constraints of generators between consecutive time periods cannot be incorporated. As a result, operational infeasibility or additional operation costs could be incurred in practice. Secondly, statistical moments (mean and covariance) used in O-DRO are assumed to be exact while they are in fact derived from historical samples and may deviate from actual values, especially when the available data is limited or with inferior quality, which could lead to sub-optimal solutions. Thirdly, in O-DRO, unlimited load shedding operation is allowed to avoid power imbalance, but could lead to undesirable load curtailment and thus degrade system security. To address these issues, a multi-period security-constrained ED model, M-SCED, is proposed here.

In M-SCED, a two-stage formulation is adopted to accurately model recourse actions with respect to uncertainty realizations. To tackle the excessive computational difficulty of multi-period two-stage models, decision variables after the first period are approximated through SLDR, which assumes that optimal decisions are of piecewise-affine functions of earlier realized uncertainty. Such formulation ensures the computational tractability of M-SCED while the model accuracy can be mostly maintained. Besides, a realistic ambiguity set is applied in M-SCED to model possible distributions of the first-period RES uncertainty. In the ambiguity set, uncertainty support is incorporated to embody the boundedness of RES uncertainty, and possible deviations of statistical moments are considered to guarantee DRO's performance under inaccurate uncertainty information. The explicit expression of the worst expectation over the ambiguity set in M-SCED is derived through exploiting the dual second-stage problem of the first period and is simplified through a tailor-made Constraint Generation algorithm when M-SCED is solved. Moreover, load shedding is limited in M-SCED to enhance system security. The solution difficulty caused by such limits is overcome with Farkas' Lemma. The proposed M-SCED is then transformed into a deterministic problem using RO and DRO techniques.

3.2 Nomenclature

Indices, decision variables and uncertainty are printed in italics while parameters are in non-italics.

3.2.1 Indices

i	Index of generators.
j	Index of RES
k	Index of loads
h	Index of transmission lines
t	Index of operation periods

3.2.2 Parameters

$\mathrm{a}_i^{\mathrm{g},1}$, $\mathrm{a}_i^{\mathrm{g},2}$	Generation cost coefficients of Generator i
$\mathrm{a}_i^{\mathrm{r}+}$, $\mathrm{a}_i^{\mathrm{r}-}$	Up, down reserve cost coefficient of Generator i
$\mathrm{b}_i^{\mathrm{p}+}$, $\mathrm{b}_i^{\mathrm{p}-}$	Up, down regulation cost coefficient of Generator i
$\mathrm{b}_k^{\mathrm{ls}}$	Load shedding penalty coefficient of Load k
$\mathrm{b}_j^{\mathrm{w}}$	Regulation cost coefficient of RES j
$\mathrm{p}_i^{\mathrm{u}}$, $\mathrm{p}_i^{\mathrm{l}}$	Maximal, minimal output limit of Generator i
Ra_i^{+}, Ra_i^{-}	Up, down ramping limit of Generator i
Re_i^{+}, Re_i^{-}	Up, down reserve capacity limit of Generator i
$\lambda_{h,i}, \lambda_{h,j}, \lambda_{h,k}$	Power transfer distribution factor of Line h from Generator i, RES j and Load k
Fl_h	Power flow limit of Line h
T	Number of periods in the operation horizon
$\mathrm{N_G}$, $\mathrm{N_W}$, $\mathrm{N_L}$	Number of generators, RES and loads
$\mathrm{w}_j^{\mathrm{f},t}$	Power forecast of RES j in Period t
d_k^t	Power demand of Load k in Period t
$\mathrm{d}_k^{\mathrm{lim},t}$	Allowed load shedding amount of Load k in Period t

3.2.3 First-stage Decision Variables

p_i^t	Scheduled output of Generator i in Period t
w_j^t	Scheduled output of RES j in Period t
$re_i^{t,+},\ re_i^{t,-}$	Up, down reserve capacity offered by Generator i in Period t
$\boldsymbol{x}^t$	Vector of first-stage decision variables in Period t

3.2.4 Second-stage Decision Variables

$p_i^{\mathrm{r},t}$	Regulated output of Generator i in Period t
$d_k^{\mathrm{ls},t}$	Load shedding amount of Load k in Period t
$w_j^{\mathrm{r},t}$	Regulated output of RES j in Period t
$\boldsymbol{y}^t$	Vector of second-stage decision variables in Period t

3.2.5 Uncertainty

$\boldsymbol{\xi}^t, \boldsymbol{\xi}$	Uncertainty of power forecast of RES in Period t and the entire operation horizon, $\boldsymbol{\xi} = [\boldsymbol{\xi}^1; \ldots; \boldsymbol{\xi}^{\mathrm{T}}]$
$\boldsymbol{\xi}_{\mathrm{seg}}$	Segregated uncertainty of $\boldsymbol{\xi}$
$\boldsymbol{\mu}_0$	Statistical mean of $\boldsymbol{\xi}^1$
$\boldsymbol{\Sigma}_0$	Statistical covariance of $\boldsymbol{\xi}^1$
S_0, S	Support of $\boldsymbol{\xi}^1,\ \boldsymbol{\xi}$
$f_{\boldsymbol{\xi}^1},\ f_{\boldsymbol{\xi}}$	Distribution of $\boldsymbol{\xi}^1,\ \boldsymbol{\xi}$
D_1, D_2	Distributional set for $\boldsymbol{\xi}^1,\ \boldsymbol{\xi}$

3.2.6 Functions

$\mathrm{E}(\,)$	Expectation
$\Pr(\,)$	Probability of events
$(x)^+, (x)^-$	Positive and negative operator, $(x)^+ = \max\{x, 0\},\ (x)^- = \max\{-x, 0\}$

3.3 DRO Techniques

In [63, 64], ambiguity sets are constructed by setting the expectation and covariance matrix of uncertainties to certain values as shown in (3.1). The first line in (3.1) sets the uncertainty support, limiting the possible range of $\boldsymbol{\xi}^1$. The second and third line give the expectation and covariance matrix, respectively. The worst expectation over D_0 can be written explicitly as (3.2)-(3.6) with (3.4)-(3.6) transformed from the first to the third line in (3.1), respectively. Probability densities $f_{\xi^1}(\boldsymbol{\xi}^1)$ are decision variables, so there are infinite variables and finite constraints in (3.2)-(3.6). According to the duality theory, the optimal value of (3.2)-(3.6) is equal to that of its dual problem (3.7)-(3.8) [63, 64]. The dual problem has finite variables and infinite constraints and is easier to solve. r^{d}, $\boldsymbol{p}^{\mathrm{d}}$, $\boldsymbol{Q}^{\mathrm{d}}$ in (3.7)-(3.8) are dual variables. $\mathrm{Tr}\left(\boldsymbol{\Sigma}_0 \cdot \boldsymbol{Q}^{\mathrm{d}}\right)$ in (3.7) stands for the trace of the matrix $\boldsymbol{\Sigma}_0 \cdot \boldsymbol{Q}^{\mathrm{d}}$, which is the sum of all elements in the main diagonal of $\boldsymbol{\Sigma}_0 \cdot \boldsymbol{Q}^{\mathrm{d}}$.

$$\mathrm{D}_0 = \left\{ f_{\xi^1} \middle| \begin{matrix} \Pr(\boldsymbol{\xi}^1 \in \mathrm{S}_0) = 1 \\ \mathrm{E}[\boldsymbol{\xi}^1] = \boldsymbol{\mu}_0 \\ \mathrm{E}[(\boldsymbol{\xi}^1 - \boldsymbol{\mu}_0) \cdot (\boldsymbol{\xi}^1 - \boldsymbol{\mu}_0)'] = \boldsymbol{\Sigma}_0 \end{matrix} \right\} \tag{3.1}$$

$$\sup_{f_{\xi^1} \in \mathrm{D}_0} \mathrm{E}[\Omega] = \sup_{f_{\xi^1} \in \mathrm{D}_0} \int_{\mathrm{S}_0} \Omega \cdot f_{\xi^1}(\boldsymbol{\xi}^1) \mathrm{d}\boldsymbol{\xi}^1 \tag{3.2}$$

$$\text{s.t.} \quad f_{\xi^1}(\boldsymbol{\xi}^1) \geq 0 \ \ \forall \boldsymbol{\xi}^1 \in \mathrm{S}_0 \tag{3.3}$$

$$\int_{\mathrm{S}_0} f_{\xi^1}(\boldsymbol{\xi}^1) \mathrm{d}\boldsymbol{\xi}^1 = 1 \tag{3.4}$$

$$\int_{\mathrm{S}_0} \boldsymbol{\xi}^1 f_{\xi^1}(\boldsymbol{\xi}^1) \mathrm{d}\boldsymbol{\xi}^1 = \boldsymbol{\mu}_0 \tag{3.5}$$

$$\int_{\mathrm{S}_0} (\boldsymbol{\xi}^1 - \boldsymbol{\mu}_0) \cdot (\boldsymbol{\xi}^1 - \boldsymbol{\mu}_0)' f_{\xi^1}(\boldsymbol{\xi}^1) \mathrm{d}\boldsymbol{\xi}^1 = \boldsymbol{\Sigma}_0 \tag{3.6}$$

$$\Lambda_1(\Omega) = \inf \ \mathrm{Tr}\left(\boldsymbol{\Sigma}_0 \cdot \boldsymbol{Q}^{\mathrm{d}}\right) + \boldsymbol{\mu}_0{}' \boldsymbol{p}^{\mathrm{d}} + r^{\mathrm{d}} \tag{3.7}$$

$$s.t. \ (\boldsymbol{\xi}^1)' \boldsymbol{Q}^{\mathrm{d}} \boldsymbol{\xi}^1 + (\boldsymbol{\xi}^1)' \boldsymbol{p}^{\mathrm{d}} + r^{\mathrm{d}} \geq \Omega \ \ \forall \boldsymbol{\xi}^1 \in \mathrm{S}_0 \tag{3.8}$$

To improve the accuracy of the model proposed in this chapter, an ambiguity set that is more realistic than (3.1) is adopted for the uncertainty in the first period as shown

in (3.9) [29]. The second and third line in (3.9) describe the possible range of uncertainty mean and covariance matrix based on their statistical values $\boldsymbol{\mu}_0$ and $\boldsymbol{\Sigma}_0$, which can be calculated from the historical samples of uncertainties. The second line bounds the mean within an ellipsoid centered at $\boldsymbol{\mu}_0$ and the third line sets up a positive semidefinite cone for the covariance. r_1 and r_2 are parameters that limit the possible range of uncertainty mean and covariance and decide the size of D_1. Values of r_1 and r_2 can be decided by using the analytical methods in [29] or according to the experience of the decision maker. The worst expectation over D_1 can be written as (3.10)-(3.14) with (3.12)-(3.14) rewritten from the first to the third line in (3.9), respectively. According to the duality theory, it can be known that the optimal value of (3.10)-(3.14) is equal to that of its dual problem (3.15)-(3.18) [29], in which r^{d}, s^{d}, $\boldsymbol{p}^{\mathrm{d}}$, $\boldsymbol{P}^{\mathrm{d}}$, $\boldsymbol{Q}^{\mathrm{d}}$ are dual variables. Compared with D_0, D_1 describes uncertainty moments by proper inequalities rather than equalities and thus attains the important condition (3.17), which facilitates the incorporation of uncertainty support information. Further discussions will be made in Section 3.5.

As decision variables after the first period are approximated by SLDR in M-SCED, modeling for the multi-period uncertainty $\boldsymbol{\xi}$ needs not to be as accurate as that for $\boldsymbol{\xi}^1$. Therefore, a simpler distributional set D_2 is adopted for $\boldsymbol{\xi}$ as in (3.19), where the mean of the segregated uncertainty under SLDR lies in a tractable conic representable set Ψ, and the worst expectation over D_2 is covered in Section 3.6.1.

$$\mathrm{D}_1 = \left\{ f_{\xi^1} \middle| \begin{array}{l} \Pr(\boldsymbol{\xi}^1 \in \mathrm{S}_0) = 1 \\ (\mathrm{E}[\boldsymbol{\xi}^1] - \boldsymbol{\mu}_0)' \cdot {\boldsymbol{\Sigma}_0}^{-1} \cdot (\mathrm{E}[\boldsymbol{\xi}^1] - \boldsymbol{\mu}_0) \le \mathrm{r}_1 \\ \mathrm{E}[(\boldsymbol{\xi}^1 - \boldsymbol{\mu}_0) \cdot (\boldsymbol{\xi}^1 - \boldsymbol{\mu}_0)'] \preccurlyeq \mathrm{r}_2 \boldsymbol{\Sigma}_0 \end{array} \right\} \tag{3.9}$$

$$\sup_{f_{\xi^1} \in \mathrm{D}_1} \mathrm{E}[\Omega] = \sup_{f_{\xi^1} \in \mathrm{D}_1} \int_{\mathrm{S}_0} \Omega \cdot f_{\xi^1}(\boldsymbol{\xi}^1) \mathrm{d}\boldsymbol{\xi}^1 \tag{3.10}$$

$$\text{s.t. } f_{\xi^1}(\boldsymbol{\xi}^1) \ge 0 \ \ \forall \boldsymbol{\xi}^1 \in \mathrm{S}_0 \tag{3.11}$$

$$\int_{\mathrm{S}_0} f_{\xi^1}(\boldsymbol{\xi}^1) \mathrm{d}\boldsymbol{\xi}^1 = 1 \tag{3.12}$$

$$\int_{\mathrm{S}_0} \begin{bmatrix} \boldsymbol{\Sigma}_0 & \boldsymbol{\xi}^1 - \boldsymbol{\mu}_0 \\ (\boldsymbol{\xi}^1 - \boldsymbol{\mu}_0)' & \mathrm{r}_1 \end{bmatrix} f_{\xi^1}(\boldsymbol{\xi}^1) \mathrm{d}\boldsymbol{\xi}^1 \succcurlyeq \mathbf{0} \tag{3.13}$$

$$\int_{S_0} (\boldsymbol{\xi}^1 - \boldsymbol{\mu}_0) \cdot (\boldsymbol{\xi}^1 - \boldsymbol{\mu}_0)' f_{\xi^1}(\boldsymbol{\xi}^1) \mathrm{d}\boldsymbol{\xi}^1 \preccurlyeq \mathrm{r}_2 \boldsymbol{\Sigma}_0 \tag{3.14}$$

$$\inf \mathrm{r}_2 \cdot \mathrm{Tr}\left(\boldsymbol{\Sigma}_0 \cdot \boldsymbol{Q}^{\mathrm{d}}\right) - \boldsymbol{\mu}_0' \boldsymbol{Q}^{\mathrm{d}} \boldsymbol{\mu}_0 + r^{\mathrm{d}} + \mathrm{Tr}\left(\boldsymbol{\Sigma}_0 \cdot \boldsymbol{P}^{\mathrm{d}}\right) - 2\boldsymbol{\mu}_0' \boldsymbol{p}^{\mathrm{d}} + \mathrm{r}_1 s^{\mathrm{d}} \tag{3.15}$$

$$s.t. \begin{bmatrix} \boldsymbol{P}^{\mathrm{d}} & \boldsymbol{p}^{\mathrm{d}} \\ \left(\boldsymbol{p}^{\mathrm{d}}\right)' & s^{\mathrm{d}} \end{bmatrix} \succcurlyeq \mathbf{0} \tag{3.16}$$

$$\boldsymbol{Q}^{\mathrm{d}} \succcurlyeq \mathbf{0} \tag{3.17}$$

$$(\boldsymbol{\xi}^1)' \boldsymbol{Q}^{\mathrm{d}} \boldsymbol{\xi}^1 + 2(\boldsymbol{\xi}^1)' \left(-\boldsymbol{p}^{\mathrm{d}} - \boldsymbol{Q}^{\mathrm{d}} \boldsymbol{\mu}_0\right) + r^{\mathrm{d}} \geq \Omega \ \ \forall \boldsymbol{\xi}^1 \in \mathrm{S}_0 \tag{3.18}$$

$$\mathrm{D}_2 = \left\{ f_{\xi} \middle| \begin{matrix} \Pr(\boldsymbol{\xi} \in \mathrm{S}) = 1 \\ \mathrm{E}\left[\boldsymbol{\xi}_{\mathrm{seg}}\right] \in \Psi \end{matrix} \right\} \tag{3.19}$$

3.4 Multi-period Economic Dispatch Model

In this part, separate models for first-stage and second-stage problems of the two-stage formulation are presented first. Multi-period modeling and SLDR are discussed next. At last, the multi period ED model M-SCED is established.

3.4.1 Separate Models for First-stage and Second-stage Problems

As in (3.20)-(3.27), first-stage problems determine initial operation plans with respect to forecasts of RES power. The sum of the first and second item in the objective (3.20) is the generation cost. The third and fourth item in (3.20) are costs for up and down reserve capacities, respectively. (3.21) ensures system power balance. (3.22) prevents overloading of transmission lines. (3.23) ensures scheduled RES power not exceeded the forecast values. (3.24)-(3.27) are power output and reserve capacity limits of generators. Quadratic generation costs in (3.20) can be approximated by piecewise-linear functions. Then, first-stage problems can be rewritten in compact forms as (3.28)-(3.29).

$$\inf \sum_{i=1}^{\mathrm{N_G}} \left[a_i^{\mathrm{g},1} (p_i^t)^2 + a_i^{\mathrm{g},2} p_i^t + a_i^{\mathrm{r}+} re_i^{t,+} + a_i^{\mathrm{r}-} re_i^{t,-} \right] \tag{3.20}$$

$$\text{s.t.} \sum_{i=1}^{\mathrm{N_G}} p_i^t + \sum_{j=1}^{\mathrm{N_W}} w_j^t = \sum_{k=1}^{\mathrm{N_L}} \mathrm{d}_k^t \tag{3.21}$$

$$-\mathrm{Fl}_h \le \sum_{i=1}^{\mathrm{N_G}} \lambda_{h,i} p_i^t + \sum_{j=1}^{\mathrm{N_W}} \lambda_{h,j} w_j^t - \sum_{k=1}^{\mathrm{N_L}} \lambda_{h,k} \mathrm{d}_k^t \le \mathrm{Fl}_h, \forall h \tag{3.22}$$

$$0 \le w_j^t \le w_j^{\mathrm{f},t}, \forall j \tag{3.23}$$

$$p_i^t + re_i^{t,+} \le \mathrm{p}_i^{\mathrm{u}}, \forall i \tag{3.24}$$

$$\mathrm{p}_i^{\mathrm{l}} \le p_i^t - re_i^{t,-}, \forall i \tag{3.25}$$

$$0 \le re_i^{t,+} \le \mathrm{Re}_i^{+}, \forall i \tag{3.26}$$

$$0 \le re_i^{t,-} \le \mathrm{Re}_i^{-}, \forall i \tag{3.27}$$

$$\inf\ (\boldsymbol{a}^t)' \cdot \boldsymbol{x}^t \tag{3.28}$$

$$\text{s.t.}\ \mathbf{A}^t \cdot \boldsymbol{x}^t \le \mathbf{c}^t \tag{3.29}$$

Second-stage problems determine recourse actions according to actual realizations of RES uncertainty. The first and second item in (3.30) are up and down regulation costs of generators, respectively. The third item is the regulation cost of RES. The last item is the penalty for load shedding. (3.31) and (3.32) avoid real-time power imbalance and overloading of transmission lines under recourse actions. (3.33) and (3.34) are constraints on availability of RES power and reserve capacity. (3.35) limits load shedding amounts, guaranteeing system security. By introducing slack variables and adding constraints (3.36)-(3.41), the objective (3.30) can be replaced by (3.42). Then, the second-stage problems can be rewritten in compact forms as (3.43)-(3.45).

$$\inf \sum_{i=1}^{\mathrm{N_G}} \mathrm{b}_i^{\mathrm{p}+} \left(p_i^{r,t} - p_i^t\right)^+ + \sum_{i=1}^{\mathrm{N_G}} \mathrm{b}_i^{\mathrm{p}-} \left(p_i^{r,t} - p_i^t\right)^- + \sum_{j=1}^{\mathrm{N_W}} \mathrm{b}_j^{\mathrm{w}} \left|w_j^{r,t} - w_j^t\right| + \sum_{k=1}^{\mathrm{N_L}} \mathrm{b}_k^{\mathrm{ls}} d_k^{\mathrm{ls},t} \tag{3.30}$$

$$\text{s.t.} \sum_{k=1}^{\mathrm{N_L}} \left(\mathrm{d}_k^t - d_k^{\mathrm{ls},t}\right) = \sum_{j=1}^{\mathrm{N_W}} w_j^{r,t} + \sum_{i=1}^{\mathrm{N_G}} p_i^{r,t} \tag{3.31}$$

$$-\mathrm{Fl}_h \le \sum_{i=1}^{\mathrm{N_G}} \lambda_{h,i} p_i^{r,t} + \sum_{j=1}^{\mathrm{N_W}} \lambda_{h,j} w_j^{r,t} - \sum_{k=1}^{\mathrm{N_L}} \lambda_{h,k} \left(\mathrm{d}_k^t - d_k^{\mathrm{ls},t}\right) \le \mathrm{Fl}_h, \forall h \quad (3.32)$$

$$0 \le w_j^{r,t} \le \mathrm{w}_j^{\mathrm{f},t} + \xi_j^t, \forall j \quad (3.33)$$

$$p_i^t - re_i^{t,-} \le p_i^{r,t} \le p_i^t + re_i^{t,+}, \forall i \quad (3.34)$$

$$0 \le d_k^{\mathrm{ls},t} \le \mathrm{d}_k^{\mathrm{lim},t}, \forall k \quad (3.35)$$

$$\mathrm{v}_i^1 \ge \mathrm{b}_i^{\mathrm{p}+}\left(p_i^{r,t} - p_i^t\right) \quad (3.36)$$

$$\mathrm{v}_i^1 \ge 0 \quad (3.37)$$

$$\mathrm{v}_i^2 \ge -\mathrm{b}_i^{\mathrm{p}-}\left(p_i^{r,t} - p_i^t\right) \quad (3.38)$$

$$\mathrm{v}_i^2 \ge 0 \quad (3.39)$$

$$\mathrm{v}_j^3 \ge \mathrm{b}_j^{\mathrm{w}}\left(w_j^{r,t} - w_j^t\right) \quad (3.40)$$

$$\mathrm{v}_j^3 \ge \mathrm{b}_j^{\mathrm{w}}\left(w_j^t - w_j^{r,t}\right) \quad (3.41)$$

$$\inf \sum_{i=1}^{\mathrm{N_G}} \mathrm{v}_i^1 + \sum_{i=1}^{\mathrm{N_G}} \mathrm{v}_i^2 + \sum_{j=1}^{\mathrm{N_W}} \mathrm{v}_j^3 + \sum_{k=1}^{\mathrm{N_L}} \mathrm{b}_k^{\mathrm{ls}} d_k^{\mathrm{ls},t} \quad (3.42)$$

$$\Omega_t = \inf\ (\boldsymbol{b}^t)' \cdot \boldsymbol{y}^t \quad (3.43)$$

$$\text{s.t. } \mathbf{B}^t \cdot \boldsymbol{y}^t \le \mathbf{g}^t - \mathbf{E}^t \cdot \boldsymbol{x}^t - \mathbf{F}^t \cdot \boldsymbol{\xi}^t \quad (3.44)$$

$$\boldsymbol{y}^t \ge \mathbf{0} \quad (3.45)$$

3.4.2 Multi-period Modeling and Segregated Linear Decision Rules

The single-period two-stage O-DRO has the formulation as (3.46)-(3.47), in which $\Omega_1(\boldsymbol{x}^1, \boldsymbol{\xi}^1)$ represents the optimal value of the second-stage problem and implies satisfaction of relevant constraints. To solve this problem, the inexplicit term $\Omega_1(\boldsymbol{x}^1, \boldsymbol{\xi}^1)$ is eliminated through exploiting the dual second-stage problem. Although such formulation is accurate, it cannot be directly extended to multi-period as it would be too difficult to solve [95, 96].

$$\inf\ (\boldsymbol{a}^1)' \cdot \boldsymbol{x}^1 + \sup_{f_{\xi^1} \in \mathrm{D}_1} \mathrm{E}[\Omega_1(\boldsymbol{x}^1, \boldsymbol{\xi}^1)] \tag{3.46}$$

$$\text{s.t. } \mathbf{A}^1 \cdot \boldsymbol{x}^1 \leq \mathbf{c}^1 \tag{3.47}$$

In multi-period ED problems, different periods in the operation horizon are not independent from each other, but are linked through ramping constraints of generators. As a result, for M-SCED, only $\boldsymbol{x}^1$ in the first period can be decided independently from actual realizations of uncertainty, while all later decisions, $\boldsymbol{x}^2, \cdots, \boldsymbol{x}^{\mathrm{T}}$ and $\boldsymbol{y}^1, \cdots, \boldsymbol{y}^{\mathrm{T}}$, are influenced by relevant early uncertainty realizations. Because of this consistency requirement of time sequences, multi-period problems are difficult to solve and thus often approximated through LDR in literatures, which is shown to be effective and computationally efficient [69, 95-98].

The relationship between optimal decisions and realized uncertainty can be very complicated. Instead of considering the true relationship, LDR assumes that the optimal decision is of affine functions of relevant uncertainty realizations. For example, in the case of O-DRO, the second-stage optimal decision of $\boldsymbol{y}^1$ is influenced by the realization of $\boldsymbol{\xi}^1$ and is decided by the second-stage optimization problem (3.43)-(3.45). The relationship between optimal $\boldsymbol{y}^1$ and $\boldsymbol{\xi}^1$ generally cannot be expressed in closed forms, but will be assumed as (3.48) if LDR is adopted, where $\widehat{\boldsymbol{y}}^1$ represents the approximation of $\boldsymbol{y}^1$. In fact, two-stage models are equivalent to single-stage ones under LDR approximation. In multi-period problems, the relationship between optimal decisions in Period 2 to Period T and relevant uncertainty realizations is more complicated than that between optimal $\boldsymbol{y}^1$ and $\boldsymbol{\xi}^1$ in O-DRO, and will also be assumed to be affine under LDR.

Generally, either load shedding or curtailing renewable energy should be adopted depending on realizations of uncertainties in RES outputs under the proposed M-SCED, which however cannot be achieved by using LDR. Therefore, SLDR instead of LDR is adopted here. SLDR extends LDR by segregating the primitive uncertainty and applying LDR on the segregated uncertainty to achieve better approximation. Under SLDR, the primitive uncertainty $\boldsymbol{\xi}$ is segregated into $(\boldsymbol{\xi})^+$ and $(\boldsymbol{\xi})^-$, and the

segregated uncertainty is $\boldsymbol{\xi}_{\text{seg}} = [(\boldsymbol{\xi})^+; (\boldsymbol{\xi})^-]$, where $(\boldsymbol{\xi})^+$ is the vector after element-wise operation $(\xi_i)^+ = \max\{\xi_i, 0\}$ to all elements in $\boldsymbol{\xi}$. Original decision variables are replaced by affine functions of the segregated uncertainty $\boldsymbol{\xi}_{\text{seg}}$, which are equivalent to piecewise-affine functions of the primitive uncertainty $\boldsymbol{\xi}$ as shown in (3.49). An illustrative figure of LDR and SLDR is given in Fig. 3.1. Coefficients of SLDR are optimized when M-SCED is solved. Details on LDR and SLDR can be found in [99, 100]. Under LDR or SLDR, time sequences can be regarded as being squeezed together. As a result, multi-period problems become mathematically equivalent to single-period ones as in [69], which greatly reduces the difficulty of solving them and improves their scalability.

$$\hat{\boldsymbol{y}}^1(\boldsymbol{\xi}) = \boldsymbol{\beta}_{\text{con}} + \boldsymbol{\beta} \cdot \boldsymbol{\xi} \tag{3.48}$$

$$\hat{\boldsymbol{y}}^1(\boldsymbol{\xi}) = \beta_{\text{con}} + \boldsymbol{\beta} \cdot \boldsymbol{\xi}_{\text{seg}} = \boldsymbol{\beta}_{\text{con}} + \boldsymbol{\beta}^+ \cdot (\boldsymbol{\xi})^+ + \boldsymbol{\beta}^- \cdot (\boldsymbol{\xi})^- \tag{3.49}$$

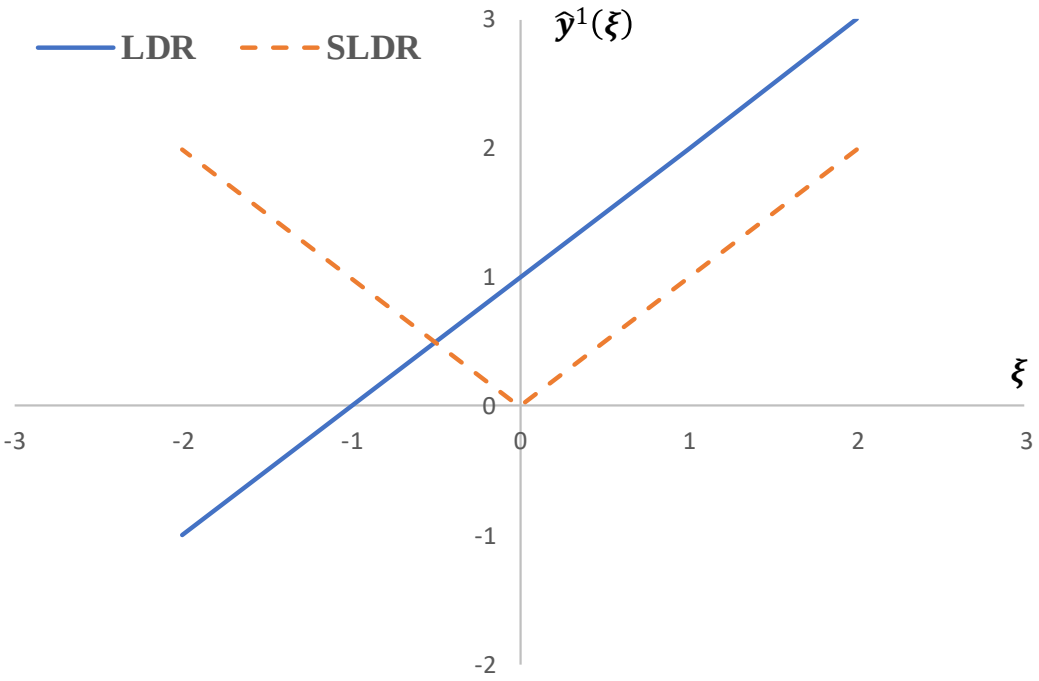

Fig. 3.1 Illustration of LDR and SLDR

3.4.3 Multi-period Economic Dispatch Model M-SCED

In M-SCED, all later decision variables after $\boldsymbol{x}^1$ can be approximated by SLDR. But, to maintain modeling accuracy, $\boldsymbol{y}^1$ is remained intact and handled as in O-DRO. The multi-period model M-SCED is established as (3.50)-(3.56).

$$\inf\left\{(\boldsymbol{a}^1)'\cdot\boldsymbol{x}^1+\sup_{f_{\xi^1}\in \mathrm{D}_1}\mathrm{E}[\Omega_1(\boldsymbol{x}^1,\boldsymbol{\xi}^1)]+\sup_{f_{\xi}\in \mathrm{D}_2}\mathrm{E}\left[\sum_{t=2}^{\mathrm{T}}[(\boldsymbol{a}^t)'\cdot\widehat{\boldsymbol{x}}^t+(\boldsymbol{b}^t)'\cdot\widehat{\boldsymbol{y}}^t]\right]\right\} \quad (3.50)$$

$$\triangleq \inf\ (\boldsymbol{a}^1)'\cdot\boldsymbol{x}^1+\Lambda_1+\Lambda_2 \quad (3.51)$$

$$\text{s.t. } \mathbf{A}^1\cdot\boldsymbol{x}^1\le\mathbf{c}^1 \quad (3.52)$$

$$\mathbf{A}^t\cdot\widehat{\boldsymbol{x}}^t\le\mathbf{c}^t,\forall\boldsymbol{\xi}\ for\ t=2,\dots,\mathrm{T} \quad (3.53)$$

$$\mathbf{B}^t\cdot\widehat{\boldsymbol{y}}^t\le\mathbf{g}^t-\mathbf{E}^t\cdot\widehat{\boldsymbol{x}}^t-\mathbf{F}^t\cdot\boldsymbol{\xi}^t,\forall\boldsymbol{\xi}\ for\ t=2,\dots,\mathrm{T} \quad (3.54)$$

$$\widehat{\boldsymbol{y}}^t\ge\mathbf{0},\forall\boldsymbol{\xi}\ for\ t=2,\dots,\mathrm{T} \quad (3.55)$$

$$-\mathrm{Ra}_i^-\le\hat{p}_i^{r,t}-\hat{p}_i^{r,t-1}\le\mathrm{Ra}_i^+,\forall\boldsymbol{\xi}\ \forall i\ for\ t=2,\dots,\mathrm{T} \quad (3.56)$$

In M-SCED, $\Omega_1(\boldsymbol{x}^1,\boldsymbol{\xi}^1)$ is the optimal second-stage cost of the first period. The second item in (3.50) is the worst expectation of $\Omega_1(\boldsymbol{x}^1,\boldsymbol{\xi}^1)$ and is represented by Λ_1. The last item in (3.50) is the worst expectation of the total costs from Period 2 to Period T and is represented by Λ_2. They are minimized together with the deterministic first-stage cost of the first period. (3.52) is the deterministic first-stage constraints of the first period. (3.53)-(3.55) are constraints from Period 2 to Period T and (3.56) is ramping constraints. Constraints in M-SCED are required to be robust to all possible uncertainty realizations in uncertainty supports in order to ensure secure system operation, while the worst expected operation costs are minimized to pursue superior average economic performance with respect to the worst possible uncertainty distribution.

M-SCED only requires to solve for $\boldsymbol{x}^1$ and other variables help make the right decision for $\boldsymbol{x}^1$ by taking future circumstances into consideration. In rolling-plan operation, second-stage decisions $\boldsymbol{y}^t$ are solved from (3.43)-(3.45) when they need to

be carried out. First-stage decisions of Period 2 to Period T are solved later from updated M-SCED.

With this in mind, it is reasonable to keep $\boldsymbol{y}^1$ intact and approximate variables after $\boldsymbol{y}^1$, because $\boldsymbol{y}^1$ has the most direct influence on the optimal decision of $\boldsymbol{x}^1$. Load shedding is not modeled from Period 2 to Period T in M-SCED, because it cannot be properly approximated by LDR or SLDR. Relevant decision variables of load shedding are deleted from second-stage problems of Period 2 to Period T in M-SCED, and relevant constraints are accordingly modified. This means that the current decision $\boldsymbol{x}^1$ needs to be made to ensure feasible system operation even with no load shedding allowed in Period 2 to Period T. However, it should be noted that the current decision $\boldsymbol{x}^1$ has more direct influence on load shedding in the first period than in Period 2 to Period T, and load shedding in the first period is still modeled in $\boldsymbol{y}^1$ to help making a proper decision for $\boldsymbol{x}^1$. Load shedding in Period 2 to Period T will be modeled later in $\boldsymbol{y}^1$ when M-SCED is updated in rolling-plan operation. With such formulation, M-SCED achieves tractable multi-period modeling while ensuring the quality of the current decision $\boldsymbol{x}^1$. A schematic diagram of M-SCED is given in Fig. 3.2.

While the consideration of RES uncertainty in the proposed model has just been presented, load uncertainty can also be incorporated into the model and handled similarly as the RES uncertainty. The incorporation of load uncertainty and its impacts will further be discussed in Section 3.6.4.

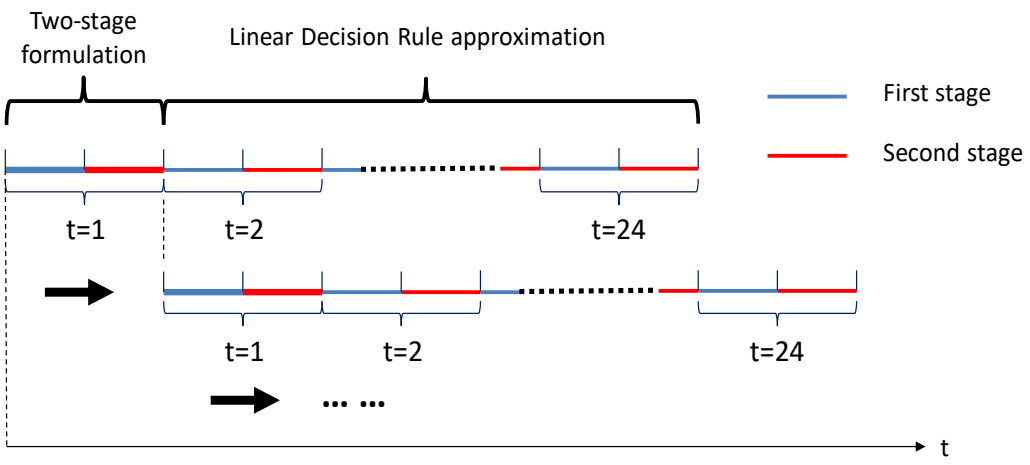

Fig. 3.2 Schematic diagram of M-SCED

3.5 Solution Method

In M-SCED, uncertainty supports of $\boldsymbol{\xi}^{\mathbf{1}}$ and $\boldsymbol{\xi}$, S_0 and S, are taken as ellipsoids and polytopes respectively due to the computation considerations. Ellipsoidal S_0 makes it possible to derive the deterministic explicit expression of Λ_1 through S-lemma, and polyhedral S keeps the robust counterparts of (3.53)-(3.56) linear. Though ellipsoid and polytope may not be the best uncertainty support shapes, both ellipsoidal and polyhedral supports are acceptable if they contain the clear majority of possible uncertainty realizations with reasonable sizes. In this thesis, S_0 and S are set to cover all historical samples of uncertainties with the sizes as small as possible. Here, M-SCED is transformed into an equivalent deterministic problem first and a Constraint Generation algorithm is proposed to solve the problem efficiently.

3.5.1 Equivalent Deterministic Problem

Under SLDR, total costs from Period 2 to Period T are of affine functions of the segregated uncertainty $\boldsymbol{\xi}_{\text{seg}}$. Therefore, Λ_2 can be rewritten as (3.57). If the mean of $\boldsymbol{\xi}_{\text{seg}}$ is expressed as $\bar{\boldsymbol{\xi}}_{\text{seg}}$, Λ_2 can be further transformed into (3.58) and thus can be replaced by its robust counterpart through standard RO techniques. Constraints (3.53)-(3.56) can be replaced by their robust counterparts as well. To avoid the over-conservativeness of RO, uncertainty budgets can be adopted to limit the realizations of multiple scaler uncertainties [101], and techniques used in [58-60] can also be considered. The explicit expression of Λ_1 is (3.15)-(3.18). Then, the only inexplicit term in M-SCED is $\Omega_1(\boldsymbol{x}^1, \boldsymbol{\xi}^1)$ in (3.18).

$$\Lambda_2 = \sup_{f_{\xi} \in \mathrm{D}_2} \mathrm{E}\left[\beta_{\text{con}} + \left(\boldsymbol{\beta}_{\text{seg}}\right)' \cdot \boldsymbol{\xi}_{\text{seg}}\right] \tag{3.57}$$

$$\Lambda_2 = \beta_{\text{con}} + \sup_{\bar{\xi}_{\text{seg}} \in \Psi} \left(\boldsymbol{\beta}_{\text{seg}}\right)' \cdot \bar{\boldsymbol{\xi}}_{\text{seg}} \tag{3.58}$$

According to the following proposition, $\Omega_1(\boldsymbol{x}^1, \boldsymbol{\xi}^1)$ in (3.18) can be eliminated. Different from O-DRO, load shedding is limited in M-SCED. As a result, under improper first-stage decisions $\boldsymbol{x}^1$, the second-stage problem of the first period could be

infeasible because of power imbalance and $\Omega_1(\boldsymbol{x}^1, \boldsymbol{\xi}^1)$ would become plus infinity. To overcome this, Farkas' Lemma is utilized to guarantee the second-stage feasibility in the proposition.

Proposition:

In M-SCED, (3.18) is equivalent to the combination of (3.59) and (3.60).

$$(\mathbf{g}^1 - \mathbf{E}^1 \cdot \boldsymbol{x}^1 - \mathbf{F}^1 \cdot \boldsymbol{\xi}^1)' \cdot \boldsymbol{u}_r \leq 0, \forall \boldsymbol{\xi}^1 \in \mathrm{S}_0, \forall r \tag{3.59}$$

$$(\boldsymbol{\xi}^1)' \boldsymbol{Q}^{\mathrm{d}} \boldsymbol{\xi}^1 + 2(\boldsymbol{\xi}^1)' \left(-\boldsymbol{p}^{\mathrm{d}} - \boldsymbol{Q}^{\mathrm{d}} \boldsymbol{\mu}_0\right) + r^{\mathrm{d}} \geq (\mathbf{g}^1 - \mathbf{E}^1 \cdot \boldsymbol{x}^1 - \mathbf{F}^1 \cdot \boldsymbol{\xi}^1)' \cdot \boldsymbol{u}_e, \forall \boldsymbol{\xi}^1 \in \mathrm{S}_0, \forall e \tag{3.60}$$

where $\boldsymbol{u}_r,\ r = 1, \ldots, \mathrm{N_R}$ and $\boldsymbol{u}_e,\ e = 1, \ldots, \mathrm{N_E}$ are all extreme rays and extreme points of the set $\mathrm{U} = \{\boldsymbol{u} | (\mathbf{B}^1)' \cdot \boldsymbol{u} \leq \mathbf{b}^1,\ \boldsymbol{u} \leq \mathbf{0}\}$, which is the dual feasible region of the second-stage problem (3.43)-(3.45) of the first period.

Proof:

According to Farkas' Lemma as given in Appendix, the feasibility of the second-stage problem (3.43)-(3.45) of the first period is equivalent to the infeasibility of (3.61) and thus can be further transformed into (3.62). Because $\mathrm{U_c}$ is a polyhedral cone, every element in it can be expressed as a nonnegative linear combination of its extreme rays, which are the same as those of U. As a result, when $\boldsymbol{x}^1$ is fixed, (3.62) is equivalent to (3.59). Under the feasibility guarantee (3.59), the optimal value $\Omega_1(\boldsymbol{x}^1, \boldsymbol{\xi}^1)$ is attained at one of the extreme points of the dual feasible set U and thus (3.63) holds [102, 103]. Therefore, (3.18) is equivalent to (3.60) under (3.59).

$$\begin{Bmatrix} \boldsymbol{u} \in \mathrm{U_c} = \{\boldsymbol{u} | (\mathbf{B}^1)' \cdot \boldsymbol{u} \leq \mathbf{0}, \boldsymbol{u} \leq \mathbf{0}\} \\ (\mathbf{g}^1 - \mathbf{E}^1 \cdot \boldsymbol{x}^1 - \mathbf{F}^1 \cdot \boldsymbol{\xi}^1)' \cdot \boldsymbol{u} > 0 \end{Bmatrix} \tag{3.61}$$

$$(\mathbf{g}^1 - \mathbf{E}^1 \cdot \boldsymbol{x}^1 - \mathbf{F}^1 \cdot \boldsymbol{\xi}^1)' \cdot \boldsymbol{u} \leq 0, \forall \boldsymbol{u} \in \mathrm{U_c} \tag{3.62}$$

$$\Omega_1(\boldsymbol{x}^1, \boldsymbol{\xi}^1) = \max_{e \in \{1,2,\ldots,\mathrm{N_E}\}} \{(\mathbf{g}^1 - \mathbf{E}^1 \cdot \boldsymbol{x}^1 - \mathbf{F}^1 \cdot \boldsymbol{\xi}^1)' \cdot \boldsymbol{u}_e\} \tag{3.63}$$

□

(3.59) guarantees the feasibility of the second-stage problem of the first period within the framework of DRO, and its effect is requiring enough reserve capacity for

scheduled RES power. (3.60) ensures the optimality of $\boldsymbol{x}^1$. (3.59) can be replaced by its deterministic robust counterpart through standard RO techniques. (3.60) can be rewritten as (3.64). Because S_0 is an ellipsoid as shown in (3.65), (3.64) can be transformed into (3.66)-(3.67) by using S-lemma. S-lemma and the transformation from (3.64) to (3.66)-(3.67) are given in Appendix. At last, M-SCED becomes a deterministic semidefinite program, which can be solved by off-the-shelf solvers.

$$[(\boldsymbol{\xi}^1)' \quad 1]\begin{bmatrix} \boldsymbol{Q}^{\mathrm{d}} & -\boldsymbol{p}^{\mathrm{d}} - \boldsymbol{Q}^{\mathrm{d}}\boldsymbol{\mu}_0 + (\mathbf{F}^1)'\boldsymbol{u}_e/2 \\ \left(-\boldsymbol{p}^{\mathrm{d}} - \boldsymbol{Q}^{\mathrm{d}}\boldsymbol{\mu}_0 + (\mathbf{F}^1)'\boldsymbol{u}_e/2\right)' & r^{\mathrm{d}} + (\mathbf{E}^1 \cdot \boldsymbol{x}^1 - \mathbf{g}^1)'\boldsymbol{u}_e \end{bmatrix}\begin{bmatrix} \boldsymbol{\xi}^1 \\ 1 \end{bmatrix} \geq 0, \forall \boldsymbol{\xi}^1 \in \mathrm{S}_0, \forall e \quad (3.64)$$

$$\mathrm{S}_0 = \{\boldsymbol{\xi}^1 | (\boldsymbol{\xi}^1 - \boldsymbol{\mu}_0)' \cdot \mathbf{M} \cdot (\boldsymbol{\xi}^1 - \boldsymbol{\mu}_0) \leq 1\} \quad (3.65)$$

$$\begin{bmatrix} \boldsymbol{Q}^{\mathrm{d}} & -\boldsymbol{p}^{\mathrm{d}} - \boldsymbol{Q}^{\mathrm{d}}\boldsymbol{\mu}_0 + (\mathbf{F}^1)'\boldsymbol{u}_e/2 \\ \left(-\boldsymbol{p}^{\mathrm{d}} - \boldsymbol{Q}^{\mathrm{d}}\boldsymbol{\mu}_0 + (\mathbf{F}^1)'\boldsymbol{u}_e/2\right)' & r^{\mathrm{d}} + (\mathbf{E}^1 \cdot \boldsymbol{x}^1 - \mathbf{g}^1)'\boldsymbol{u}_e \end{bmatrix} \succcurlyeq -\tau_e \begin{bmatrix} \mathbf{M} & -\mathbf{M} \cdot \boldsymbol{\mu}_0 \\ -(\mathbf{M} \cdot \boldsymbol{\mu}_0)' & (\boldsymbol{\mu}_0)'\mathbf{M}\boldsymbol{\mu}_0 - 1 \end{bmatrix}, \forall e \quad (3.66)$$

$$\tau_e \geq 0, \forall e \quad (3.67)$$

3.5.2 Constraint Generation Algorithm

Although M-SCED is transformed into a deterministic problem as in Section 3.5.1, constraints from (3.59) and (3.60) can be in vast numbers, relating with extreme rays and points of U, and only parts of them are active for the optimal solution. To solve the problem efficiently, a Constraint Generation algorithm is proposed here based on the structure of M-SCED. The core idea is to relax M-SCED by considering only parts of constraints from (3.59) and (3.60). Necessary constraints from (3.59) and (3.60) are found iteratively by solving the relaxed M-SCED and two sub-problems until the optimal solution is reached. The relaxed M-SCED is in the form of (3.68), where Φ_e and Φ_r are sets of necessary extreme points and rays. Sub-problem 1 and 2 are set as (3.69)-(3.70) and (3.71)-(3.73), respectively, where $\boldsymbol{x}^{1,*}$, $\boldsymbol{p}^{\mathrm{d},*}$, $\boldsymbol{Q}^{\mathrm{d},*}$ and $r^{\mathrm{d},*}$ are optimal values solved from the relaxed M-SCED.

$$\begin{aligned} &\inf\ (\mathbf{a}^1)' \cdot \boldsymbol{x}^1 + \Lambda_2 + (3.15) \\ &\text{s.t.}\ (3.52) - (3.56), (3.16) - (3.17) \\ &\quad (3.59), \forall r \in \Phi_r \\ &\quad (3.60), \forall e \in \Phi_e \end{aligned} \tag{3.68}$$

$$\inf_{\boldsymbol{\xi}^1, \boldsymbol{u}}\ (\boldsymbol{\xi}^1)' \boldsymbol{Q}^{\mathrm{d},*} \boldsymbol{\xi}^1 + 2(\boldsymbol{\xi}^1)' \left(-\boldsymbol{p}^{\mathrm{d},*} - \boldsymbol{Q}^{\mathrm{d},*} \boldsymbol{\mu}_0\right) + r^{\mathrm{d},*} - (\mathbf{g}^1 - \mathbf{E}^1 \cdot \boldsymbol{x}^{1,*} - \mathbf{F}^1 \cdot \boldsymbol{\xi}^1)' \cdot \boldsymbol{u} \tag{3.69}$$

$$\text{s.t.}\ \ \boldsymbol{\xi}^1 \in \mathrm{S}_0, \boldsymbol{u} \in \mathrm{U} \tag{3.70}$$

$$\sup_{\boldsymbol{\xi}^1, \boldsymbol{u}}\ (\mathbf{g}^1 - \mathbf{E}^1 \cdot \boldsymbol{x}^{1,*} - \mathbf{F}^1 \cdot \boldsymbol{\xi}^1)' \cdot \boldsymbol{u} \tag{3.71}$$

$$s.t.\ \ \boldsymbol{\xi}^1 \in \mathrm{S}_0, \boldsymbol{u} \in \mathrm{U}_\mathrm{c} \tag{3.72}$$

$$(\mathbf{g}^1 - \mathbf{E}^1 \cdot \boldsymbol{x}^{1,*} - \mathbf{F}^1 \cdot \boldsymbol{\xi}^1)' \cdot \boldsymbol{u} \leq 1 \tag{3.73}$$

If there is any extreme ray $\boldsymbol{u}_r$ violating (3.59), Sub-problem 1 will be unbounded and the optimal $\boldsymbol{u}$ of Sub-problem 2 corresponds to the most violating extreme ray for (3.59), which should be added to Φ_r. If there is no violating extreme ray for (3.59) but are some violating extreme points for (3.60), the optimal value of Sub-problem 1 will be a finite negative value and the optimal $\boldsymbol{u}$ corresponds to the most violating extreme point for (3.60), which should be added to Φ_e. The complete algorithm of solving M-SCED is as follows.

1) Initialize Φ_e and Φ_r with proper extreme points and rays of U.
2) Solve the relaxed M-SCED (20) with parts of constraints from (15) and (16) corresponding to Φ_r and Φ_e, respectively.
3) Substitute the optimal $\boldsymbol{x}^{1,*}$, $\boldsymbol{p}^{\mathrm{d},*}$, $\boldsymbol{Q}^{\mathrm{d},*}$ and $r^{\mathrm{d},*}$ obtained in step 2 into Sub-problem 1 and 2, and solve Sub-problem 1.
4) If the optimal value of Sub-problem 1 is not less than zero, the optimal solution of M-SCED is attained and the algorithm ends. If the optimal value is less than zero but not minus infinity, add the corresponding extreme point into Φ_e. Otherwise, solve Sub-problem 2 and add the corresponding extreme ray into Φ_r.

5) Repeat Step 2-4 until the algorithm ends.

Sub-problem 1 and 2 are both biconvex problems. When u is fixed, they are both convex in $\boldsymbol{\xi}^1$. When $\boldsymbol{\xi}^1$ is fixed, they are both linear in u. Biconvex problems are non-convex and difficult to solve. To solve the biconvex Sub-problem 1 and 2 efficiently, a sequentially alternating approach is adopted here, which solves the problems by fixing $\boldsymbol{\xi}^1$ and $\boldsymbol{u}$ as constants alternatively until a local optimum is attained [104]. Though this approach cannot guarantee to find the global optimal solutions of Sub-problem 1 and 2, its solution quality could be improved with the use of multiple initial values [63]. Similar heuristic methods have been widely adopted to effectively solve bilinear and biconvex problems in literatures adopting two-stage formulations [60, 63, 64, 74, 101], and the suggested sequentially alternating approach has also been shown to be effective in the case studies. The procedure of the sequentially alternating approach is as follows.

1) Choose a set of initial vales of $\boldsymbol{\xi}^1$.
2) Set $\boldsymbol{\xi}^1$ to an initial value or $\boldsymbol{\xi}^{1,*}$, solve the subproblem with respect to $\boldsymbol{u}$. Record the optimal value of the subproblem as o^1 and the solution of $\boldsymbol{u}$ as $\boldsymbol{u}^*$.
3) Set $\boldsymbol{u}$ to $\boldsymbol{u}^*$, solve the subproblem with respect to $\boldsymbol{\xi}^1$. Record the optimal value of the subproblem as o^2 and the solution of $\boldsymbol{\xi}^1$ as $\boldsymbol{\xi}^{1,*}$.
4) If the difference between o^1 and o^2 is within the tolerance, go to Step 5. Otherwise, repeat Set 2-3 until the difference between o^1 and o^2 is within the tolerance.
5) Check whether Step 2-4 have been conducted for all chosen initial values of $\boldsymbol{\xi}^1$. If yes, go to Step 6. Otherwise, go to Step 2 for an initial value of $\boldsymbol{\xi}^1$ that has not been attempted.
6) Compare the solutions corresponding to each chosen initial value of $\boldsymbol{\xi}^1$. Choose the one that has the best optimal value as the optimal solution of the subproblem.

It should be noted that Sub-problem 1 is convex because of (3.17), which is attained in the dual problem for evaluating worst expectations of uncertainty-affected costs.

However, if equalities were used instead of inequalities to describe uncertainty moments in the distributional set as in D_0, condition (3.17) could not be attained in this way. In [63], S_0 in D_0 is set as the entire real space $\mathbb{R}^{\mathrm{N}_{\xi^1}}$. N_{ξ^1} is the dimension of $\boldsymbol{\xi}^1$. As a result, instead of (3.60), there will be constraints in the form of (3.74), which can be rewritten as (3.75) and further replaced by (3.76), from which (3.17) can be obtained. However, if S_0 in D_0 is set to ellipsoids as in D_1, there will be only constraints in the form of (3.66) but not (3.76). As a result, (3.17) cannot be contained and thus the biconvexity of subproblems in the Constraint Generation algorithm cannot be guaranteed, which will lead to extra computational difficulty. To conclude, compared with D_0, D_1 incorporates ellipsoidal uncertainty support without increasing the computational complexity.

$$(\boldsymbol{\xi}^1)'\boldsymbol{Q}^{\mathrm{d}}\boldsymbol{\xi}^1 + (\boldsymbol{\xi}^1)'\boldsymbol{p}^{\mathrm{d}} + r^{\mathrm{d}} \geq (\mathbf{g}^1 - \mathbf{E}^1 \cdot \boldsymbol{x}^1 - \mathbf{F}^1 \cdot \boldsymbol{\xi}^1)' \cdot \boldsymbol{u}_e, \forall \boldsymbol{\xi}^1 \in \mathbb{R}^{\mathrm{N}_{\xi^1}}, \forall e \quad (3.74)$$

$$\begin{bmatrix}(\boldsymbol{\xi}^1)' & 1\end{bmatrix}\begin{bmatrix}\boldsymbol{Q}^{\mathrm{d}} & \left(\boldsymbol{p}^{\mathrm{d}} + (\mathbf{F}^1)'\boldsymbol{u}_e\right)/2 \\ \left(\boldsymbol{p}^{\mathrm{d}} + (\mathbf{F}^1)'\boldsymbol{u}_e\right)'/2 & r^{\mathrm{d}} + (\mathbf{E}^1 \cdot \boldsymbol{x}^1 - \mathbf{g}^1)'\boldsymbol{u}_e\end{bmatrix}\begin{bmatrix}\boldsymbol{\xi}^1 \\ 1\end{bmatrix} \geq 0, \quad \forall \boldsymbol{\xi}^1 \in \mathbb{R}^{\mathrm{N}_{\xi^1}}, \forall e \quad (3.75)$$

$$\begin{bmatrix}\boldsymbol{Q}^{\mathrm{d}} & \left(\boldsymbol{p}^{\mathrm{d}} + (\mathbf{F}^1)'\boldsymbol{u}_e\right)/2 \\ \left(\boldsymbol{p}^{\mathrm{d}} + (\mathbf{F}^1)'\boldsymbol{u}_e\right)'/2 & r^{\mathrm{d}} + (\mathbf{E}^1 \cdot \boldsymbol{x}^1 - \mathbf{g}^1)'\boldsymbol{u}_e\end{bmatrix} \succcurlyeq 0 \quad (3.76)$$

3.6 Results and Discussions

Effects of DRO in improving the economy of ED operation are firstly demonstrated here to show the necessity of utilizing DRO. Superiority of two-stage models over single-stage ones is illustrated next. Lastly, M-SCED is benchmarked against O-DRO [63] to show its improvements and the effects of incorporating load uncertainty are discussed.

3.6.1 Necessity of Using DRO in Economic Dispatch

In ED, RO has been commonly used to minimize the objective in the worst possible case. However, because the worst case rarely happens, the solution can often be over-

conservative. In contrast, M-SCED can greatly improve the economic efficiency through evaluating the expected second-stage cost by DRO. The traditional RO model in [63] is here referred as T-RO. Because both T-RO and O-DRO are single-period, only the first-period sub-model of M-SCED is used for comparison here by removing components after the first period in M-SCED, and it is referred as S-SCED.

Case studies in this part are conducted on a modified IEEE 118-bus system from [63], where all RES have power forecast of 100 MW. For simplicity, all RES uncertainty is assumed to have zero mean, the same variance and no correlation with each other. T-RO has a parameter called uncertainty budget Γ, which controls the size of uncertainty sets and decides the conservatism level of T-RO. To make a fair comparison, ED is solved by S-SCED, O-DRO and T-RO of different Γ under RES uncertainty of different variances. Their calculated total costs for two stages are shown in Fig. 3.3. Costs of T-RO are much higher than those of S-SCED and O-DRO, which overlap each other in the figure.

To obtain the average performance of different models, for each set of variances, 3000 simulated uncertainty realizations are generated by normal distributions. Based on the first-stage decisions of different models, recourse actions are solved from the second-stage problem (3.43)-(3.45) under simulated uncertainty realizations. The average total costs are shown in Fig. 3.4, which are the sum of deterministic first-stage costs and average second-stage costs with respect to all simulated uncertainty realizations. Average costs of T-RO are lower than its calculated costs, but still much higher than average costs of S-SCED and O-DRO. This is because T-RO is designed for the worst case when actual available RES power is much lower than the forecast value. With this anticipation, T-RO schedules only part of forecasted RES power and thus plans more outputs from generators than S-SCED and O-DRO in the first stage, leading to unnecessary extra costs under most uncertainty realizations. Although T-RO will have lower total costs when the worst case does occur [63], the probability is small. Therefore, in terms of average economic performance, S-SCED and O-DRO are better than T-RO, proving the necessity of utilizing DRO in ED operation.

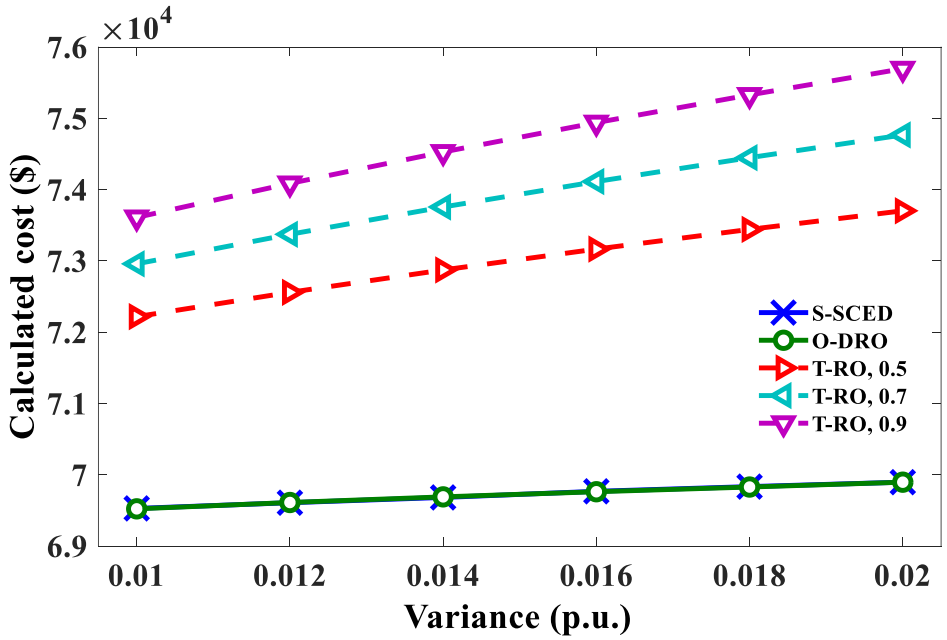

Fig. 3.3 Calculated costs from different models

Computation times of different models are recorded in Table 3.1 which shows that S-SCED is comparable with O-DRO while the computation times of T-RO depend on Γ and could vary widely. Here, T-RO is solved by a column-and-constraint algorithm as in [63] with the bilinear sub-problem transformed into a MILP. This bilinear sub-problem can also be solved by the sequentially alternating approach as adopted for S-SCED with the sacrifice of global optimality by solving a series of linear programs. While the method of transforming bilinear optimization problems into MILP is more computation demanding, it has been widely adopted in various applications [48, 57, 63, 105, 106] because of its good solution quality, and hence is adopted here for benchmarking.

Table 3.1 Computation times of different models

Variance (p.u.)	S-SCED (s)	O-DRO (s)	T-RO (s)		
			Γ=0.5	Γ=0.7	Γ=0.9
0.01	119.50	89.88	149.61	119.59	30.99
0.014	116.52	107.24	132.86	122.42	29.86
0.018	114.35	107.66	166.70	121.89	34.42
0.02	113.51	113.02	150.10	121.86	30.28

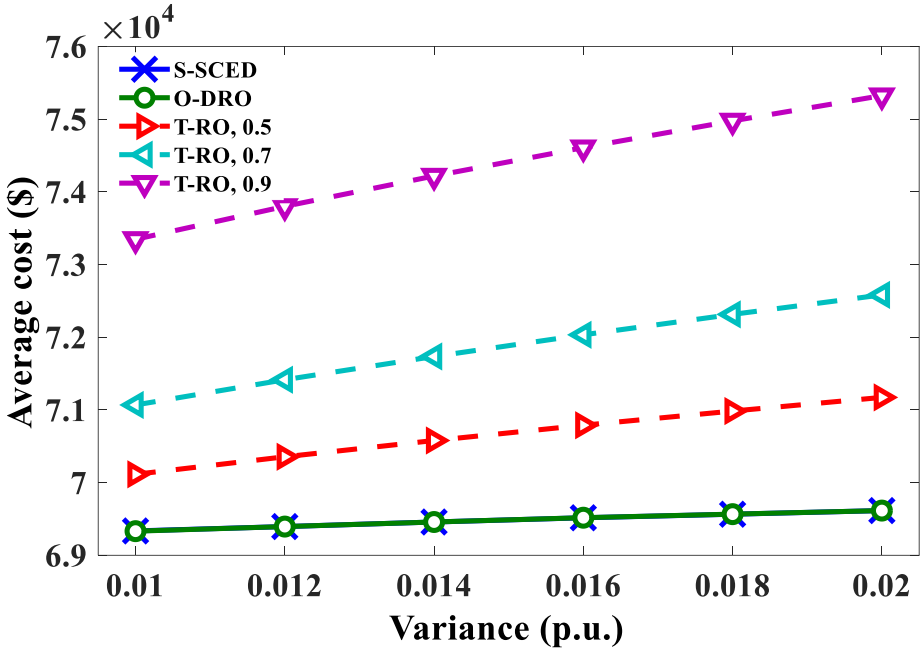

Fig. 3.4 Average costs from different models

3.6.2 Comparison Between Two-stage and Single-stage Models

Both S-SCED and O-DRO are two-stage models with recourse actions fully modeled in the second stage. In contrast, single-stage models simply assume that recourse actions respond affinely to uncertainty realizations. To illustrate the superiority of the two-stage S-SCED over single-stage models, comparison is made here between S-SCED and its single-stage counterpart, which is referred as S-S-SCED.

Case studies in this and following parts are conducted on a modified IEEE 30-bus system, where two RES are connected to Bus 22 and 25 with forecast power of 60 MW each. Variances of RES uncertainty are set to 0.02 p.u. and parameters of generators are given in Table 3.2. Up and down reserve cost coefficients of all generators, a_i^{r+} and a_i^{r-}, are set to 1.2 \$/MW. 3000 simulated uncertainty realizations are generated by normal distributions to test S-SCED and S-S-SCED.

Under this set of parameter settings, wind curtailment is cheaper than adjusting generators' outputs downwards. Therefore, in this and following case studies, only up reserve capacity is scheduled and presented in the results. The results of S-SCED and S-S-SCED are recorded in Table 3.3. S-S-SCED schedules much less RES power than

S-SCED and thus has much higher first-stage costs, leading to higher total costs than S-SCED. The reason is that the affine assumption on recourse actions of S-S-SCED is far from the optimal case. Taking load shedding as an example, if the first-stage plan of S-S-SCED is fixed to be the same as S-SCED, its decision rule for load shedding will be the dashed curve in Fig. 3.5 when no transmission capacity constraint is binding. However, the optimal load shedding decision shall be the solid curve instead, as load shedding is the most expansive recourse action and should only be carried out when generators cannot provide enough regulation power. Besides load shedding, nonlinearity can also exist in other recourse actions, such as power regulation of generators. When the costs of generators are different, power regulation should be provided by lower cost generators first if possible; whereas under affine assumptions of single-stage models, regulation power is always provided by all generators.

Table 3.2 Generator parameters in IEEE 30-bus system

Bus No.	p_i^l (MW)	p_i^u (MW)	Re_i^+,Re_i^- (MW)	$a_i^{g,1}$ ($/MW^2)	$a_i^{g,2}$ ($/MW)	b_i^{p+}, b_i^{p-} ($/MW)
1	50	100	20	3.75e-3	3	5
2	20	80	16	3.75e-3	3	5
5	15	50	10	3.75e-3	3	5
8	10	35	7	3.75e-3	3	5
11	12	60	10	3.75e-3	3	5
13	20	80	16	3.75e-3	3	5

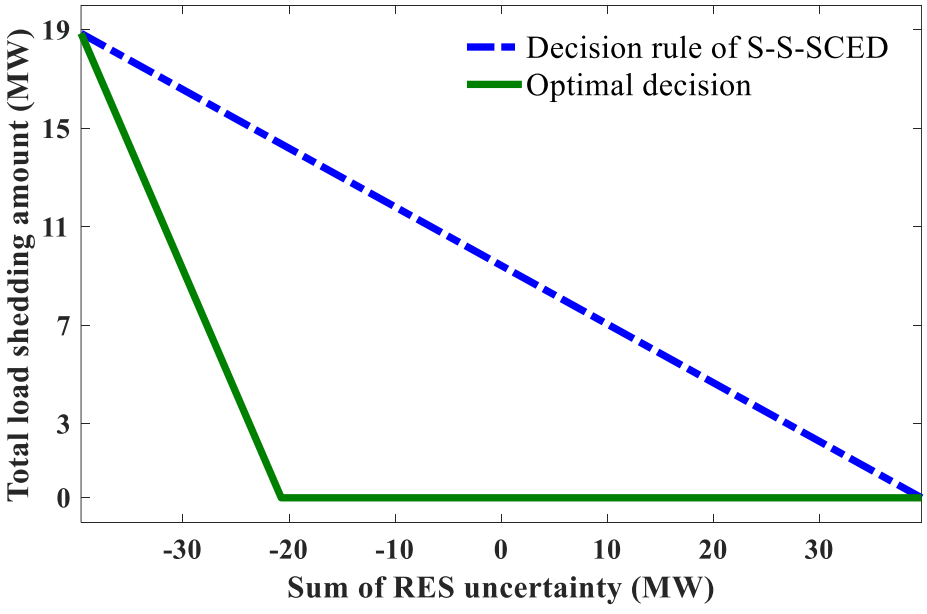

Fig. 3.5 Decision rule of S-S-SCED and the optimal decision on load shedding

The affine assumption on recourse actions leads to much more conservative anticipated costs of recourse actions for S-S-SCED. As a result, here S-S-SCED reduces the amount of scheduled RES power to avoid recourse actions as much as possible. The decision rule of S-SCED for recourse actions cannot be derived explicitly and thus cannot be directly compared with that of S-S-SCED. However, as shown in Table 3.3, S-SCED achieves much better results than S-S-SCED, illustrating that it captures the nonlinearity of recourse actions better.

Table 3.3 Results of S-SCED and S-S-SCED

MODEL	S-SCED	S-S-SCED
SCHEDULED GENERATOR OUTPUTS (MW)	226.0	266.1
SCHEDULED RES OUTPUTS (MW)	120.0	80.0
SCHEDULED RESERVE CAPACITY (MW)	20.7	0.0
FIRST-STAGE COSTS ($)	735.5	842.9
AVERAGE SECOND-STAGE COSTS ($)	29.9	2.0
AVERAGE TOTAL COSTS ($)	765.4	844.8

Though the global optimal solutions of the biconvex sub-problems in S-SCED cannot be guaranteed as explained in Section 3.5.2, it is verified through case studies that the solution quality of S-SCED is better than that of single-stage models and is basically satisfactory.

3.6.3 Further Comparison between S-SCED and O-DRO

In this part, the advantages of S-SCED over O-DRO will be shown from different aspects. Again, 3000 simulated uncertainty realizations are generated by normal distributions in each coming experiment and are used to obtain second-stage decisions from (3.43)-(3.45).

1) Effects of strict constraints on load shedding

Here, O-DRO is compared with S-SCED under different load shedding limits. In all considered circumstances, S-SCED schedules all forecasted RES power, and results of S-SCED are shown in Table 3.4. Reserve capacity scheduled in the first stage increases as the limit becomes stricter. As a result, load shedding is reduced in the second stage with corresponding reduced penalty. As the expense of ensuring system

security, costs of the first stage are increased under stricter shedding limits because of increased reserve capacity, which also leads to higher average total costs of the two stages.

Table 3.4 Results of S-SCED under different load shedding limits

Allowed total load shedding amounts (%)	Scheduled reserve capacity (MW)	First-stage costs ($)	Average load shedding penalty ($)	Average total costs ($)
100	20.74	735.49	2.556	765.4
3	29.22	745.67	0.352	774.0
2.5	30.95	747.75	0.226	776.0
2	32.68	749.82	0.125	778.0
1.5	34.41	751.90	0.054	780.1
1	36.11	753.93	0.021	782.1
0.5	37.87	756.05	0.004	784.2

In contrast with S-SCED, O-DRO does not impose any load shedding limit. It schedules all forecasted RES power and 18.99 MW of reserve capacity. Because of the insufficient reserve capacity scheduled, load shedding limits will be violated in the second stage under O-DRO as shown in Table 3.5. In this study, O-DRO has a probability up to 3.42% in having extra load shedding beyond the limit, which could be unacceptable. Although the load shedding penalty in O-DRO can be increased to reduce load shedding operation in the second stage, it is not clear how much the penalty should be set such that the load shedding limit will not be violated. Therefore, S-SCED is more capable to maintain system security compared with O-DRO.

Table 3.5 Probability of violating load shedding limits

Allowed total load shedding amounts (%)		3	2.5	2	1.5	1	0.5
Probability of violation (%)	S-SCED	0.00	0.00	0.00	0.00	0.00	0.00
	O-DRO	0.58	0.81	1.20	1.78	2.65	3.42

2) Effects of incorporating uncertainty support

RES uncertainty is always bounded with finite supports, because the power output of RES cannot be negative values nor exceed the installed capacity. As compared to O-

DRO, S-SCED would incorporate uncertainty support information. Here, both O-DRO and S-SCED are used to solve ED problems under different load shedding penalty and a summary of their dispatch plans is shown in Table 3.6. Under both models, scheduled reserve capacity increases as the shedding penalty grows, because in such circumstances, possibility of load shedding operation should be reduced accordingly to avoid excessive total costs. However, the reserve capacity gradually stops increasing under S-SCED when the penalty is high enough while it continues to increase under O-DRO. This is because uncertainty support information is absent in O-DRO and the solution becomes over-pessimistic in preventing cases that hardly happen. As a result, under high shedding penalty (75-135), the unnecessary reserve capacity scheduled by O-DRO makes its first-stage costs higher than those of S-SCED as shown in Table 3.7, which also leads to higher average total costs for O-DRO. Therefore, S-SCED can prevent over-conservative solutions compared with O-DRO by incorporating uncertainty support information.

Besides, under high shedding penalty (45-135), S-SCED schedules only part of forecasted RES power while O-DRO schedules all as shown in Table 3.6. This is not the major reason causing differences between the total costs of O-DRO and S-SCED. However, to avoid confusion, the reason of this phenomenon is briefly explained as follows. For S-SCED, its optimal dispatch plan of scheduling part of forecasted RES power can achieve a lower total cost compared with the plan of scheduling all forecasted RES power because of reduced reserve costs in the first stage and reduced recourse costs in the second stage. However, different from S-SCED, O-DRO has no support limitation for uncertainty distribution and thus the worst distribution it considers is more dispersed than that considered by S-SCED. As a result, the benefit of reducing recourse costs in the second stage for O-DRO by taking S-SCED's optimal plan is less than that for S-SCED and scheduling all forecasted RES power is still the optimal plan for O-DRO.

Table 3.6 Summary of dispatch plans of S-SCED and O-DRO under different load shedding penalties

Load shedding penalty ($)		15	45	75	105	135
Scheduled generator outputs (MW)	S-SCED	226.0	228.0	228.5	228.8	228.9
	O-DRO	226.0	226.0	226.0	226.0	226.0
Scheduled RES outputs (MW)	S-SCED	120.0	118.0	117.5	117.2	117.1
	O-DRO	120.0	120.0	120.0	120.0	120.0
Scheduled reserve capacity (MW)	S-SCED	20.74	35.46	36.03	36.17	36.24
	O-DRO	18.99	35.40	46.36	55.20	63.93

Table 3.7 Operation costs of S-SCED and O-DRO under different load shedding penalties

Load shedding penalty ($)		15	45	75	105	135
First-stage costs ($)	S-SCED	735.5	759.6	762.1	763.0	763.5
	O-DRO	733.4	753.1	766.2	776.8	787.3
Average second-stage costs ($)	S-SCED	29.34	22.58	21.29	20.88	20.70
	O-DRO	30.13	27.56	27.35	27.35	27.35
Average total costs ($)	S-SCED	764.8	782.1	783.4	783.9	784.1
	O-DRO	763.5	780.7	793.6	804.2	814.7

3) Effects of considering deviations of uncertainty moments

Here, S-SCED is set with $r_1 = 0.2$ and $r_2 = 0$ to consider possible deviation of uncertainty mean. O-DRO and S-SCED are both used to solve ED problems and the summary of their dispatch plans is recorded in Table 3.8. O-DRO schedules all forecasted RES power, 120.0MW, while S-SCED anticipates possible deviation of uncertainty mean and schedules only 116.0MW. Meanwhile, S-SCED schedules more power outputs from generators and thus has a higher first-stage cost than O-DRO.

An indicator, r_1^*, is used to measure the actual deviation of uncertainty mean. When $r_1^* = 0$, there is no deviation. When $r_1^* = r_1$, uncertainty mean deviates to the boundary of D_1 and has the lowest sum in D_1. Simulated uncertainty realizations are generated by normal distributions according to the actual moments under different r_1^*. Operation costs of S-SCED and O-DRO are presented in Table 3.9. S-SCED has lower second-stage costs than O-DRO because it schedules less RES power and thus needs

less recourse operation in the second stage. When $r_1^* = 0$, S-SCED has slightly higher average total cost than O-DRO. While in other cases recorded in Table 3.9, uncertainty mean deviates to be smaller than the statistical value, so there will be less available RES power on average than anticipated by O-DRO. As a result, O-DRO will have unexpected regulation costs on average in the second stage and thus has higher average total costs than S-SCED. Compared with O-DRO, cost savings of S-SCED, when uncertainty mean deviates to be smaller than the statistical value, are generally higher than its extra cost under no mean deviation. Besides, although the advantages of S-SCED over O-DRO shown here are not that significant, they will be amplified when RES penetration level increases or costs of recourse actions become more expansive. Therefore, it is more reasonable to adopt S-SCED rather than O-DRO. Besides, r_1, r_2 of S-SCED can be adjusted based on historical uncertainty samples.

Table 3.8 Summary of dispatch plans of S-SCED and O-DRO when mean deviations considered

Model	Scheduled generator outputs (MW)	Scheduled RES outputs (MW)	Scheduled reserve capacity (MW)	First-stage costs ($)
S-SCED	230.0	116.0	17.46	744.6
O-DRO	226.0	120.0	18.99	733.4

Table 3.9 Operation costs of S-SCED and O-DRO under different mean deviations

r_1^*		0	0.02	0.04	0.12	0.20
Deviation of average available RES power (MW)		0.00	-1.70	-2.40	-4.16	-5.37
Average second-stage costs ($)	S-SCED	19.75	23.50	25.97	30.70	35.77
	O-DRO	30.06	36.05	39.21	44.99	51.52
Average total costs ($)	S-SCED	764.3	768.1	770.5	775.3	780.3
	O-DRO	763.5	769.4	772.6	778.4	784.9

3.6.4 Incorporation of Load Uncertainty

As mentioned in Section 3.4.3, load uncertainty can also be incorporated into the model exactly like RES uncertainty. Here, the effects of incorporating load uncertainty are discussed. Loads at Bus 2, 5, 7, 8, 21 and 30 contribute to 70% of the total load and they are assumed to be with uncertainty in this study. Results of comparison between models with and without load uncertainty are presented in Table 3.10. Load uncertainty makes the ED problem more unpredictable, thus more reserve capacity is scheduled, and the operation costs increase as well.

Table 3.10 Effects of incorporating load uncertainties

With load uncertainty	Scheduled reserve capacity (MW)	First-stage costs ($)	Average second-stage costs ($)	Average total costs ($)
No	20.74	735.5	30.32	765.8
Yes	25.35	741.0	41.46	782.5

Correlation between uncertainty can be considered by the model through the covariance matrix. Effects of load uncertainty's correlation are also studied here. Load at Bus 5 is the largest and makes up of 31.5% of the total load. To simulate circumstances of different uncertainty correlation, a covariance matrix Δ is generated by assuming that uncertainties of loads at Bus 2, 7, 8, 21 and 30 are of 0.2, 0.2, 0.25, 0.15, and 0.2 times of the uncertainty of the load at Bus 5 respectively, and Δ_α with different α are generated by multiplying the covariance terms in Δ between uncertainty of the load at Bus 5 and other load uncertainties by α. Δ_α is adopted as the covariance matrix of load uncertainty in the ED problem. Under positive and negative α, uncertainty of load at Bus 5 has positive and negative correlation respectively with other load uncertainties. The correlation is stronger with larger absolute value of α. Results of ED problems under Δ_α with different α are shown in Fig. 3.6. Under stronger negative correlation, load uncertainties tend to offset each other better, thus less reserve capacity is scheduled and the operation cost decreases.

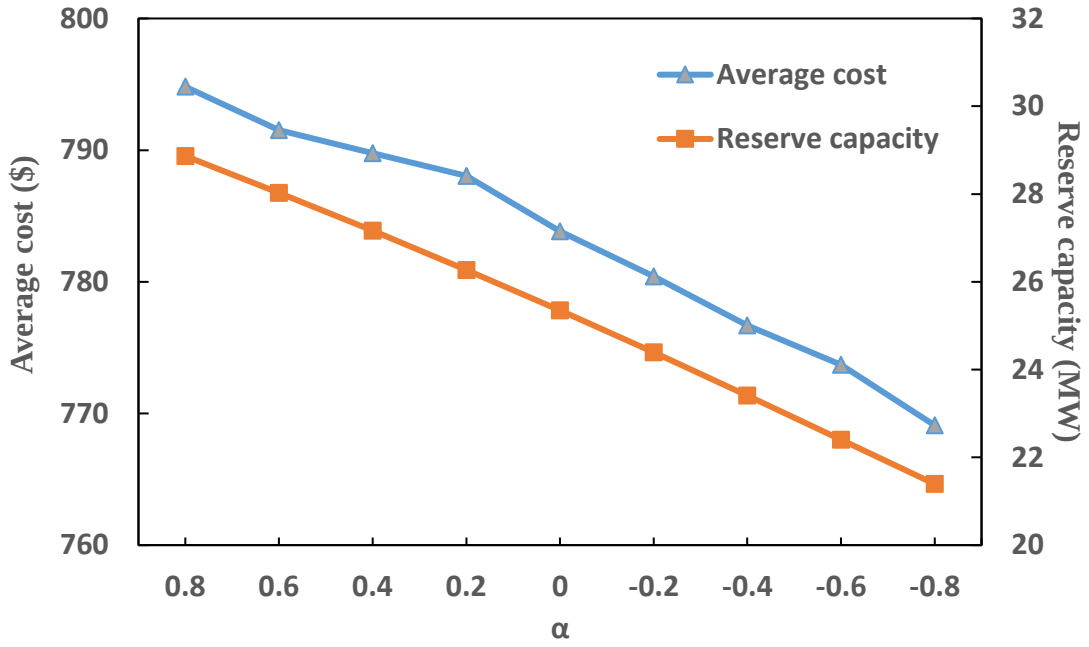

Fig. 3.6 Effects of the correlation between load uncertainties

3.6.5 Necessity of Multi-period Modeling

Here, M-SCED is compared with O-DRO to illustrate the necessity of multi-period modeling for ED problems. M-SCED can incorporate any reasonable number of time periods. Here, for simplicity, T is set to three. Duration of each period is set to one hour. Generator 5 is set to be more expansive than Generator 1-4, and Generator 6 is set to be more expansive than Generator 5. Cost difference between Generator 6 and Generator 5 is more significant than that between Generator 5 and Generator 1-4. Up and down ramping limits of all generators, Ra_i^+ and Ra_i^-, are set to two times of their up and down reserve capacity limits, respectively. Power forecasts of all RES in all periods are set as 30 MW. Total loads in the system are set as 318.4, 380.4, 380.4 MW from Period 1 to 3. In rolling-plan operation, with ramping constraints coupled with the previous period, M-SCED is updated in each period and O-DRO is adopted repeatedly for each period respectively to obtain ED operation plans. 1000 simulated uncertainty realizations are generated by normal distributions to evaluate the performance of M-SCED and O-DRO in multi-period ED operation.

Because Generator 6 is the most expensive, power generation should be preferentially scheduled to other generators if possible. As shown in Fig. 3.7, without anticipating future circumstances, O-DRO schedules Generator 5 and 6 at their minimum generation in Period 1. In Period 2 and 3, to meet the increased load, Generator 1-4 increase their power outputs to their maximum capacities, Generator 5 increases its power output and reserve capacity by reaching its up ramping limit, and the most expensive Generator 6 needs to increase its power output as well. In contrast, under M-SCED, because the load increase is anticipated, Generator 5 is scheduled with higher generation in Period 1 and thus it can provide enough power in Period 2 and 3, avoiding power output increase from expensive Generator 6.

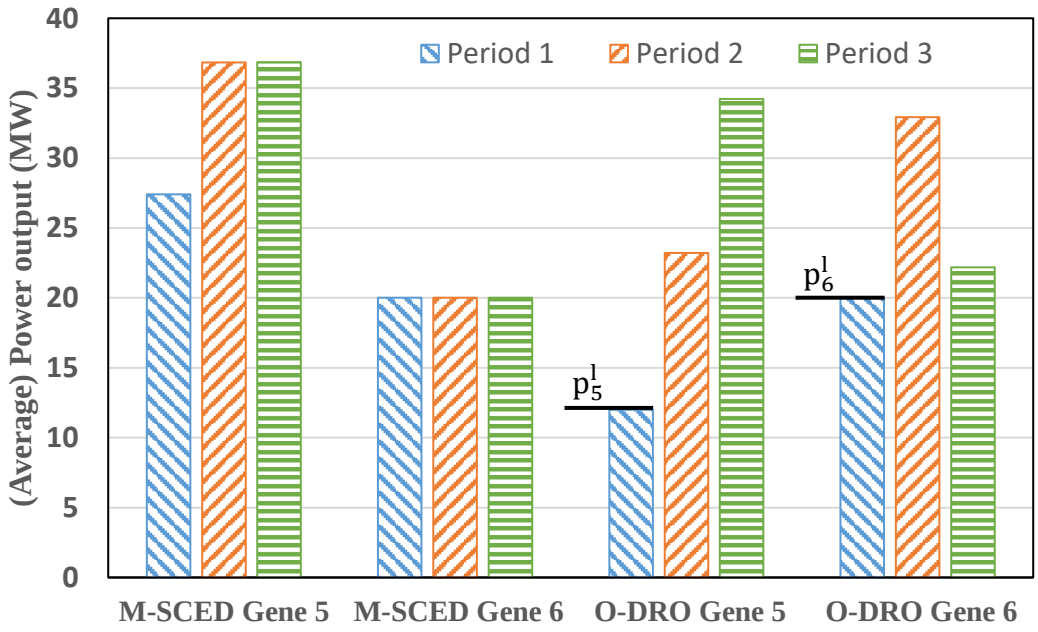

Fig. 3.7 Power outputs of Generator 5 and 6 under different models

As shown in Table 3.11, M-SCED has higher cost in Period 1 but lower costs in following periods than O-DRO, matching the results in Fig. 3.7. The total cost of M-SCED is lower as well. This is because M-SCED has an overall consideration over the entire operation horizon and sacrifices short-term benefit to pursue long-term profit. In contrast, O-DRO is shortsighted in considering only the current period. In more severe situations such as when the total load in Period 2 is 410 MW, O-DRO will even meet infeasible operation situations, leading to more serious consequences, while M-SCED

will not. Besides, as stated earlier, O-DRO cannot be directly extended to be multi-period because of the complicated consistency requirement of time sequences. While according to Table 3.11, M-SCED achieves effective multi-period modeling without causing excessive computational burden.

Table 3.11 Computation times of M-SCED and O-DRO and their operation costs of multi-period ED

	Computation times (s)	Average costs in Period 1 ($)	Average costs in Period 2 ($)	Average costs in Period 3 ($)	Average total costs ($)
M-SCED	36.71	977.8	1204.9	1203.1	3385.8
O-DRO	18.72	967.9	1242.3	1208.7	3418.9

3.7 Summary

In this chapter, a multi-period economic dispatch model M-SCED is established to accommodate uncertainty from renewable energy, in which a two-stage formulation is adopted to effectively model recourse actions with respect to uncertainty realizations. Compared with traditional robust optimization based economic dispatch, M-SCED greatly reduces average operation costs through application of DRO. Compared with the previous work based on DRO, M-SCED avoids over-conservative solutions and prevents inferior performance under inaccurate uncertainty information through more realistic modeling of uncertainty as well as enhances system security by limiting load shedding in recourse actions. In addition, the efficient multi-period modeling guarantees economical and secure long-term economic dispatch operation without causing excessive computational burden.

Chapter IV

A Model to Mitigate Forecast Uncertainties in Balance Responsible Distribution Systems Using the Flexibility of EVAs

4.1 Introduction

In power systems, energy supplies and demands need to be balanced all the time. To maintain the balance under forecast uncertainties, reserve needs to be prepared, which is traditionally achieved by using generators and hydropower stations [63, 64]. As EVs become common, they can also participate in energy balancing through regulation markets in some deregulated power systems [107, 108]. While for power systems without regulation markets, other mechanisms to make use of EVs need to be designed. As EVs are connected to distribution systems, one possible alternative is to let each distribution system mitigate its forecast uncertainties [78, 109]. Then, each distribution system becomes a BRDS and can be penalized if its actual energy consumption fails to match the plan [22]. With each BRDS mitigating its own uncertainties, the transmission system operator needs to prepare less reserve.

If BRDS directly dispatches each EV, the arrival times, departure times, SOC at arrival and target SOC at departure of all EVs need to be taken into consideration. However, considering these uncertain parameters will be very cumbersome when a large number of EVs are involved. Instead, it is more reasonable for system operators to dispatch EVAs and let EVAs control EVs. [110, 111] adopt such schemes, but their models are not designed for BRDS and do not use EVAs to mitigate uncertainties.

By making use of the flexibility of EVs, EVAs possess flexibilities in accepting disturbance to their charging. The disturbance to EVAs is called over-charging if they receive more energy than their needs and is called charging deficiency if they receive

less energy than their needs. Besides, EVAs also have forecast uncertainties in their charging demands as a result of unpredictable behaviors of EVs. Because of the large volume of charging demands of EVAs in the future, their potential deviations from forecast can be considerable although they have relatively predictable patterns. But by using the flexibility of EVAs, their charging rates can be kept as scheduled at the cost of their over-charging or charging deficiency depending on the signs of their uncertainty realizations, which means that their uncertainties can be eliminated by themselves.

In consideration of the features of EVAs, a tailored model is established to use the flexibility of EVAs to mitigate forecast uncertainties in BRDSs. Charging demands of EVAs are required to be fulfilled at the end of the day in order to guarantee driving activities of EVs in the next day. As a result, over-charging and charging deficiency of EVAs incurred from mitigating uncertainties should be recovered later in the day. So, contributions of EVAs in mitigating uncertainties are actually delaying uncertainties, and thus the deviation of the energy consumption of BRDS from the plan in an hour depends on uncertainties from different hours, which may offset each other. In the established model, DRO is adopted to optimize the average performance of the operation plans. Because movements of EVs possess distinct spatial-temporal features [112], uncertainties in charging demands of EVAs may have prominent temporal and spatial correlations. Therefore, the ambiguity set under DRO is constructed with the statistical expectation and covariance matrix of uncertainties.

Components of distribution systems can have intertemporal constraints, such as those on ramping rates of DGs, SOC of ES and accumulated disturbance to the charging of EVAs. With these constraints, earlier decisions influence later operation. Therefore, it is necessary to properly take real-time recourse operation into consideration when making day-ahead operation decisions. Otherwise, inferior results could be incurred. For example, reserve capacities are scheduled from DGs and ES to tackle uncertainties in energy supplies without considering the real-time operation in [78]. As a consequence, DGs and ES are poorly coordinated. Different from [78], [80] considers

real-time operation in advance through a two-stage framework. But the second stage of the framework assumes that real-time decisions at all times are made simultaneously knowing realizations of uncertainties at all times, which neglects the fact that earlier decisions are made without knowing realizations of later uncertainties. As a result, operational infeasibility may be encountered. To consider real-time operation without violating temporal sequences of uncertainty realizations, LDR is adopted here, which assumes that real-time decisions are affine functions of realizations of earlier uncertainties. Details about LDR will be given in Section 4.4.2.

Charging rates of EVAs can be kept as scheduled by using their flexibility, which is equivalent to having each EVA mitigate its own uncertainties. Then, charging of different EVAs is disturbed independently. Without any influence on the total energy consumption of BRDS, a scheme of uncertainty transferring is proposed based on LDR. Under this scheme, EVAs can transfer their uncertainties to each other. In other words, an EVA can mitigate uncertainties of other EVAs. As a result, disturbance to the charging of an EVA depends on uncertainties of different EVAs and may be relieved because uncertainties of different EVAs may offset each other. This scheme also has other potential benefits, which will be further discussed in Section 4.4.2.

4.2 Nomenclature

Sets, decision variables and uncertainties are printed in italics while others are in non-italics. Decision variables depending on uncertainty realizations are marked with tildes.

4.2.1 Sets

$\mathcal{N}$	Set of all nodes in BRDS
$\mathcal{N}_{\mathrm{AVR}}$	Set of nodes that automatic voltage regulators (AVRs) are connected to
$\mathcal{N}_{\mathrm{EVA}}$	Set of nodes that EVAs are connected to
$a(i)$	Parent node of node i

$\mathcal{B}(i)$	Set of child nodes of node i

4.2.2 Parameters

Δt	An hour
T	Number of hours in a day
$c_i^{r,over}$, $c_i^{r,def}$	Price of reserve capacity for over-charging, charging deficiency of the EVA at node i
$c_i^{in,over}$, $c_i^{in,def}$	Regular compensation rate to the EVA at node i for over-charging, charging deficiency
$c_i^{out,over}$,$c_i^{out,def}$	Punitive compensation rate to the EVA at node i for over-charging, charging deficiency
$c^{pen,+}$, $c^{pen,-}$	Penalty coefficient for positive, negative deviations of BRDS' energy consumptions
v_0	Base voltage
$R_{i,j}$, $X_{i,j}$	Resistance, reactance of the feeder between node i and j
$p_{t,i}^d$, $q_{t,i}^d$	Active, reactive load at node i in hour t
$e_{t,i}^{EVA,p}$	Planned charging demand of the EVA at node i in hour t
β_i	Power factor of the EVA at node i
$e_{t,i}^{cap,over}$,$e_{t,i}^{cap,def}$	Dispatchable range for over-charging, charging deficiency of the EVA at node i in hour t
$q_i^{AVR,cap}$	Capacity of the AVR at node i

4.2.3 Uncertainties

$\xi_{t,i}$	Uncertain deviation of the charging demand of the EVA at node i in hour t from the plan
$\boldsymbol{\xi}$	Vector of $\xi_{t,i}$ for all EVAs and all hours
N_{ξ}	Dimension of $\boldsymbol{\xi}$
$\boldsymbol{\mu}$	Statistical mean of $\boldsymbol{\xi}$
$\boldsymbol{\Sigma}$	Statistical covariance matrix of $\boldsymbol{\xi}$

f_{ξ}	Distribution of $\boldsymbol{\xi}$
D	Family of distributions that satisfy the statistical mean and covariance matrix of $\boldsymbol{\xi}$

4.2.4 Decision Variables

e_t^{p}	Planned energy consumption of BRDS in hour t
$r_{t,i}^{\mathrm{over}}$, $r_{t,i}^{\mathrm{def}}$	Reserve purchased from the EVA at node i for over-charging, charging deficiency in hour t
$\tilde{p}_{t,i}^{\mathrm{EVA}}$, $\tilde{q}_{t,i}^{\mathrm{EVA}}$	Active and reactive charging power of the EVA at node i in hour t
$\tilde{e}_{t,i}^{\mathrm{EVA,dis}}$	Accumulated disturbance to the charging of the EVA at node i in hour t
$\tilde{q}_{t,i}^{\mathrm{AVR}}$	Reactive power output of the AVR at node i in hour t
$\tilde{p}_{t,i,j}^{\mathrm{fl}}$, $\tilde{q}_{t,i,j}^{\mathrm{fl}}$	Active, reactive power flow from node i to node j in hour t
$\tilde{p}_t^{\mathrm{in}}$, $\tilde{q}_t^{\mathrm{in}}$	Active, reactive power input from the main grid in hour t
$\tilde{v}_{t,i}$	Voltage of node i in hour t
$\alpha_{\hat{t},j}^{t,i}$	Proportion of the uncertainty of the EVA at node i in hour t allocated to the EVA at node j in hour $\hat{t}$

4.3 Settings on BRDS Operation

It is assumed that energy consumptions of BRDS at different hours in a day should be planned in advance. Similar to [75, 113], penalties are assumed to be applied on deviations of BRDS' energy consumptions from the plan. In terms of dispatching EVAs, BRDS is assumed to purchase reserves from EVAs ahead of time. During the operation, the disturbance to the charging of EVAs within the purchased reserves is compensated by BRDS at regular rates and the other beyond the purchased reserves is compensated at punitive rates, which are higher than regular rates.

The interaction mechanism between BRDS and EVAs is as follows. First, EVAs plan their charging demands by collecting information from EV owners. Based on

energy requirements of EVs, revenue from BRDS and potential compensations to EVs, EVAs decide their dispatchable ranges for BRDS. Planned charging demands and dispatchable ranges of EVAs are reported to BRDS. After that, BRDS decides its energy consumption plans and its dispatching plans for EVAs and purchases reserves from EVAs. Knowing the reserves purchased by BRDS, EVAs can make plans on controlling EVs. At last, as uncertainties realize in real-time operation, BRDS gives dispatch to EVAs within their dispatchable ranges, and EVAs control EVs to follow the dispatch of BRDS. It should be noted that the dispatch of BRDS on EVAs should respect the dispatchable ranges reported by EVAs and constraints of the distribution system.

The EVAs studied here can be operators of EV parking lots or providers of smart-charging service to EVs at home. They can also be affiliated departments of BRDS. In the latter case, it is equivalent to simplifying BRDS operation by adopting hierarchical dispatching schemes. This chapter focuses on BRDS operation under the above interaction mechanism between BRDS and EVAs. Operation models of EVAs and the interaction mechanism between EVAs and EVs are beyond the scope of the study here.

4.4 Model Formulation and Transformation

In this section, the formulation of the proposed model will be given first. LDR and the uncertainty transferring scheme are then discussed. At last, the proposed model is transformed into a deterministic second-order conic program.

4.4.1 Formulation of The Proposed Model

The proposed model optimizes BRDS operation by balancing costs of dispatching EVAs and penalties for deviations of BRDS' energy consumptions from the plan while guaranteeing the system security. Its formulation is given in (4.1)-(4.19). The first item in the objective (4.1) is the cost of purchasing reserves from EVAs. The second term is the worst expected sum of compensations to EVAs and penalties for energy deviations

of BRDS over all considered uncertainty distributions. (4.2) and (4.3) are penalties when deviations of the energy consumptions of BRDS from planned values are positive and negative, respectively. (4.4) and (4.5) are compensations to EVAs when charging deficiency of EVAs is within and beyond purchased reserves, respectively. (4.6) and (4.7) are compensations to EVAs when the over-charging of EVAs is within and beyond purchased reserves, respectively. (4.8) and (4.9) indicate the active and reactive power imported from the transmission system, respectively. The node connecting the transmission system is numbered as 0. (4.10) and (4.11) ensure active and reactive power balance, respectively. AVRs are installed at certain nodes to supply reactive power in order to maintain voltage profiles. (4.12) describes the relationship between the voltage of adjacent nodes. (4.13) prevents voltage profiles from exceeding the lower and upper bound. (4.14) limits the output of AVRs. (4.15) ensures the charging power of EVAs to be non-negative. (4.16) is the relationship between the active and reactive charging power of EVAs. (4.17) describes the disturbance to the charging of EVAs. Positive values indicate charging deficiency and negative values indicate over-charging. (4.18) avoids the dispatchable ranges of EVAs from being violated. (4.19) requires that charging demands of EVAs are fulfilled at the end of the day to guarantee driving activities of EVs in the next day.

$$\inf \sum_{t=1,\dots,\mathrm{T}} \sum_{i\in\mathcal{N}_{\mathrm{EVA}}} \left(\mathrm{c}_i^{\mathrm{r,def}} \cdot r_{t,i}^{\mathrm{def}} + \mathrm{c}_i^{\mathrm{r,over}} \cdot r_{t,i}^{\mathrm{over}}\right) + \sup_{f_\xi \in \mathrm{D}} \mathrm{E}\left[\sum_{t=1,\dots,\mathrm{T}} \max_{k=1,2} f_k\left(\tilde{p}_t^{\mathrm{in}}\right) + \sum_{t=1,\dots,\mathrm{T}} \sum_{i\in\mathcal{N}_{\mathrm{EVA}}} \max_{k=1,2,3,4} g_k\left(\tilde{e}_{t,i}^{\mathrm{EVA,dis}}\right)\right] \quad (4.1)$$

$$\text{s.t. } f_1\left(\tilde{p}_t^{\mathrm{in}}\right) = \mathrm{c}^{\mathrm{pen},+} \cdot \left(\tilde{p}_t^{\mathrm{in}} \cdot \Delta\mathrm{t} - e_t^{\mathrm{p}}\right) \quad (4.2)$$

$$f_2\left(\tilde{p}_t^{\mathrm{in}}\right) = \mathrm{c}^{\mathrm{pen},-} \cdot \left(e_t^{\mathrm{p}} - \tilde{p}_t^{\mathrm{in}} \cdot \Delta\mathrm{t}\right) \quad (4.3)$$

$$g_1\left(\tilde{e}_{t,i}^{\mathrm{EVA,dis}}\right) = \mathrm{c}_i^{\mathrm{in,def}} \cdot \tilde{e}_{t,i}^{\mathrm{EVA,dis}} \quad (4.4)$$

$$g_2\left(\tilde{e}_{t,i}^{\mathrm{EVA,dis}}\right) = \mathrm{c}_i^{\mathrm{out,def}} \cdot \left(\tilde{e}_{t,i}^{\mathrm{EVA,dis}} - r_{t,i}^{\mathrm{def}}\right) + \mathrm{c}_i^{\mathrm{in,def}} \cdot r_{t,i}^{\mathrm{def}} \quad (4.5)$$

$$g_3\left(\tilde{e}_{t,i}^{\mathrm{EVA,dis}}\right) = -\mathrm{c}_i^{\mathrm{in,over}} \cdot \tilde{e}_{t,i}^{\mathrm{EVA,dis}} \quad (4.6)$$

$$g_4\left(\tilde{e}_{t,i}^{\mathrm{EVA,dis}}\right) = \mathrm{c}_i^{\mathrm{out,over}} \cdot \left(-\tilde{e}_{t,i}^{\mathrm{EVA,dis}} - r_{t,i}^{\mathrm{over}}\right) + \mathrm{c}_i^{\mathrm{in,over}} \cdot r_{t,i}^{\mathrm{over}} \tag{4.7}$$

$$\tilde{p}_t^{\mathrm{in}} = \sum_{i \in \mathcal{B}(0)} \tilde{p}_{t,0,i}^{\mathrm{fl}}, \forall \boldsymbol{\xi}, \forall t \tag{4.8}$$

$$\tilde{q}_t^{\mathrm{in}} = \sum_{i \in \mathcal{B}(0)} \tilde{q}_{t,0,i}^{\mathrm{fl}}, \forall \boldsymbol{\xi}, \forall t \tag{4.9}$$

$$\tilde{p}_{t,a(i),i}^{\mathrm{fl}} = \mathrm{p}_{t,i}^{\mathrm{d}} + \tilde{p}_{t,i}^{\mathrm{EVA}} + \sum_{j \in \mathcal{B}(i)} \tilde{p}_{t,i,j}^{\mathrm{fl}}, \forall \boldsymbol{\xi}, \forall i \in \mathcal{N}/\{0\}, \forall t \tag{4.10}$$

$$\tilde{q}_{t,a(i),i}^{\mathrm{fl}} = \mathrm{q}_{t,i}^{\mathrm{d}} + \tilde{q}_{t,i}^{\mathrm{EVA}} - \tilde{q}_{t,i}^{\mathrm{AVR}} + \sum_{j \in \mathcal{B}(i)} \tilde{q}_{t,i,j}^{\mathrm{fl}}, \forall \boldsymbol{\xi}, \forall i \in \mathcal{N}/\{0\}, \forall t \tag{4.11}$$

$$\tilde{v}_{t,a(i)} - \left(\mathrm{R}_{a(i),i} \cdot \tilde{p}_{t,a(i),i}^{\mathrm{fl}} + \mathrm{X}_{a(i),i} \cdot \tilde{q}_{t,a(i),i}^{\mathrm{fl}}\right)/\mathrm{v}_0 = \tilde{v}_{t,i}, \quad \forall \boldsymbol{\xi}, \forall i \in \mathcal{N}/\{0\}, \forall t \tag{4.12}$$

$$0.95 \cdot \mathrm{v}_0 \leq \tilde{v}_{t,i} \leq 1.05 \cdot \mathrm{v}_0 \ \ \forall \boldsymbol{\xi}, \forall i \in \mathcal{N}, \forall t \tag{4.13}$$

$$0 \leq \tilde{q}_{t,i}^{\mathrm{AVR}} \leq \mathrm{q}_i^{\mathrm{AVR,cap}} \ \ \forall \boldsymbol{\xi}, \forall i \in \mathcal{N}_{\mathrm{AVR}}, \forall t \tag{4.14}$$

$$\tilde{p}_{t,i}^{\mathrm{EVA}} \geq 0 \ \ \forall \boldsymbol{\xi}, \forall i \in \mathcal{N}_{\mathrm{EVA}}, \forall t \tag{4.15}$$

$$\beta_i \cdot \tilde{q}_{t,i}^{\mathrm{EVA}} = \sqrt{1 - {\beta_i}^2} \cdot \tilde{p}_{t,i}^{\mathrm{EVA}}, \forall \boldsymbol{\xi}, \forall i \in \mathcal{N}_{\mathrm{EVA}}, \forall t \tag{4.16}$$

$$\tilde{e}_{t,i}^{\mathrm{EVA,dis}} = \sum_{\hat{t}=1,\ldots,t} \left(\mathrm{e}_{\hat{t},i}^{\mathrm{EVA,p}} + \xi_{\hat{t},i}\right) - \sum_{\hat{t}=1,\ldots,t} \Delta\mathrm{t} \cdot \tilde{p}_{\hat{t},i}^{\mathrm{EVA}}, \forall \boldsymbol{\xi}, \forall i \in \mathcal{N}_{\mathrm{EVA}}, \forall t \tag{4.17}$$

$$-\mathrm{e}_{t,i}^{\mathrm{cap,over}} \leq \tilde{e}_{t,i}^{\mathrm{EVA,dis}} \leq \mathrm{e}_{t,i}^{\mathrm{cap,def}} \ \ \forall \boldsymbol{\xi}, \forall i \in \mathcal{N}_{\mathrm{EVA}}, \forall t \tag{4.18}$$

$$\sum_{t=1,\ldots,\mathrm{T}} \tilde{p}_{t,i}^{\mathrm{EVA}} \cdot \Delta\mathrm{t} = \sum_{t=1,\ldots,\mathrm{T}} \left(\mathrm{e}_{t,i}^{\mathrm{EVA,p}} + \xi_{t,i}\right) \ \forall \boldsymbol{\xi}, \forall i \in \mathcal{N}_{\mathrm{EVA}} \tag{4.19}$$

4.4.2 LDR Approximation and The Uncertainty Transferring Scheme

In (4.1)-(4.19), optimal values of variables with tildes are influenced by realizations of uncertainties. As uncertainty realizations cannot be foreseen, uncertainty-affected variables are decided only with information about earlier realized uncertainties but not future ones. Because there are many time periods in (4.1)-(4.19) and the relationship between the optimal values of variables and realizations of earlier uncertainties can be very complicated [95, 96], problem (4.1)-(4.19) is difficult to solve, and thus proper approximations are needed. In this respect, LDR is widely used to approximate multi-

period problems with uncertainties [95-98]. With LDR, instead of considering the actual relationship between the optimal values of variables and realizations of earlier uncertainties, affine relationships are assumed to hold in order to reduce the complexity. This is equivalent to allocating uncertainties to different hours in advance through determining the uncertainty coefficients of LDR. Under LDR, the charging power of EVAs will be as (4.20) if each EVA mitigates its own uncertainties. It should be noted that uncertainties can only be allocated to later hours but not earlier ones as uncertainty realizations cannot be foreseen. Besides, uncertainties in an hour can be allocated to more than one later hour.

$$\tilde{p}_{t,i}^{\mathrm{EVA}} = p_{t,i}^{\mathrm{EVA,con}} + \sum_{\hat{t}=1,\dots,t} \alpha_{t,i}^{\hat{t},i} \cdot \xi_{\hat{t},i}\,, \forall i \in \mathcal{N}_{\mathrm{EVA}}, \forall t \tag{4.20}$$

As discussed in Section 4.1, without influencing total energy consumptions of BRDS, EVAs can transfer their uncertainties to each other. Then, the charging power of EVAs will be as (4.21) and disturbance to the charging of an EVA depends on uncertainties of different EVAs. Because uncertainties of different EVAs may offset each other, disturbance to the charging of EVAs may be relieved. Apart from this, the uncertainty transferring scheme has other potential benefits as well. First, uncertainties of EVAs that are more expensive to dispatch can be transferred to cheaper EVAs, which is equivalent to having uncertainties of expensive EVAs mitigated by cheaper EVAs. So, BRDS needs to pay less to EVAs in total. Furthermore, it is possible that when one EVA reaches its dispatchable ranges, the others do not. With the proposed uncertainty transferring scheme, uncertainties of this EVA can be transferred to other EVAs to better utilize their spare dispatchable capacities and thus potential deviations of BRDS' energy consumptions from the plan may further decrease.

$$\tilde{p}_{t,i}^{\mathrm{EVA}} = p_{t,i}^{\mathrm{EVA,con}} + \sum_{j \in \mathcal{N}_{\mathrm{EVA}}} \sum_{\hat{t}=1,\dots,t} \alpha_{t,i}^{\hat{t},j} \cdot \xi_{\hat{t},j}\,, \forall i \in \mathcal{N}_{\mathrm{EVA}}, \forall t \tag{4.21}$$

To further illustrate the idea of allocating uncertainties to different hours and different EVAs in advance, the implication of (4.19) on the uncertainty coefficients of LDR for the charging power of EVAs is discussed here. According to (4.19), the total

energy that any EVA is charged with at the end of the day should be the sum of its uncertainties and planned demands. Therefore, for any uncertainty of any EVA, its allocation (LDR) coefficients to its EVA at all hours should sum to one, leading to (4.22). Also, (4.19) implies that the energy that any EVA is charged with at the end of the day should not be influenced by uncertainties of other EVAs. So, for any uncertainty of any EVA, its allocation (LDR) coefficients to any other EVA at all hours should sum to zero, which results in (4.23).

$$\sum_{\hat{t}=t,\dots,\mathrm{T}} \alpha_{\hat{t},i}^{t,i} = 1, \forall i \in \mathcal{N}_{\mathrm{EVA}}, \forall t \tag{4.22}$$

$$\sum_{\hat{t}=t,\dots,\mathrm{T}} \alpha_{\hat{t},j}^{t,i} = 0, \forall j \in \mathcal{N}_{\mathrm{EVA}}/\{i\}, \forall i \in \mathcal{N}_{\mathrm{EVA}}, \forall t \tag{4.23}$$

Similar to the charging power of EVAs, all other uncertainty-affected variables are also assumed to be affine functions of earlier uncertainty realizations under LDR. Then, different time periods in (4.1)-(4.19) can be regarded as being squeezed together and (4.1)-(4.19) becomes a mathematically single-period problem, which is easier to handle. Coefficients of these affine functions are determined at the beginning of the day. When uncertainties realize, real-time decisions can be made according to these affine functions. Instead of making adjustments when new information is available as done in online models for multi-period problems, the coefficients of the affine functions are fixed during the day under the proposed model because the reserves that BRDS purchased from EVAs have been fixed at the beginning of the day.

4.4.3 Deterministic Transformation of The Proposed Model

To solve problem (4.1)-(4.19), it still needs to be transformed into deterministic forms. (4.13)-(4.15) and (4.18) are linear inequality constraints involving uncertainties, and can be replaced by their deterministic counterparts through robust optimization because uncertainty realizations are assumed here to lie in proper polyhedral sets [54, 114]. Linear equality constraints involving uncertainties in (4.1)-(4.19) can be written in compact forms as (4.24), where $\boldsymbol{h}'$ is the transpose of $\boldsymbol{h}$. To ensure these constraints

are satisfied with respect to all considered uncertainty realizations, the additive coefficient for each uncertainty in each constraint needs to be zero, meaning that $\boldsymbol{h} = \mathbf{0}$ needs to hold. After removing the uncertainty-related terms, the original equality constraints in (4.1)-(4.19) become $g = 0$, which is deterministic.

$$\boldsymbol{h}'\boldsymbol{\xi} + g = 0 \tag{4.24}$$

To handle uncertainties in the objective, DRO is adopted. DRO's ambiguity set for uncertainty distribution can be constructed with different information. For example, uncertainty expectations and variances are used in [62], and [61] uses expectations, mean absolute deviations and standard deviations. As discussed in Section 4.1, uncertainties from different hours may offset each other when EVAs are used to mitigate uncertainties, whose possibility depends on uncertainty correlation. Therefore, the ambiguity set is constructed based on uncertainty expectations and covariance matrix as shown in (4.25) and represented as D. The worst expectation of a specific family of piecewise-linear utility functions over all possible distributions in D can be transformed into deterministic forms as (4.26)-(4.29), where w_1, w_2, w_3 and w_4 are slack variables [115]. However, there are summations of piecewise-linear functions within the expectation operator in the objective (4.1), impeding the direct application of (4.26)-(4.29). To overcome this difficulty, the objective (4.1) is approximated by (4.30), where the original worst expectation is replaced by its upper bound. The conservatism of such approximation is shown to be acceptable in [116]. After substituting worst expectations in the approximated objective (4.30) by (4.26)-(4.29), the proposed model becomes a deterministic second-order conic program and can be solved by off-the-shelf solvers.

At the same time of depicting uncertainty distributions by the statistical expectation and covariance matrix, DRO can also bound the range of uncertainty realizations by ellipsoidal sets as in [64]. With such DRO technique, the conservatism level of the proposed model can be adjusted by varying the sizes of the ellipsoidal sets, but also, semidefinite programs will be resulted, which are challenging and time-consuming to

solve. To avoid heavy computational burden, the DRO technique from [115] rather than that from [64] is adopted.

$$\mathrm{D} = \left\{ f_{\boldsymbol{\xi}} \middle| \begin{array}{l} \Pr\left(\boldsymbol{\xi} \in \mathbb{R}^{\mathrm{N}_{\xi}}\right) = 1 \\ \mathrm{E}[\boldsymbol{\xi}] = \boldsymbol{\mu} \\ \mathrm{E}[(\boldsymbol{\xi} - \boldsymbol{\mu}) \cdot (\boldsymbol{\xi} - \boldsymbol{\mu})'] = \boldsymbol{\Sigma} \end{array} \right\} \tag{4.25}$$

$$\begin{aligned} &\sup_{f_{\xi} \in \mathrm{D}} \mathrm{E}\left[\max_{k=1,\ldots,\mathrm{K}} \{m_k(y_0 + \boldsymbol{y}'\boldsymbol{\xi}) + n_k\}\right] \\ &= \inf \ w_4 - w_3 && (4.26) \\ &\quad \text{s.t. } w_3 \leq -m_k(y_0 + \boldsymbol{y}'\boldsymbol{\mu}) - n_k - {m_k}^2 w_1 - m_k w_2, \forall k && (4.27) \\ &\qquad w_1 + w_4 \geq \sqrt{\boldsymbol{y}'\boldsymbol{\Sigma}\boldsymbol{y} + {w_2}^2 + (w_1 - w_4)^2} && (4.28) \\ &\qquad w_1 \geq 0 && (4.29) \end{aligned}$$

$$\begin{aligned} \sum_{t=1,\ldots,\mathrm{T}} \sum_{i \in \mathcal{N}_{\mathrm{EVA}}} \left(\mathrm{c}_i^{\mathrm{r,def}} \cdot r_{t,i}^{\mathrm{def}} + \mathrm{c}_i^{\mathrm{r,over}} \cdot r_{t,i}^{\mathrm{over}}\right) + \sum_{t=1,\ldots,\mathrm{T}} \sup_{f_{\xi} \in \mathrm{D}} \mathrm{E}\left[\max_{k=1,2} f_k\left(\tilde{p}_t^{\mathrm{in}}\right)\right] \\ + \sum_{t=1,\ldots,\mathrm{T}} \sum_{i \in \mathcal{N}_{\mathrm{EVA}}} \sup_{f_{\xi} \in \mathrm{D}} \mathrm{E}\left[\max_{k=1,2,3,4} g_k\left(\tilde{e}_{t,i}^{\mathrm{EVA,dis}}\right)\right] \end{aligned} \tag{4.30}$$

4.5 Simulation of the Charging Demands of EVAs

As charging demands of EVAs are greatly influenced by the travel of EVs, a travel survey in Atlanta [117] with 119480 trip records is used to simulate the daily operation of EVs, which is used to simulate charging demands of EVAs. Instead of accurate and complex analysis, simple settings are adopted because the charging demands simulated here are only used to validate the effectiveness of the proposed model. In real operation, real data will be used.

The simulation here focuses on charging at home by assuming that the simulated EVAs are in residential areas. From the 119480 trip records of the survey, 26617 home-to-home (h2h) trips are sorted out, each of which may be made up of itself or several connected non-h2h trips. The 26617 h2h trips further constitute 18553 records of daily operation, forming the database. Each simulated EV is assigned with a random daily

operation record from the database. The energy consumption rate of EVs is assumed to be 0.22 kWh per mile. Charging demands of EVAs are calculated by assuming that EVs are charged at the maximum rate once they arrive home until they are fully charged. The charging efficiency is assumed to be 90%. The maximum charging rate is assumed to be 6 kW. Charging demands of EVAs at each hour are measured in kWh. As there is a relatively large number of EVs under each EVA, different energy consumption rates, charging efficiencies and maximum charging rates are not considered. 10000 sets of simulated daily charging demand of an EVA with 450 EVs are presented in Fig. 4.1 and used in Section 4.6.1 to Section 4.6.3.

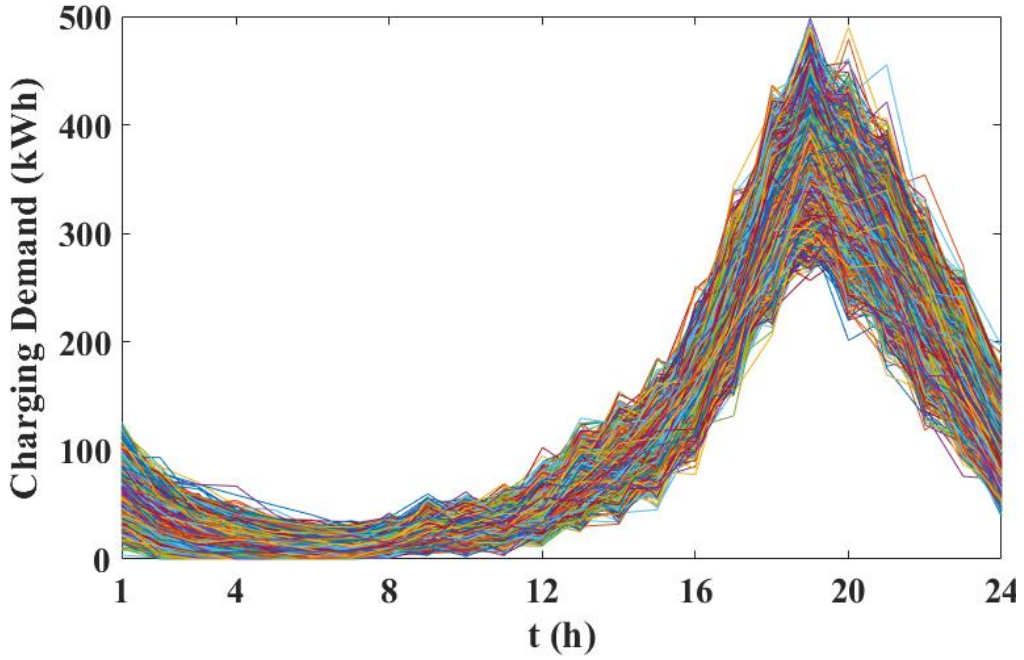

Fig. 4.1 10000 sets of simulated daily charging demand of an EVA with 450 EVs

Traffic congestion is further considered in simulation to reflect spatial correlations of the charging demands of EVAs. Again, as the simulated data is just used for validating the proposed model, only the influence of traffic congestion on travel speeds of EVs is considered with simple settings. The congestion period is assumed to be the 18th to 20th hour in the day. As the travel routes of EVs from the same distribution system are generally near to each other, a random variable γ_t is generated to reflect the overall congestion level of this area in hour t. For every single EV, another random

variable $\lambda_{t,i}$ is generated to reflect the specific influence of traffic congestion on its travel speed. A simple assumed relationship between congestion levels and travel speeds of EVs is adopted as (4.31), where $s_{t,i}$ and $\hat{s}_{t,i}$ are the original speed and the speed under congestion of EV i in hour t, respectively. The smaller γ_t and $\lambda_{t,i}$ become, the slower EVs travel. 10000 sets of simulated daily charging demand of an EVA with 450 EVs considering traffic congestion are presented in Fig. 4.2 and used in Section 4.6.4.

$$\hat{s}_{t,i} = \gamma_t \cdot \lambda_{t,i} \cdot s_{t,i} \tag{4.31}$$

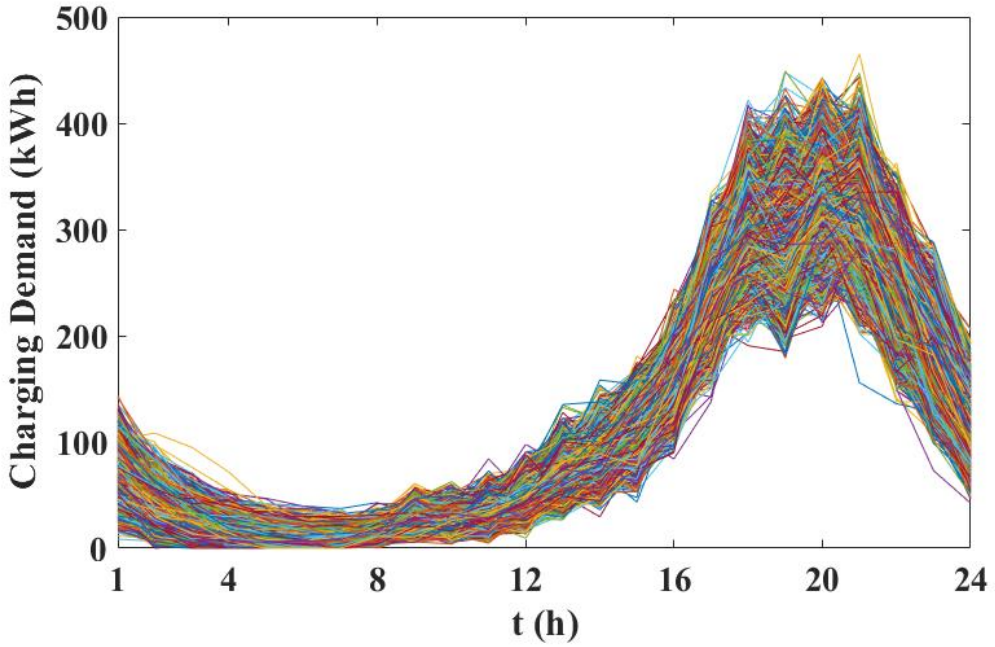

Fig. 4.2 10000 sets of simulated daily charging demand of an EVA with 450 EVs when traffic congestion is considered

4.6 Case Studies

Four sets of case studies are presented in this section. General performance of the proposed model is shown first. Next, the second set discusses the effects of the flexibility of EVAs in mitigating forecast uncertainties in BRDSs. After that, benefits of the uncertainty transferring scheme are illustrated. At last, temporal and spatial correlations of the charging demands of EVAs are qualitatively shown and the effectiveness of the proposed model in considering them is verified.

The IEEE 33-bus distribution system from [118] is adopted for case studies with the following base case settings. Three EVAs are assumed to be connected to Bus 16, 22 and 32 with 450, 450 and 600 EVs, respectively. Dispatchable ranges for over-charging and charging deficiency of the EVA at Bus 16, 22 and 32 at all hours are set to 450, 450 and 600 kWh, respectively. Power factors of all EVAs are set to 0.8. AVRs are assumed to be installed at Bus 6, 9, 15, 20, 23, 27 and 31. Each has a capacity of 500 kVar. Prices of reserves of all EVAs for over-charging and charging deficiency at all hours are set to 0.2¢ per kWh. Regular compensation rates to all EVAs for over-charging and charging deficiency at all hours are set to 1¢ per kWh. Punitive compensation rates to all EVAs for over-charging and charging deficiency at all hours are set to 5¢ per kWh. Penalty rates for positive and negative deviations of energy consumptions of BRDS from planned values at all hours are set to 15¢ per kWh. For all case studies, 10000 sets of charging demands are simulated to calculate the statistical mean and covariance matrix of uncertainties in charging demands of EVAs, based on which the operation decisions of BRDS are solved by the proposed model. After that, another 10000 sets of data are simulated independently to test the performance of the obtained solution.

4.6.1 General Performance of the Proposed Model

Case studies here are conducted by varying penalty rates. Relevant results are recorded in Table 4.1. Costs recorded in all subsequent tables are incurred from BRDS operation in the considered day. Average costs are computed based on actual outcomes under simulated charging demands of EVAs. With the increase of penalty rates, using EVAs to mitigate uncertainties becomes relatively cheaper and thus EVAs are resorted to more extensively. As a result, costs of reserves from EVAs and average compensations to EVAs increase. Besides, average penalties grow with the rise of penalty rates. But the increased percentage of average penalties is less than that of penalty rates, which is also because EVAs are used more extensively. To conclude, the

proposed model can successfully give proper operation decisions under a wide range of penalty rates.

Table 4.1 General performance of the proposed model

Penalty rates (¢/kWh)	5	10	15*	20
Reserve costs ($/day)	2.64	4.36	4.80	5.16
Average compensations to EVAs ($/day)	3.95	6.55	7.21	7.74
Average penalties ($/day)	22.03	38.09	55.89	73.60
Average total costs ($/day)	28.61	49.00	67.91	86.50

* base case

4.6.2 Effects of EVAs in Mitigating Uncertainties

In this section, case studies are first conducted by using EVAs to mitigate uncertainties or not. The average penalty at each hour under both cases are presented in Fig. 4.3. When EVAs are not used, the curve of average penalties reflects the level of uncertainties in each hour and basically matches the trend of the charging demands of EVAs. When EVAs are used, average penalties at some hours are close to zero because uncertainties in these hours are mainly mitigated by EVAs. In some other hours, over-charging and charging deficiency of EVAs incurred from mitigating uncertainties are recovered, and thus the average penalty is high. Therefore, the dashed curve in Fig. 4.3 fluctuates more severely than the solid curve. With the flexibility of EVAs, uncertainties from different hours can be delayed to the same hour and thus may offset each other. As a result, the average penalty in most hours is lower when EVAs are used to mitigate uncertainties.

Case studies are also conducted by increasing cost coefficients of EVAs to 2 to 4 times of the base setting and relevant results are recorded in Table 4.2. When EVAs are used to mitigate uncertainties, there are corresponding reserve costs and compensations to EVAs. But at the same time, average penalties decrease compared with the case that EVAs are not used, resulting in lower average total costs. When cost coefficients of EVAs increase, EVAs are used less extensively because using them becomes less economical. As a result, average penalties and average total costs increase and get

closer to the values when EVAs are not used. Reserve costs and average compensations to EVAs increase first because of higher cost coefficients but then decrease as EVAs are rarely used. When cost coefficients are high enough, the result will be the same as when EVAs are not used to mitigate uncertainties.

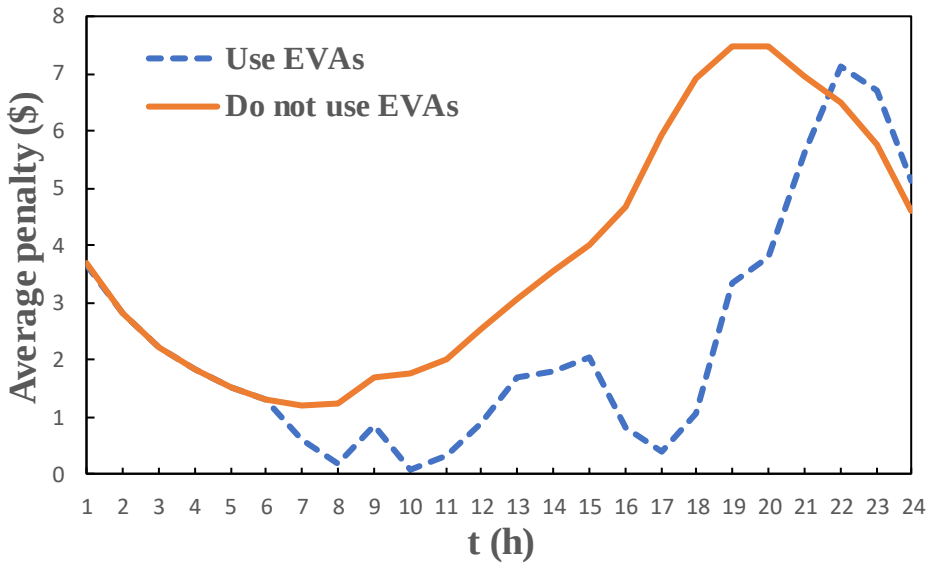

Fig. 4.3 Average penalty at each hour when EVAs are used to mitigate uncertainties and not

Table 4.2 Case studies on different cost coefficients of EVAs

Using EVAs to mitigate uncertainties	Yes				No
Cost coefficients of EVAs (times of the base setting)	1*	2	3	4	-
Reserve costs ($/day)	4.80	7.72	7.91	5.43	0
Average compensations to EVAs ($/day)	7.21	11.59	11.81	8.10	0
Average penalties ($/day)	55.89	59.11	66.09	76.10	90.65
Average total costs ($/day)	67.91	78.42	85.84	89.65	90.65

* base case

4.6.3 Benefits of the Uncertainty Transferring Scheme

Three potential benefits of the uncertainty transferring scheme are discussed in Section 4.4.2 and will be further illustrated here. Case studies are conducted with and without the uncertainty transferring scheme. As shown in Table 4.3, with uncertainty transferring, savings in reserve costs and average compensations to EVAs are about 50% because now disturbance to the charging of an EVA depends on uncertainties of several EVAs, which may offset each other. The other two benefits of the uncertainty transferring scheme are not significant under current parameters. To illustrate them more clearly, the above case studies are repeated with specific parameters modified. The original setting is represented as Setting 1, based on which Setting 2 and Setting 3 are created. In Setting 2, cost coefficients of the EVA at Bus 32 are set to half of their original values. In Setting 3, dispatchable ranges of the EVA at Bus 16 at all hours are set to 0, which implies that the EVA at Bus 16 is non-dispatchable.

Results under Setting 2 are summarized in Table 4.4. Apart from relieving disturbance to the charging of EVAs, the uncertainty transferring scheme can make use of the low cost coefficients of the EVA at Bus 32 by transferring uncertainties of other EVAs to it. As a result, savings in reserve costs and average compensations to EVAs brought by the uncertainty transferring scheme are about 76% and are higher than those under Setting 1.

Results under Setting 3 are given in Table 4.5. Without the uncertainty transferring scheme, uncertainties of the EVA at Bus 16 cannot be mitigated as it is now non-dispatchable. In contrast, its uncertainties can be transferred to other EVAs to utilize their spare dispatchable capacities under the uncertainty transferring scheme and thus can be mitigated. Therefore, when the uncertainty transferring scheme is applied, reserve costs and average compensations to EVAs are higher but average penalties are much lower. The saving in average penalties increases from 3.02% under Setting 1 to 26.77% under Setting 3.

Table 4.3 Benefits of the uncertainty transferring scheme in relieving disturbance to the charging of EVAs

With uncertainty transferring	No	Yes*	Savings brought by uncertainty transferring (%)
Reserve costs ($/day)	7.20	4.80	49.77
Average compensations to EVAs ($/day)	10.85	7.21	50.47
Average penalties ($/day)	57.58	55.89	3.02
Average total costs ($/day)	75.62	67.91	11.36

* base case

Table 4.4 Benefits of the uncertainty transferring scheme in making use of EVAs with lower cost coefficients

With uncertainty transferring	No	Yes	Savings brought by uncertainty transferring (%)
Reserve costs ($/day)	6.21	3.51	76.88
Average compensations to EVAs ($/day)	9.34	5.30	76.49
Average penalties ($/day)	56.43	55.46	1.76
Average total costs ($/day)	71.98	64.26	12.02

Table 4.5 Benefits of the uncertainty transferring scheme in relieving limitation from the dispatchable ranges of EVAs

With uncertainty transferring	No	Yes	Savings brought by uncertainty transferring (%)
Reserve costs ($/day)	4.02	4.54	-11.5
Average compensations to EVAs ($/day)	6.05	6.82	-11.3
Average penalties ($/day)	72.78	57.41	26.77
Average total costs ($/day)	82.85	68.78	20.46

4.6.4 Temporal and Spatial Correlations of Charging Demands of EVAs and Effectiveness of the Proposed Model in Considering Them

Simulated charging demands of EVAs with traffic congestion considered are adopted here. Instead of proving correlations between the charging demands of EVAs, simulation here is used only to illustrate possible correlations. For space-saving purposes, temporal and spatial correlations of the charging demands of EVAs are

illustrated through sub-matrices of the complete statistical covariance matrix. The statistical covariance matrix of charging demands of the EVA at Bus 16 from the 18th to 20th hour is represented as $\boldsymbol{\Sigma}_1$ and shown in (4.32). Significant positive temporal correlations between charging demands in adjacent hours can be observed, which is because the charging of EVs may not finish in the hour when EVs arrive home and may last to the following hour. The statistical covariance matrix of charging demands of all EVAs in the 19th hour is represented as $\boldsymbol{\Sigma}_2$ and shown in (4.33). There are significant positive spatial correlations between charging demands of different EVAs because traffic conditions pose similar influences on the travel of EVs from different EVAs and thus on charging demands of different EVAs as well.

$$\boldsymbol{\Sigma}_1 = \begin{bmatrix} 1031.7 & \mathbf{555.3} & 46.7 \\ \mathbf{555.3} & 1520.1 & \mathbf{513.9} \\ 46.7 & \mathbf{513.9} & 1150.3 \end{bmatrix} \tag{4.32}$$

$$\boldsymbol{\Sigma}_2 = \begin{bmatrix} 1520.1 & \mathbf{555.0} & \mathbf{735.7} \\ \mathbf{555.0} & 1554.6 & \mathbf{728.0} \\ \mathbf{735.7} & \mathbf{728.0} & 2313.4 \end{bmatrix} \tag{4.33}$$

Because temporal and spatial correlations of the charging demands of EVAs can be significant, it is crucial to consider them when making operation decisions of BRDS. Otherwise, sub-optimal solutions may be obtained. Case studies are conducted here to show the necessity of considering the correlations of charging demands of EVAs and the effectiveness of the proposed model in this aspect. A modified covariance matrix is generated by setting all covariance terms in the original statistical covariance matrix to zero. The proposed model is solved to obtain operation decisions with the original and the modified covariance matrix. The average performance of obtained operation decisions is recorded in Table 4.6. Under positive correlations, it is easier for disturbance to the charging of EVAs to be greater than a fixed amount of purchased reserves as the possibility that uncertainties offset each other decreases. Therefore, reserves should be properly purchased from EVAs to avoid excessive compensations to them. In this regard the proposed model is effective. Overall, the average total cost is lower when uncertainty correlations are properly considered by the proposed model.

Table 4.6 Case studies with uncertainty correlations considered and not

Considering uncertainty correlations	Yes	No
Reserve costs ($/day)	5.76	5.52
Average compensations to EVAs ($/day)	8.48	14.17
Average penalties ($/day)	58.66	60.38
Average total costs ($/day)	72.90	80.07

4.7 Further Discussions

By setting the dispatchable ranges of EVAs to zero as shown in Section 4.6.3, the proposed model could consider EVAs to choose to not follow the dispatch of BRDS or have no flexibility. Other loads with uncertainties can also be considered by the proposed model as they are the same as non-dispatchable EVAs from the perspective of BRDS. Besides, the proposed model can incorporate renewable energy sources as well. Uncertainties of these system components can be mitigated by dispatchable EVAs through the proposed uncertainty transferring scheme. The methodology adopted to solve the proposed model remains valid with respect to such modifications.

Linearized power flow equations for distribution networks from [80] are adopted here, which neglects non-linear terms of power losses. As power losses are much smaller than power flows in distribution networks [80], neglecting them has little influences on the result but can greatly reduce the computational complexity. To further improve the accuracy of the proposed model, the linearized equations from [74] can be employed to approximates the non-linear power losses by piecewise-linear functions.

4.8 Summary

In this chapter, a comprehensive model is established to mitigate forecast uncertainties in BRDSs by using EVAs. With their flexibility, uncertainties from different hours can be delayed to the same hour and thus may offset each other. The established model obtains the operation decisions by balancing costs of dispatching

EVAs and penalties for deviations of BRDS' energy consumptions from planned values. Therefore, as dispatching EVAs becomes cheaper, they will be used more extensively. Various benefits of the proposed uncertainty transferring scheme for the established model are verified through case studies. Furthermore, the adopted DRO technique is shown to be effective in avoiding unnecessary costs by taking temporal and spatial correlations of the charging demands of EVAs into consideration.

Chapter V

An Operation Model for Balance Responsible Distribution Companies Using the Flexibility of EVAs

5.1 Introduction

Based on the model proposed for BRDS in Chapter 4, operation of BR-DISCO is studied with better utilized EVA flexibility through more flexible settings in this chapter. Different from BRDS, BR-DISCO needs to purchase energy that it plans to import from the transmission system. So, apart from being used to mitigate uncertainties as done in Chapter 4, EVA flexibility can be used by BR-DISCO to shift EVA charging demands to hours with lower energy prices. Using EVAs to mitigate uncertainties can reduce penalties for energy deviations, and shifting EVA charging demands can decrease energy costs. Besides, both the EVA applications are constrained by EVA capacity for charging disturbance, which will be further illustrated in Section 5.3. If EVAs are used to mitigate uncertainties more extensively, they can shift less charging demands and vice versa. So, the two EVA applications are correlated. The model proposed for BR-DISCO here obtains the optimal solution by coordinating the two EVA applications.

In Chapter 4, it is assumed that the disturbance to EVA charging should be fully recovered by the end of the day. While, to further utilize EVA flexibility, it is assumed here that the disturbance to EVAs needs not be fully recovered by the end of the day given EVA capacity for charging disturbance being respected. Depending on whether recovering the corresponding disturbance to EVAs in the current day, using EVAs to mitigate uncertainties is classified into delaying uncertainties and eliminating uncertainties here. Further discussions will be made in Section 5.4.2.

In Chapter 4, EVAs can only charge. In contrast, they are also allowed here to discharge and thus may provide greater flexibility. To avoid their simultaneous charging and discharging, corresponding binary variables are introduced for them. Power losses incurred by their charging and discharging can be evaluated through their average charging and discharging efficiencies, respectively. Because of power losses in EVA charging, the power supplied by the distribution system is greater than that received by EVAs. Similarly, the power received by the distribution system is smaller than that supplied by EVAs when EVAs discharge. Such phenomenon is utilized by the proposed model to reduce the scale of uncertainties from the perspective of BR-DISCO. Relevant illustration is given in Section 5.7.3.

5.2 Nomenclature

5.2.1 Parameters

a_{e}^{t}	Energy price in Hour t
$a_{\mathrm{r,def}}^{t,i}$, $a_{\mathrm{r,over}}^{t,i}$	Price of reserves for EVA charging deficiency, over-charging at Node i in Hour t
$b_{\mathrm{r,def}}^{t,i}$, $b_{\mathrm{r,over}}^{t,i}$	Regular compensation rate for EVA charging deficiency, over-charging at Node i in Hour t
$b_{\mathrm{p,def}}^{t,i}$, $b_{\mathrm{p,over}}^{t,i}$	Punitive compensation rate for EVA charging deficiency, over-charging at Node i in Hour t
$b_{\mathrm{p,pos}}^{t}$, $b_{\mathrm{p,neg}}^{t}$	Penalty coefficient for positive, negative deviations of BR-DISCO from its energy purchase in Hour t
b_{d}^{i}	Compensation rate for EVA battery degradation at Node i
v_{b}	Base voltage
$x_{i,j}$, $r_{i,j}$	Line reactance, resistance between Node i and j
$p_{\mathrm{l}}^{t,i}$, $q_{\mathrm{l}}^{t,i}$	Active, reactive load at Node i in Hour t
$p_{\mathrm{RES,f}}^{t,i}$	RES power forecast at Node i in Hour t
$p_{\mathrm{EVA,p}}^{t,i}$	EVA planned charging demand at Node i in Hour t

λ_i	EVA power factor at Node i
η_{ch}^i, η_{dis}^i	Average EVA charging, discharging efficiency at Node i
$p_{\mathrm{ch,max}}^i$, $p_{\mathrm{dis,max}}^i$	Maximum EVA charging, discharging rate at Node i
$e_{\mathrm{def,max}}^{t,i}$	Acceptable EVA charging deficiency at Node i in Hour t
$e_{\mathrm{over,max}}^{t,i}$	Acceptable EVA over-charging at Node i in Hour t
T	Number of hours in the time horizon
Δt	An hour
N_{sys}	Set of nodes in the distribution system
$N_{\mathrm{p}}(i)$	Parent node of Node i
$N_{\mathrm{c}}(i)$	Set of children nodes of Node i
N_{EVA}	Set of nodes with EVAs
N_{RES}	Set of nodes with RESs

5.2.2 Uncertainties

$\xi_{\mathrm{EVA}}^{t,i}$	Deviation of EVA actual charging demand from EVA planned charging demand at Node i in Hour t
$\xi_{\mathrm{RES}}^{t,i}$	Error of RES power forecast at Node i in Hour t
$\boldsymbol{\xi}$	Vector of EVA and RES uncertainties in all hours
d_{ξ}	Dimension of $\boldsymbol{\xi}$
f_{ξ}	Probability distribution of $\boldsymbol{\xi}$
$A(\boldsymbol{\xi})$	Ambiguity set for $\boldsymbol{\xi}$
$\boldsymbol{\mu}$	Statistical expectation of $\boldsymbol{\xi}$
$\boldsymbol{\Sigma}$	Statistical covariance matrix of $\boldsymbol{\xi}$

5.2.3 Variables

$r_{\mathrm{def}}^{t,i}$, $r_{\mathrm{over}}^{t,i}$	Purchased reserves for EVA charging deficiency, over-charging at Node i in Hour t
e_{pur}^t	Purchased energy for Hour t
$\sigma_{t,i}$	EVA status at Node i in Hour t

$p_{\text{sys,EVA}}^{t,i}$	EVA active power supplied by the distribution system at Node i in Hour t
$p_{\text{ch}}^{t,i}$, $p_{\text{dis}}^{t,i}$	EVA active charging, discharging power at Node i in Hour t
$e_{\text{dist}}^{t,i}$	Cumulative disturbance to EVA at Node i between Hour 1 and t
$fl_{\text{p}}^{t,i,j}$, $fl_{\text{q}}^{t,i,j}$	Active, reactive power flow between Node i and j in Hour t
p_{in}^{t}	Active power imported from the transmission system
$v_{t,i}$	Voltage of Node i in Hour t

5.3 Background Settings

The proposed model considers two stages, i.e., day-ahead and real-time stage. Actual EVA charging demands and RES outputs are known only in the real-time stage, which means that there are EVA and RES uncertainties in the day-ahead stage. In consideration of real-time operation under possible realizations of EVA and RES uncertainties, the proposed model makes day-ahead decisions and real-time operation plans for BR-DISCO with the aim of minimizing total operation costs of BR-DISCO in the two stages. Real-time operation plans are functions of uncertainties and will give real-time decisions when uncertainties realize. Further discussions about real-time operation plans will be made in Section 5.4 and 5.5.2. The schematic diagram of the proposed model is given in Fig. 5.1, where TSO stands for transmission system operator. Similar as in Chapter 4, interactions between EVAs and EVs are beyond the scope of the study here.

In the day-ahead stage, BR-DISCO purchases energy that it plans to import from the transmission system. Because of uncertainties in EVA charging demands and RES outputs, the actual energy import of BR-DISCO in the real-time stage may deviate from its energy purchase. BR-DISCO needs to pay penalties for the deviation no matter it is positive or negative.

In the day-ahead stage, EVAs are required to report their planned charging demands to BR-DISCO. The actual EVA charging demands in the real-time stage will be the

sum of planned charging demands and EVA uncertainties $\xi_{\mathrm{EVA}}^{t,i}$. Disturbance to EVAs is defined in (5.1). When EVAs receive more energy than their needs, $e_{\mathrm{dist}}^{t,i}$ is negative and EVA over-charging happens. When EVAs receive less energy than their needs, $e_{\mathrm{dist}}^{t,i}$ is positive and EVA charging deficiency happens. In the day-ahead stage, EVAs report their acceptable amounts for over-charging and charging deficiency to BR-DISCO.

$$e_{\mathrm{dist}}^{t,i} = \sum_{\bar{t}=1,\dots,t} \left(\left(p_{\mathrm{EVA,p}}^{\bar{t},i} + \xi_{\mathrm{EVA}}^{\bar{t},i} - p_{\mathrm{ch}}^{\bar{t},i} + p_{\mathrm{dis}}^{\bar{t},i} \right) \cdot \Delta t \right) \tag{5.1}$$

BR-DISCO pays EVAs for disturbance to them in two steps. First, in the day-ahead stage, BR-DISCO reserves certain amounts for EVA over-charging and charging deficiency and pays EVAs for the reserves. As uncertainties realize, disturbance to EVAs is known in the real-time stage. Regular compensations are given to EVAs by BR-DISCO for the disturbance within the reserves purchased by BR-DISCO, and punitive compensations that are of higher rates are given for the disturbance beyond the reserves. Besides, BR-DISCO compensates EVA battery degradation.

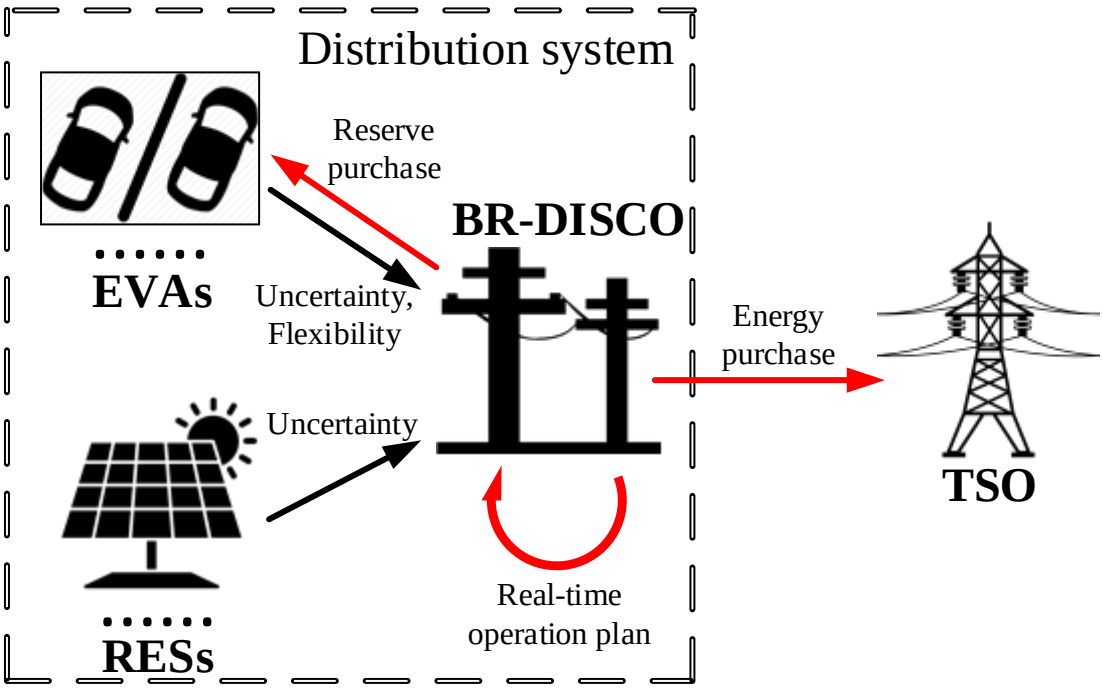

Fig. 5.1 Schematic diagram of the proposed model

5.4 Applications of EVA Flexibility

The key of the proposed model lies in applications of EVA flexibility, which are further elaborated in this section.

5.4.1 BR-DISCO's Real-time Operation Plans for EVA Charging and Discharging Power

BR-DISCO's real-time operation plan for EVA charging power is given in (5.2). If BR-DISCO does not disturb EVAs, EVA charging power will be the sum of EVA planned charging demands and EVA uncertainties, which means $\alpha_{\mathrm{ch}}^{t,i} = p_{\mathrm{EVA,p}}^{t,i}$ and $f_{\mathrm{ch}}^{t,i}(\boldsymbol{\xi}) = \xi_{\mathrm{EVA}}^{t,i}$. By choosing proper $f_{\mathrm{ch}}^{t,i}(\boldsymbol{\xi})$, BR-DISCO can use EVAs to mitigate uncertainties. For example, if $f_{\mathrm{ch}}^{t,i}(\boldsymbol{\xi}) = 0$, EVA i mitigates its own uncertainty because its charging power is now constant. If $f_{\mathrm{ch}}^{t,i}(\boldsymbol{\xi}) = \xi_{\mathrm{EVA}}^{t,i} - \xi_{\mathrm{EVA}}^{t,j}$, EVA i mitigates the uncertainty of EVA j. Similarly, EVAs can mitigate RES uncertainties. Besides, by setting $\alpha_{\mathrm{ch}}^{t,i}$ to proper values, BR-DISCO can shift EVA charging demands to hours with lower energy prices. If EVAs discharge in some hours, more EVA charging demands can be shifted compared with the case when EVAs never discharge. BR-DISCO's operation plan for EVA discharging power is given in (5.3). Similar as choosing proper $\alpha_{\mathrm{ch}}^{t,i}$ and $f_{\mathrm{ch}}^{t,i}(\boldsymbol{\xi})$, choosing proper $\alpha_{\mathrm{dis}}^{t,i}$ and $f_{\mathrm{dis}}^{t,i}(\boldsymbol{\xi})$ can have EVAs shift their charging demands and mitigate uncertainties, respectively.

$\alpha_{\mathrm{ch}}^{t,i}$, $\alpha_{\mathrm{dis}}^{t,i}$, $f_{\mathrm{ch}}^{t,i}(\boldsymbol{\xi})$ and $f_{\mathrm{dis}}^{t,i}(\boldsymbol{\xi})$ all influence power flows between the distribution system and EVAs. But the influence of $f_{\mathrm{ch}}^{t,i}(\boldsymbol{\xi})$ and $f_{\mathrm{dis}}^{t,i}(\boldsymbol{\xi})$ is known only after uncertainties realize. In the following parts of the paper, "shifting EVA charging demands" refers to "choosing proper $\alpha_{\mathrm{ch}}^{t,i}$ and $\alpha_{\mathrm{dis}}^{t,i}$", and "mitigating uncertainties" refers to "choosing proper $f_{\mathrm{ch}}^{t,i}(\boldsymbol{\xi})$ and $f_{\mathrm{dis}}^{t,i}(\boldsymbol{\xi})$". The schematic diagram of the proposed model's methodology is given in Fig. 5.2.

$$p_{\mathrm{ch}}^{t,i} = \alpha_{\mathrm{ch}}^{t,i} + f_{\mathrm{ch}}^{t,i}(\boldsymbol{\xi}) \tag{5.2}$$

$$p_{\mathrm{dis}}^{t,i} = \alpha_{\mathrm{dis}}^{t,i} + f_{\mathrm{dis}}^{t,i}(\boldsymbol{\xi}) \tag{5.3}$$

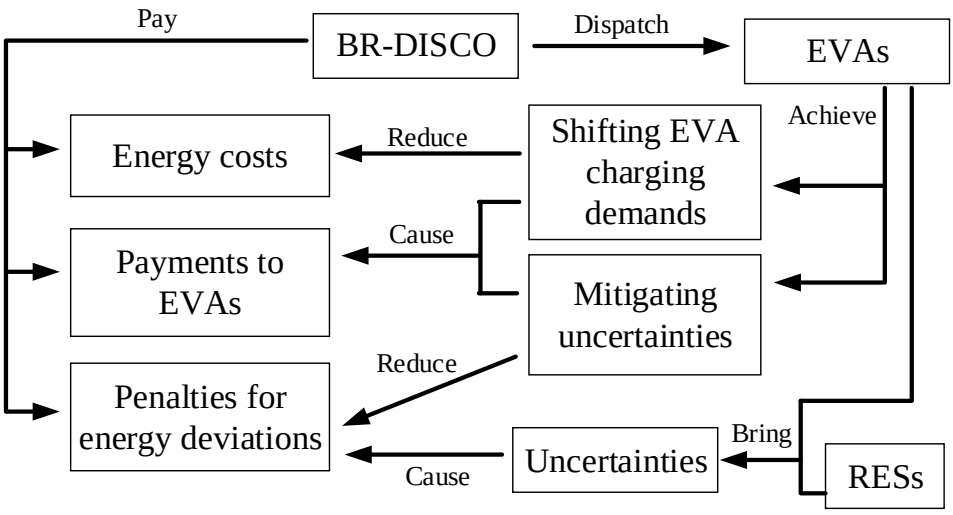

Fig. 5.2 Schematic diagram of the proposed model's methodology

5.4.2 Delaying Uncertainties and Eliminating Uncertainties

Using EVAs to mitigate uncertainties is further classified into delaying uncertainties and eliminating uncertainties. Delaying uncertainties is illustrated as follows. If $p_{\mathrm{ch}}^{1,i} = p_{\mathrm{EVA,p}}^{1,i}$, EVA i mitigates its own uncertainty in the first hour and $e_{\mathrm{dist}}^{1,i} = \xi_{\mathrm{EVA}}^{1,i}$. If disturbance to EVA i is recovered in the second hour, there is $e_{\mathrm{dist}}^{2,i} = 0$, which requires $p_{\mathrm{ch}}^{2,i} = p_{\mathrm{EVA,p}}^{2,i} + \xi_{\mathrm{EVA}}^{1,i} + \xi_{\mathrm{EVA}}^{2,i}$. So, $\xi_{\mathrm{EVA}}^{1,i}$ causes the variation of EVA charging power in the second hour rather than in the first hour, which means that $\xi_{\mathrm{EVA}}^{1,i}$ is delayed. $\xi_{\mathrm{EVA}}^{1,i}$ and $\xi_{\mathrm{EVA}}^{2,i}$ now offset each other if they are of different signs. To conclude, delaying uncertainties happens when disturbance to EVAs incurred from mitigating uncertainties is recovered within the day.

Eliminating uncertainties occurs when the disturbance to EVAs incurred from mitigating uncertainties is not fully recovered by the end of the day. The unrecovered disturbance will be merged into EVA planned charging demands when BR-DISCO makes decisions again at the beginning of the next day. In other words, the involved uncertainties will become deterministic information in the next day and will not cause energy deviations of BR-DISCO anymore, which is like the involved uncertainties being eliminated. Operation costs of BR-DISCO in the next day will be influenced by the unrecovered disturbance to EVAs incurred from mitigating uncertainties. But the

average influence is tiny because expectations of considered uncertainties are close to zero.

5.5 Proposed Model for BR-DISCO

Compensations to EVAs and penalties for energy deviations of BR-DISCO are influenced by uncertainty realizations. Obviously, BR-DISCO desires to achieve the minimum average costs. As relevant information is limited, the uncertainty distribution is hard to be acquired. But it is included in the family of all distributions satisfying known information. The set constituted by such family of distributions is just the ambiguity set under DRO. To utilize available uncertainty information and avoid being over-optimistic, the worst, i.e., largest, expected costs with respect to the ambiguity set are evaluated through DRO in the proposed model. Further discussions will be made in Section 5.6.2.

5.5.1 Formulation of the Proposed Model

The formulation of the proposed model is given in (5.4)-(5.22). In the objective (5.4), the first and second item are energy costs and reserve costs, respectively. The third item is the worst expectation of uncertainty-affected costs with respect to the ambiguity set. The first item within the worst expectation in (5.4) is the compensation for disturbance to EVAs and its explicit expressions are given in (5.5)-(5.8). (5.5)-(5.6) and (5.7)-(5.8) correspond to the cases when disturbance to EVAs is within and beyond purchased reserves, respectively. The second item within the worst expectation in (5.4) is the penalty for BR-DISCO's energy deviations and its explicit expressions are given in (5.9) and (5.10), which correspond to positive and negative energy deviations, respectively. The last item within the worst expectation in (5.4) is the compensation for EVA battery degradation. To avoid excessive degradation of EVA battery and reduce operational challenges, the status of EVAs, i.e., charging or discharging, in an hour is required to be fixed whatever uncertainty realizations are, which is achieved through

(5.12)-(5.14). Also, EVA charging and discharging power are limited in (5.13) and (5.14), respectively. (5.15) reflects power losses in EVA charging and discharging. Disturbance to EVAs is constrained within their acceptable ranges in (5.16). (5.17) implies that disturbance to EVAs incurred from shifting charging demands should be fully recovered in the end of the day. Power balances are ensured through (5.18)-(5.20). Node voltage is given in (5.21) and constrained in (5.22).

$$\inf \quad \sum_{t=1,\dots,T} a_{\mathrm{e}}^{t} \cdot e_{\mathrm{pur}}^{t} + \sum_{t=1,\dots,T} \sum_{i \in N_{\mathrm{EVA}}} \left(a_{\mathrm{r,def}}^{t,i} \cdot r_{\mathrm{def}}^{t,i} + a_{\mathrm{r,over}}^{t,i} \cdot r_{\mathrm{over}}^{t,i} \right) + \sup_{f_{\xi} \in A(\xi)} \left(\sum_{t=1,\dots,T} \sum_{i \in N_{\mathrm{EVA}}} \max_{k=1,\dots,4} f_k\left(e_{\mathrm{dist}}^{t,i}, r_{\mathrm{def}}^{t,i}, r_{\mathrm{over}}^{t,i}\right) + \sum_{t=1,\dots,T} \max_{k=1,2} g_k\left(p_{\mathrm{in}}^{t}, e_{\mathrm{pur}}^{t}\right) + \sum_{t=1,\dots,T} \sum_{i \in N_{\mathrm{EVA}}} b_{\mathrm{d}}^{i} \cdot p_{\mathrm{dis}}^{t,i} \cdot \Delta t \right) \tag{5.4}$$

$$\text{s.t.} \quad f_1\left(e_{\mathrm{dist}}^{t,i}, r_{\mathrm{def}}^{t,i}, r_{\mathrm{over}}^{t,i}\right) = b_{\mathrm{r,def}}^{t,i} \cdot e_{\mathrm{dist}}^{t,i} \tag{5.5}$$

$$f_2\left(e_{\mathrm{dist}}^{t,i}, r_{\mathrm{def}}^{t,i}, r_{\mathrm{over}}^{t,i}\right) = -b_{\mathrm{r,over}}^{t,i} \cdot e_{\mathrm{dist}}^{t,i} \tag{5.6}$$

$$f_3\left(e_{\mathrm{dist}}^{t,i}, r_{\mathrm{def}}^{t,i}, r_{\mathrm{over}}^{t,i}\right) = b_{\mathrm{p,def}}^{t,i} \cdot \left(e_{\mathrm{dist}}^{t,i} - r_{\mathrm{def}}^{t,i}\right) + b_{\mathrm{r,def}}^{t,i} \cdot r_{\mathrm{def}}^{t,i} \tag{5.7}$$

$$f_4\left(e_{\mathrm{dist}}^{t,i}, r_{\mathrm{def}}^{t,i}, r_{\mathrm{over}}^{t,i}\right) = b_{\mathrm{p,over}}^{t,i} \cdot \left(-e_{\mathrm{dist}}^{t,i} - r_{\mathrm{over}}^{t,i}\right) + b_{\mathrm{r,over}}^{t,i} \cdot r_{\mathrm{over}}^{t,i} \tag{5.8}$$

$$g_1\left(p_{\mathrm{in}}^{t}, e_{\mathrm{pur}}^{t}\right) = b_{\mathrm{p,pos}}^{t} \cdot \left(p_{\mathrm{in}}^{t} \cdot \Delta t - e_{\mathrm{pur}}^{t}\right) \tag{5.9}$$

$$g_2\left(p_{\mathrm{in}}^{t}, e_{\mathrm{pur}}^{t}\right) = b_{\mathrm{p,neg}}^{t} \cdot \left(e_{\mathrm{pur}}^{t} - p_{\mathrm{in}}^{t} \cdot \Delta t\right) \tag{5.10}$$

$$e_{\mathrm{dist}}^{t,i} = \sum_{\bar{t}=1,\dots,t} \left(\left(p_{\mathrm{EVA,p}}^{\bar{t},i} + \xi_{\mathrm{EVA}}^{\bar{t},i} - p_{\mathrm{ch}}^{\bar{t},i} + p_{\mathrm{dis}}^{\bar{t},i}\right) \cdot \Delta t \right), \forall \boldsymbol{\xi}, \forall t, \forall i \in N_{\mathrm{EVA}} \tag{5.11}$$

$$\sigma_{t,i} \in \{0,1\}, \forall t, \forall i \in N_{\mathrm{EVA}} \tag{5.12}$$

$$0 \le p_{\mathrm{ch}}^{t,i} \le \sigma_{t,i} \cdot p_{\mathrm{ch,max}}^{i}, \forall \boldsymbol{\xi}, \forall t, \forall i \in N_{\mathrm{EVA}} \tag{5.13}$$

$$0 \le p_{\mathrm{dis}}^{t,i} \le \left(1 - \sigma_{t,i}\right) \cdot p_{\mathrm{dis,max}}^{i}, \forall \boldsymbol{\xi}, \forall t, \forall i \in N_{\mathrm{EVA}} \tag{5.14}$$

$$p_{\mathrm{sys,EVA}}^{t,i} = p_{\mathrm{ch}}^{t,i} / \eta_{\mathrm{ch}}^{i} - p_{\mathrm{dis}}^{t,i} \cdot \eta_{\mathrm{dis}}^{i}, \forall \boldsymbol{\xi}, \forall t, \forall i \in N_{\mathrm{EVA}} \tag{5.15}$$

$$-e_{\mathrm{over,max}}^{t,i} \le e_{\mathrm{dist}}^{t,i} \le e_{\mathrm{def,max}}^{t,i}, \forall \boldsymbol{\xi}, \forall t, \forall i \in N_{\mathrm{EVA}} \tag{5.16}$$

$$\sum_{t=1,\dots,T} \left(p_{\mathrm{EVA,p}}^{t,i} - p_{\mathrm{ch}}^{t,i} + p_{\mathrm{dis}}^{t,i}\right) = 0 \text{ if } \boldsymbol{\xi} = \mathbf{0}\,, \forall i \in N_{\mathrm{EVA}} \tag{5.17}$$

$$fl_{\mathrm{p}}^{t,N_{\mathrm{p}}(i),i} = p_{\mathrm{l}}^{t,i} + p_{\mathrm{sys,EVA}}^{t,i} - p_{\mathrm{RES,f}}^{t,i} - \xi_{\mathrm{RES}}^{t,i} + \sum_{j \in N_{\mathrm{c}}(i)} fl_{\mathrm{p}}^{t,i,j}\,,$$

$$\forall \boldsymbol{\xi}, \forall t, \forall i \in N_{\mathrm{sys}}/\{1\} \tag{5.18}$$

$$fl_{\mathrm{q}}^{t,N_{\mathrm{p}}(i),i} = q_{\mathrm{l}}^{t,i} + p_{\mathrm{sys,EVA}}^{t,i} \cdot \sqrt{1 - {\lambda_i}^2}/\lambda_i + \sum_{j \in N_{\mathrm{c}}(i)} fl_{\mathrm{q}}^{t,i,j}\,,$$

$$\forall \boldsymbol{\xi}, \forall t, \forall i \in N_{\mathrm{sys}}/\{1\} \tag{5.19}$$

$$p_{\mathrm{in}}^{t} = fl_{\mathrm{p}}^{t,1,2} \tag{5.20}$$

$$v_{t,i} + \left(r_{N_{\mathrm{p}}(i),i} \cdot fl_{\mathrm{p}}^{t,N_{\mathrm{p}}(i),i} + x_{N_{\mathrm{p}}(i),i} \cdot fl_{\mathrm{q}}^{t,N_{\mathrm{p}}(i),i}\right)/v_{\mathrm{b}} = v_{t,N_{\mathrm{p}}(i)}\,,$$

$$\forall \boldsymbol{\xi}, \forall t, \forall i \in N_{\mathrm{sys}}/\{1\} \tag{5.21}$$

$$0.95 \cdot v_{\mathrm{b}} \le v_{t,i} \le 1.05 \cdot v_{\mathrm{b}}\,, \forall \boldsymbol{\xi}, \forall t, \forall i \in N_{\mathrm{sys}} \tag{5.22}$$

5.5.2 Linear Decision Rules Approximation

To reduce computational complexity, LDR approximation is adopted by assuming that BR-DISCO's real-time operation plans are affine functions of uncertainty realizations in earlier hours. Then, (5.2) can be rewritten as (5.23), where $\beta_{t,i}^{\bar{t},j}$ and $\gamma_{t,i}^{\bar{t},j}$ are uncertainty coefficients. Under LDR, using EVAs to mitigate uncertainties is equivalent to allocating uncertainties to EVAs in advance through uncertainty coefficients of $p_{\mathrm{ch}}^{t,i}$ and $p_{\mathrm{dis}}^{t,i}$.

$$p_{\mathrm{ch}}^{t,i} = \alpha_{\mathrm{ch}}^{t,i} + \sum_{\bar{t}=1,\dots,t} \left(\sum_{j \in N_{\mathrm{EVA}}} \beta_{t,i}^{\bar{t},j} \cdot \xi_{\mathrm{EVA}}^{\bar{t},j} + \sum_{j \in N_{\mathrm{RES}}} \gamma_{t,i}^{\bar{t},j} \cdot \xi_{\mathrm{RES}}^{\bar{t},j} \right) \tag{5.23}$$

5.6 Transformation of the Proposed Model

The proposed model contains robust equality and inequality constraints, which are both linear under LDR. With the same techniques as used in Section 4.4.3, they can be transformed into deterministic forms, and an upper bound (5.24) can be used to approximate the original worst expectation in (5.4). As the compensation for EVA

battery degradation depends linearly on uncertainties under LDR, its expectation can be calculated directly from uncertainty expectations. By using the same DRO technique as in Section 4.4.3, the first two terms in (5.24) can be transformed into deterministic forms. At last, the proposed model becomes a deterministic mixed-integer second-order conic program and can be solved by off-the-shelf solvers.

$$\sum_{t=1,\dots,T}\sum_{i\in N_{\mathrm{EVA}}}\sup_{f_\xi\in A(\xi)}\left(\max_{k=1,\dots,4} f_k\left(e_{\mathrm{dist}}^{t,i}, r_{\mathrm{def}}^{t,i}, r_{\mathrm{over}}^{t,i}\right)\right)$$

$$+\sum_{t=1,\dots,T}\sup_{f_\xi\in A(\xi)}\left(\max_{k=1,2} g_k\left(p_{\mathrm{in}}^{t}, e_{\mathrm{pur}}^{t}\right)\right)+\sum_{t=1,\dots,T}\sum_{i\in N_{\mathrm{EVA}}}\mathrm{E}\left[b_{\mathrm{d}}^{i}\cdot p_{\mathrm{dis}}^{t,i}\cdot\Delta t\right] \quad (5.24)$$

5.7 Case Studies and Discussions

Case studies are conducted based on a modified IEEE 33-node system, in which Node 16 and 22 each has an EVA, and Node 13 and 30 each has an RES. Average charging and discharging efficiencies of both EVAs are set to 0.9. To evaluate the performance of obtained decisions, uncertainty realizations are generated according to normal distributions. In Section 5.7.1 to 5.7.4, the time horizon is assumed to contain only 2 hours to demonstrate the proposed model more clearly. In Section 5.7.5, the time horizon is assumed to contain 24 hours.

In Section 5.7.1 to 5.7.4, disturbance to EVAs is assumed to be completely recovered at the end of the time horizon, which means that EVAs are used to only delay but not eliminate uncertainties according to the definitions in Section 5.4.2. Prices of reserves for over-charging and charging deficiency of both EVAs are set to 0.2¢/kWh. Regular compensation rates for over-charging and charging deficiency to both EVAs are set to 2¢/kWh. Punitive compensation rates for over-charging and charging deficiency to both EVAs are set to 6¢/kWh. Compensation rates for battery degradation to both EVAs are set to 0.05¢/kWh.

5.7.1 Using EVAs to Delay Uncertainties

In this part, energy prices in both hours are set to 4¢/kWh. Penalty coefficients for positive and negative energy deviations of BR-DISCO are set to 10¢/kWh. As discussed in Section 5.5.2, using EVAs to mitigate uncertainties under LDR is equivalent to allocating uncertainties to EVAs in advance, which is illustrated here.

According to the solution of the proposed model, the active power that the distribution system supplies for EVA 1 in the first hour is $p^{1,1}_{\mathrm{sys,EVA}} = 222.222 + 1.111\xi^{1,1}_{\mathrm{EVA}}$ when EVA flexibility is not used. So, the coefficient of $p^{1,1}_{\mathrm{sys,EVA}}$ for $\xi^{1,1}_{\mathrm{EVA}}$ is 1.111 and the coefficients of $p^{1,1}_{\mathrm{sys,EVA}}$ for other uncertainties are 0. For clearer illustration, uncertainty coefficients of certain decision variables when EVA flexibility is used and not are given in Table 5.2 and 5.1, respectively. As shown in Table 5.1, coefficients for EVA uncertainties are greater than 1 because of power losses in EVA charging. As EVA flexibility is not used, each variable in Table 5.1 depends and only depends on uncertainties in its hour. In contrast, when EVA flexibility is used, the active power imported from the transmission system in the first hour, i.e., p^{1}_{in}, is not influenced by uncertainties as shown in Table 5.2. In the second hour, because disturbance to EVAs incurred from uncertainty mitigation is recovered, variables depend on uncertainties from both hours. So, uncertainties in the first hour are delayed to the second hour.

Uncertainty-affected costs when EVA flexibility is used and not are recorded in Table 5.3, where the total uncertainty-affected costs are the sum of reserve costs, compensations to EVAs and penalties for energy deviations minus the reduction in energy costs. As uncertainties from different hours can offset each other, average penalties for energy deviations of BR-DISCO decrease when EVA flexibility is used. Meanwhile, corresponding reserve costs and compensations to EVAs are incurred. Overall, the average total uncertainty-affected costs are reduced because of EVA flexibility.

Table 5.1 Uncertainty coefficients when EVA flexibility is not used

Uncertainty	Variables in the first hour			Variables in the second hour		
	$p_{\text{sys,EVA}}^{1,1}$	$p_{\text{sys,EVA}}^{1,2}$	p_{in}^{1}	$p_{\text{sys,EVA}}^{2,1}$	$p_{\text{sys,EVA}}^{2,2}$	p_{in}^{2}
$\xi_{\text{EVA}}^{1,1}$	1.111	0	1.111	0	0	0
$\xi_{\text{EVA}}^{1,2}$	0	1.111	1.111	0	0	0
$\xi_{\text{RES}}^{1,1}$	0	0	-1	0	0	0
$\xi_{\text{RES}}^{1,2}$	0	0	-1	0	0	0
$\xi_{\text{EVA}}^{2,1}$	0	0	0	1.111	0	1.111
$\xi_{\text{EVA}}^{2,2}$	0	0	0	0	1.111	1.111
$\xi_{\text{RES}}^{2,1}$	0	0	0	0	0	-1
$\xi_{\text{RES}}^{2,2}$	0	0	0	0	0	-1

Table 5.2 Uncertainty coefficients when EVA flexibility is used

Uncertainty	Variables in the first hour			Variables in the second hour		
	$p_{\text{sys,EVA}}^{1,1}$	$p_{\text{sys,EVA}}^{1,2}$	p_{in}^{1}	$p_{\text{sys,EVA}}^{2,1}$	$p_{\text{sys,EVA}}^{2,2}$	p_{in}^{2}
$\xi_{\text{EVA}}^{1,1}$	0.600	-0.600	0	0.512	0.600	1.111
$\xi_{\text{EVA}}^{1,2}$	-0.512	0.512	0	0.512	0.600	1.111
$\xi_{\text{RES}}^{1,1}$	0.460	0.540	0	-0.460	-0.540	-1
$\xi_{\text{RES}}^{1,2}$	0.460	0.540	0	-0.460	-0.540	-1
$\xi_{\text{EVA}}^{2,1}$	0	0	0	1.111	0	1.111
$\xi_{\text{EVA}}^{2,2}$	0	0	0	0	1.111	1.111
$\xi_{\text{RES}}^{2,1}$	0	0	0	0	0	-1
$\xi_{\text{RES}}^{2,2}$	0	0	0	0	0	-1

Table 5.3 Uncertainty-affected costs when EVA flexibility is used and not

Using EVA flexibility	No	Yes
Reduction in energy costs brought by EVA flexibility (¢)	0.0	0.0
Reserve costs (¢)	0.0	8.6
Average compensations for disturbance to EVAs (¢)	0.0	26.8
Average compensations for EVA battery degradation (¢)	0.0	0.0
Average penalties for energy deviations (¢)	258.5	182.5
Average total uncertainty-affected costs (¢)	258.5	217.9

5.7.2 Trade-off between Cost Savings Brought by Using EVA Flexibility and Corresponding Payments to EVAs

In Section 5.7.1, each uncertainty in the first hour is completely delayed to the second hour, which however is not always the case. In this part, case studies are conducted under varying penalty coefficients for energy deviations of BR-DISCO. Energy prices are set to be the same as in Section 5.7.1. Under all considered penalty coefficients, each uncertainty in the first hour has the same percentage delayed to the second hour. Relevant results are recorded in Table 5.4. When penalty coefficients decrease, using EVAs to mitigate uncertainties becomes less attractive. As a result, EVA flexibility is used less extensively, and thus lower percentage of each uncertainty is delayed to the second hour, resulting in fewer reserve costs and average compensations for disturbance to EVAs.

Table 5.4 Results under different penalty coefficients

$b^1_{\mathrm{p,pos}},\ b^1_{\mathrm{p,neg}},\ b^2_{\mathrm{p,pos}},\ b^2_{\mathrm{p,neg}}$ (¢/kWh)	10	9	8	7	6
Percentage of each uncertainty delayed to the second hour (%)	100	100	97.5	86.7	74.5
Reserve costs (¢)	8.6	8.6	8.4	7.5	6.4
Average compensations for disturbance to EVAs (¢)	26.8	26.8	26.2	23.3	20.0

5.7.3 Effects of Power Losses in EVA Charging and Discharging on Uncertainties

Case studies are conducted in this part under three settings for energy prices as shown in Table 5.5. Penalty coefficients are set to be the same as in Section 5.7.1. Under all three settings in Table 5.5, each uncertainty in the first hour is completely delayed to the second hour. Uncertainty coefficients of p^2_{in} are shown in Fig. 5.3. Average penalties for energy deviations of BR-DISCO are given in Table 5.6.

Table 5.5 Settings for energy prices

Setting	C-I	C-II	C-III
a^1_{e} (¢/kWh)	4	7	4
a^2_{e} (¢/kWh)	4	4	7

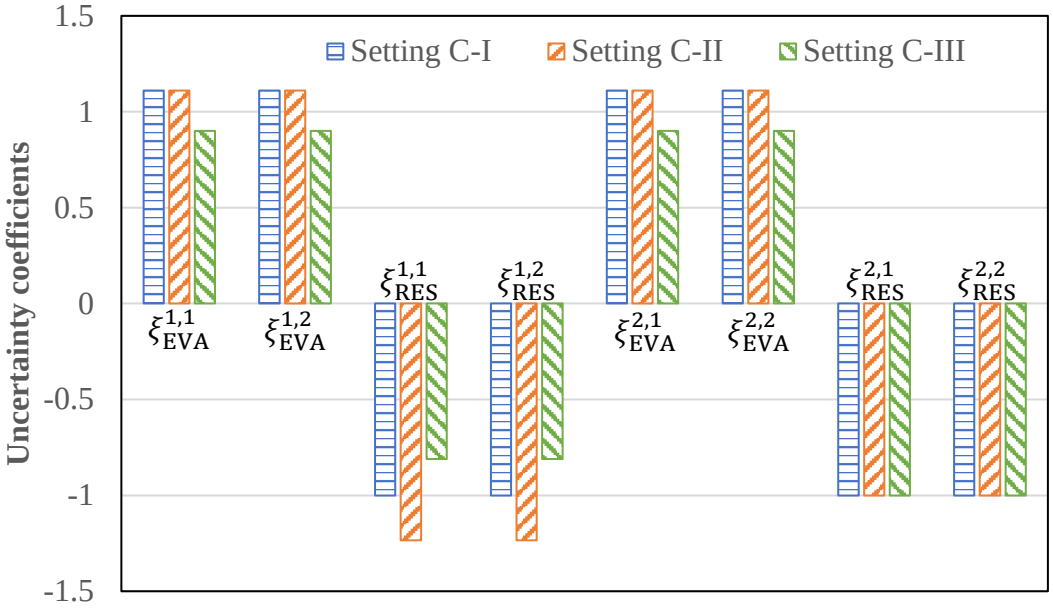

Fig. 5.3 Uncertainty coefficients of p_{in}^{2}

Table 5.6 Average penalties for BR-DISCO's energy deviations under different settings

Setting	C-I	C-II	C-III
Average penalties for energy deviations (¢)	182.5	183.5	148.8

As average charging and discharging efficiencies of both EVAs have been set to 0.9, they are all represented by η in the following illustration. Uncertainty coefficients of p_{in}^{2} under Setting C-I are the same with those in Table 5.2 and can be regarded as the reference for Setting C-II and C-III. Under Setting C-II, because of the significant difference in energy prices in the two hours, EVAs discharge in the first hour and charge in the second hour. To offset RES uncertainties, the total power that the distribution system receives from EVAs in the first hour, i.e., $-p_{\mathrm{sys,EVA}}^{1,1}-p_{\mathrm{sys,EVA}}^{1,2}$, contains $-\left(\xi_{\mathrm{RES}}^{1,1}+\xi_{\mathrm{RES}}^{1,2}\right)$. Because of power losses in EVA discharging, the total EVA discharging power, i.e., $p_{\mathrm{dis}}^{1,1}+p_{\mathrm{dis}}^{1,2}$, contains $-\left(\xi_{\mathrm{RES}}^{1,1}+\xi_{\mathrm{RES}}^{1,2}\right)/\eta$. In the second hour, disturbance to EVAs is recovered. As a result, the total EVA charging power, i.e., $p_{\mathrm{ch}}^{2,1}+p_{\mathrm{ch}}^{2,2}$, contains $-\left(\xi_{\mathrm{RES}}^{1,1}+\xi_{\mathrm{RES}}^{1,2}\right)/\eta$. Because of power losses in EVA charging, $p_{\mathrm{sys,EVA}}^{2,1}+p_{\mathrm{sys,EVA}}^{2,2}$ and p_{in}^{2} contains $-\left(\xi_{\mathrm{RES}}^{1,1}+\xi_{\mathrm{RES}}^{1,2}\right)/(\eta^{2})$. As shown in Fig. 5.3, coefficients for $\xi_{\mathrm{RES}}^{1,1}$ and $\xi_{\mathrm{RES}}^{1,2}$ have greater absolute values under Setting C-II than

under Setting C-I. So, under Setting C-II, these uncertainties are magnified from the perspective of BR-DISCO, and average penalty for energy deviations is higher than that under Setting C-I as shown in Table 5.6. Under Setting C-III, EVAs charge in the first hour and discharge in the second hour. With similar analysis as for Setting C-II, it can be told that p_{in}^2 contains $-(\xi_{\text{RES}}^{1,1}+\xi_{\text{RES}}^{1,2})\eta^2$ and $(\xi_{\text{EVA}}^{1,1}+\xi_{\text{EVA}}^{1,2}+\xi_{\text{EVA}}^{2,1}+\xi_{\text{EVA}}^{2,2})\eta$ under Setting C-III, which matches the results in Fig. 5.3. So, these uncertainties are minified from the perspective of BR-DISCO, and average penalty for energy deviations is now lower than under Setting C-I.

5.7.4 Interactions between Mitigating Uncertainties and Shifting Charging Demands

In this part, energy price in the first hour is set to 4¢/kWh and energy price in the second hour, i.e., a_{e}^2, is set to varying values. Penalty coefficients are set to be the same as in Section 5.7.1. Constant components of the total EVA active power supplied by the distribution system are recorded in Fig. 5.4. Average penalties for energy deviations of BR-DISCO are shown in Fig. 5.5.

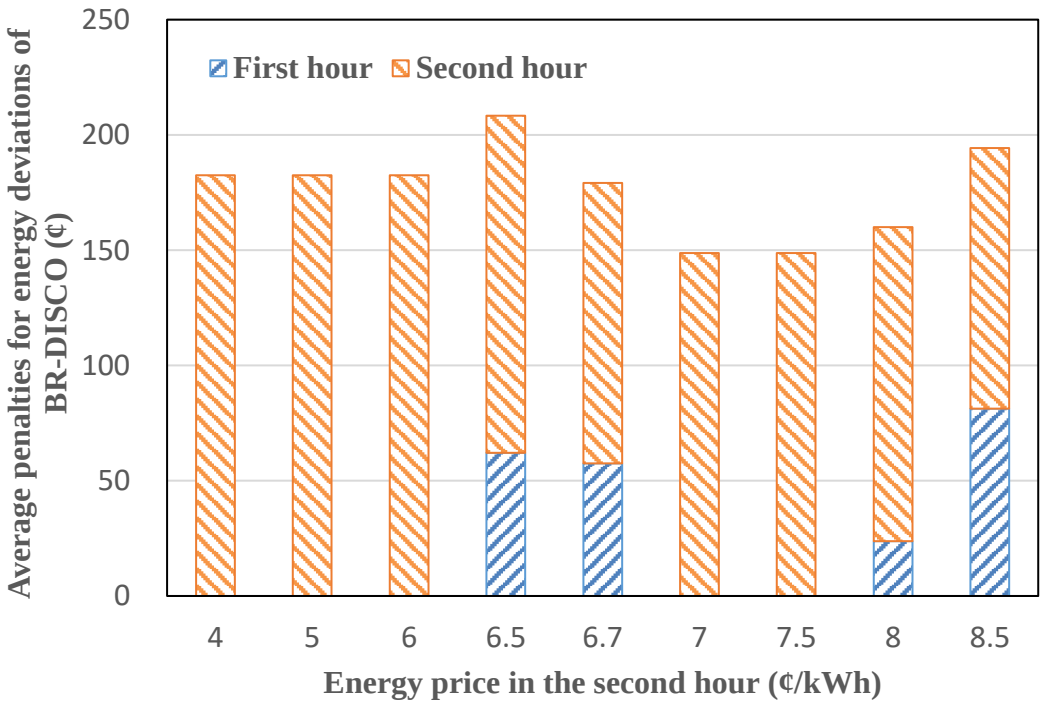

Fig. 5.4 Constant components of the total EVA active power supplied by the distribution system under varying energy price in the second hour

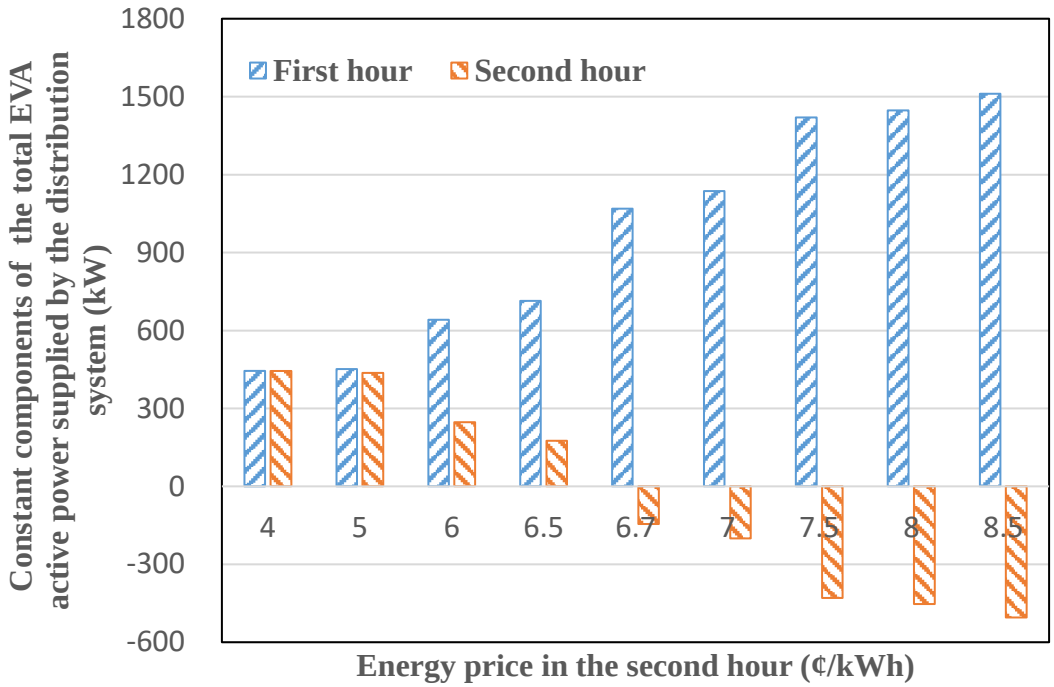

Fig. 5.5 Average penalties for energy deviations of BR-DISCO under varying energy price in the second hour

When a_e^2 is 4¢/kWh, there is no shifted EVA charging demand, and each uncertainty in the first hour is completely delayed to the second hour. Therefore, there is no penalty for energy deviations in the first hour as shown in Fig. 5.5. When a_e^2 rises to 5¢/kWh, savings in energy costs brought by shifting EVA charging demands are fewer than corresponding payments to EVAs. But shifting EVA charging demands may alleviate the disturbance to EVAs incurred from uncertainty mitigation. For the sake of minimizing overall costs, there is a slight amount of EVA charging demands shifted from the second hour to the first hour as shown in Fig. 5.4. When a_e^2 equals to 6¢/kWh, the difference in energy prices in the two hours becomes large enough and shifted EVA charging demands greatly increase compared with earlier cases. As a_e^2 increases to 6.5¢/kWh, shifted EVA charging demands grow further. To guarantee that EVA status is fixed in the second hour, each uncertainty in the first hour is only partially delayed to the second hour. So, the average penalty in the first hour is now positive and the average total penalty in the two hours is higher than those under earlier cases as shown in Fig. 5.5.

When a_e^2 is 6.7¢/kWh, EVA discharging is uneconomical in terms of the sum of energy costs and payments to EVAs. However, EVAs still discharge in the second hour because uncertainties will thus be minified as illustrated in Section 5.7.3 and thus lower overall costs will be achieved. To avoid EVA status swinging between discharging and charging in the second hour, each uncertainty in the first hour is only partially delayed to the second hour, which leads to positive average penalty in the first hour as shown in Fig. 5.5. When a_e^2 grows to 7¢/kWh, EVAs further discharge in the second hour and each uncertainty in the first hour is completely delayed to the second hour. Compared with the cases when EVAs charge in the second hour, the average total penalty is now lower because uncertainties are minified. When a_e^2 increases to 7.5¢/kWh, EVA discharging power in the second hour significantly increases and is bounded by EVAs' acceptable amounts for over-charging in the first hour. As a_e^2 keeps increasing to 8 and 8.5¢/kWh, each uncertainty in the first hour is only partially delayed to the second hour to have more EVA charging demands shifted from the second hour to the first hour, which causes growth in penalties but achieves optimal overall costs because of savings in energy costs.

5.7.5 Effects of Delaying Uncertainties and Eliminating Uncertainties

In this part, the time horizon contains 24 hours. Prices of reserves for EVA over-charging and charging deficiency are set to 0.1 time of energy prices. Regular compensation rates for EVA over-charging and charging deficiency are set to be equal to energy prices. Punitive compensations rates for EVA over-charging and charging deficiency are set to 3 times of energy prices. Compensation rates for EVA battery degradation are set to 0.05 time of energy prices. Penalty coefficients for energy deviations of BR-DISCO are set to 3 times of energy prices. As compensations to EVAs will keep increasing as time goes if disturbance to EVAs is not recovered, it is assumed here that disturbance to EVAs incurred from uncertainty mitigation needs to be recovered in 5 hours unless the time horizon ends. Such restriction has tiny influence on the results but can greatly reduce the computational complexity. Case studies are

conducted under three settings as given in Table 5.7. Average penalties for energy deviations of BR-DISCO are shown in Fig. 5.6.

Table 5.7 Three settings for uncertainty mitigation

Setting	E-I	E-II	E-III
Using EVAs to delay uncertainties	No	Yes	Yes
Using EVAs to eliminate uncertainties	No	No	Yes

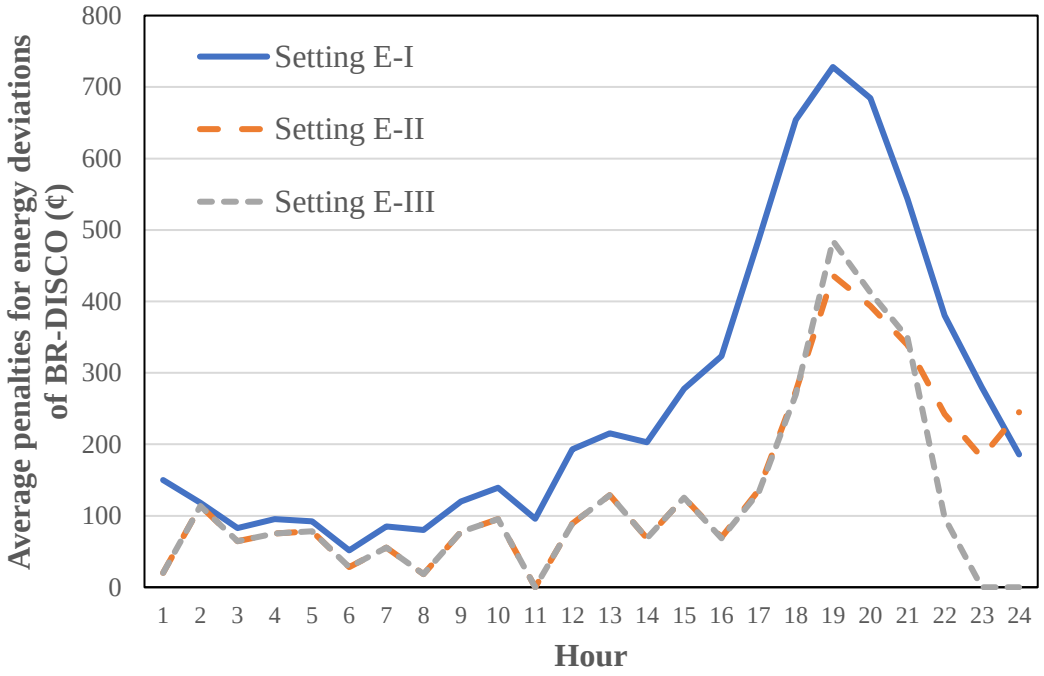

Fig. 5.6 Average penalties for energy deviations of BR-DISCO under different settings

The curve of Setting E-I reflects the scale of uncertainties in each hour as EVAs are not used to mitigate uncertainties. Under Setting E-II, average penalties are generally lower than those under Setting E-I, which is because uncertainties are delayed through EVAs and thus can offset uncertainties in later hours. Under Setting E-III, EVAs eliminate or partially eliminate uncertainties in the last several hours. As a result, average penalties in these hours are lower than those under Setting E-II. Uncertainty-affected costs under Setting E-I to E-III are recorded in Table 5.8. As shown by the results under Setting E-I and E-II, using EVAs to delay uncertainties brings significant reduction in average penalties and thus achieves lower average total uncertainty-

affected costs, which are consistent with the results in Section 5.7.1. By comparing the results under Setting E-II and E-III, it can be further noticed that having EVAs eliminate uncertainties creates extra savings based on those achieved by using EVAs to delay uncertainties.

Table 5.8 Uncertainty-affected costs under different settings

Setting	E-I	E-II	E-III
Reduction in energy costs brought by EVA flexibility (¢)	0.0	5.4	6.7
Reserve costs (¢)	0.0	562.1	642.6
Average compensations for disturbance to EVAs (¢)	0.0	1369.6	1629.3
Average compensations for EVA battery degradation (¢)	0.0	0.0	0.0
Average penalties for energy deviations (¢)	6265.6	3356.8	2853.2
Average total uncertainty-affected costs (¢)	6265.6	5283.2	5118.4

5.8 Summary

With the proposed model, flexibility of EVAs is explored by BR-DISCO to shift EVA charging demands to hours with lower energy prices and mitigate uncertainties in EVA charging demands and renewable power outputs. If the corresponding disturbance to EVAs is recovered within the time horizon, using EVAs to mitigate uncertainties is equivalent to delaying uncertainties; otherwise, it is equivalent to eliminating uncertainties. With comprehensive case studies, it is found that (1) the proposed model is successful in simultaneously utilizing both forms of uncertainty mitigation to reduce average penalties for deviations of BR-DISCO from its planned energy portfolio, (2) the proposed model is effective in coordinating EVA applications in mitigating uncertainties and shifting charging demands to achieve optimal overall costs, and (3) power losses in EVA charging and discharging are used in the proposed model to reduce the scale of uncertainties under certain circumstances.

Chapter VI

Conclusions and Future Work

6.1 Conclusions

The increasing RESs and EVs bring considerable uncertainties to the operation of power systems. Uncertainties can result in overloading of system equipment or make bus voltage exceed the allowable operation range. They can also cause the energy imbalance of the system, which will lead to the deviation of system frequency. In the worst case, blackout of vast areas will be caused. Therefore, decisions for the operation of power systems need to be carefully made to alleviate the negative effects brought by uncertainties. As many operation tasks in power systems are optimization problems, it is important to have approaches that can solve optimization problems with uncertainties effectively and efficiently. In this regard, DRO is a fast-developing approach and has been shown to be competent. However, the potentials of DRO in power system operation have not been fully explored yet. In this thesis, applications of DRO in ED are improved based on the state-of-art applications in literature. Besides, DRO is applied in managing EVAs in BRDSs for the first time. The model proposed for BRDSs is also extended for BR-DISCOs that have EVAs in their distribution systems. Specifically, primary conclusions of this thesis are concluded as follows:

i) *A comprehensive multi-period ED model is proposed using DRO techniques with more realistic modeling of uncertainty to accommodate uncertainties from RESs and is solved through a tailor-made Constraint Generation algorithm.*

The proposed model adopts two-stage frameworks to effectively model recourse actions with respect to uncertainty realizations and greatly reduces average operation costs through applying DRO. As the statistical moments of uncertainties are derived from limited historical samples, they may deviate from the actual moments. In consideration of such deviations, the adopted DRO technique prevents inferior

performance of the proposed model. Besides, the boundness of uncertainties in outputs of RESs are considered in DRO, which avoids over-conservative solutions. Moreover, RO is integrated into the framework of DRO to guarantee the system security through limiting load shedding. Furthermore, rolling-plan operation is adopted. So, only the decisions for the first period in the proposed multi-period model are carried out, and then the proposed model rolls forward and is solved again to get the decisions for the next period, which means that decisions for the first period are more important. Therefore, faced with the computational difficulty brought by temporal sequences of uncertainties and decisions in different periods, decision variables for the first period are kept intact, but those for later periods are approximated through SLDR to guarantee the tractability of the proposed model. With such formulation, the proposed model does not cause excessive computational burden when solved through the tailor-made Constraint Generation algorithm and successfully guarantees economical and secure long-term ED operation at the same time.

ii) *A model to use the flexibility of EVAs in mitigating forecast uncertainties in BRDSs is proposed with the temporal and spatial uncertainty correlations considered through DRO.*

Under the proposed model, disturbance to the charging of EVAs will be caused when EVAs are used to mitigate uncertainties and is required to be recovered by the end of the day to guarantee driving activities of EVs in the next day. As deviations of BRDS from its planned energy portfolio will still be caused when the corresponding disturbance to EVAs is recovered, using EVAs to mitigate uncertainties is equivalent to delaying uncertainties under the proposed model. Delayed uncertainties may offset uncertainties in later hours, whose probability depends on uncertainty correlations. As a result, average penalties for energy deviations of BRDS are reduced. By incorporating the statistical covariance matrix of uncertainties into the ambiguity set of DRO, the proposed model captures the correlation information of uncertainties and is effective in evaluating operation costs that are affected by uncertainties. Besides, payments are given to EVAs by BRDS to compensate for the disturbance to their charging. Trade-off

between costs of dispatching EVAs and corresponding savings in penalties for energy deviations of BRDS is achieved to obtain the optimal overall costs under the proposed model. Therefore, as dispatching EVAs becomes cheaper, they are more extensively used. Moreover, LDR is used to reduce the computational complexity. Based on LDR, a scheme of uncertainty transferring is proposed so that any EVA can mitigate uncertainties of other EVAs. As a result, the disturbance to EVAs is relieved on average as it now depends on uncertainties of different EVAs, which may offset each other. Also, EVAs that are cheaper to dispatch or have greater capacity for charging disturbance are better utilized under the scheme of uncertainty transferring.

iii) *The model proposed for BRDSs is further developed to facilitate BR-DISCOs to utilize the flexibility of EVAs to achieve optimal overall costs.*

Apart from paying penalties for its energy deviations, BR-DISCO needs to purchase energy that it plans to import from the transmission system. Therefore, for BR-DISCO, the flexibility of EVAs can be used to shift their charging demands to hours with lower energy prices to save energy costs at the same time of being used to mitigate uncertainties. As using EVAs to mitigate uncertainties and shifting EVA charging demands both disturb the charging of EVAs, these two applications of EVAs are correlated. By coordinating them, the proposed model obtains the optimal operation decisions for BR-DISCO. Moreover, EVAs can discharge in some hours to have more charging demands shifted. Power losses in the charging and discharging of EVAs influence the interaction between using EVAs to mitigate uncertainties and shifting EVA charging demands and are used to reduce the scale of uncertainties from the perspective of BR-DISCO under certain circumstances. Besides, disturbance to the charging of EVAs incurred from uncertainty mitigation is not required to be fully recovered by the end of the day as long as the limits of EVAs in accepting disturbance are not violated. If the corresponding disturbance to EVAs is recovered in the day, using EVAs to mitigate uncertainties is equivalent to having EVAs delay uncertainties. Otherwise, it is equivalent to using EVAs to eliminate uncertainties, which would have little influence on average operation costs of BR-DISCO in the next day as the

expectations of considered uncertainties are around zero. Both forms of uncertainty mitigation reduce the average penalties for energy deviations of BR-DISCO.

6.2 Future Work

i) More accurate DRO modeling.

Uncertainties usually follow unimodal distributions such as normal distributions. In other words, their distributions usually have a single peak. In this thesis, the ambiguity sets of the adopted DRO techniques are based on the expectation and covariance matrix of the uncertainty and do not exclude multimodal distributions. As a result, the decision made may be based on a multimodal distribution in the ambiguity set and thus may be over-conservative. Besides, the expectation and covariance matrix are made up of first and second-order moments of the uncertainty. There are also third-order and even higher-order moments, which all reveal different information. For example, third-order moments can disclose the dissymmetry of the uncertainty distribution, while first and second-order moments cannot. If the unimodality information and higher-order moments can be properly incorporated into ambiguity sets, the modeling accuracy of DRO and the quality of the obtained decision will be improved.

ii) More applications of the methodology developed in this thesis.

In Chapter 3, a methodology is developed based on two-stage frameworks to improve the economic efficiency of power system operation through DRO while guaranteeing system security through RO. Apart from being used for ED as in Chapter 3, this methodology can be applied to more problems. For example, in [74], a model is proposed to maximize the hosting capacity of distribution systems for EVs by using two-stage frameworks. However, only the system security is properly guaranteed, and the economic efficiency is roughly evaluated through approximating the uncertainty distribution by piecewise-linear functions. With the methodology developed in Chapter 3, solutions better than those in [74] can be obtained.

References

[1] P. Jain, *Wind energy engineering*. New York: McGraw-Hill, 2011.

[2] [Online] Available: https://data.worldbank.org/indicator/EG.ELC.RNEW.ZS

[3] "Technology Roadmap Solar Photovoltaic Energy." [Online]. Available: https://www.webcitation.org/6T92GIRhW?url=http://www.iea.org/publications/freepublications/publication/TechnologyRoadmapSolarPhotovoltaicEnergy_2014edition.pdf

[4] P. Kelly-Detwiler, "Solar Grid Parity Comes to Spain." [Online]. Available: https://www.forbes.com/sites/peterdetwiler/2012/12/26/solar-grid-parity-comes-to-spain/#6eb4c6dd5422

[5] "Science-Driven Innovation Can Reduce Wind Energy Costs by 50% by 2030." [Online]. Available: https://www.nrel.gov/news/program/2017/science-driven-innovation-can-reduce-wind-energy-costs-by-50-percent-by-2030.html

[6] "Wind Systems Integration Basics." [Online]. Available: https://web.archive.org/web/20120607000124/http://www.nrel.gov/wind/systemsintegration/system_integration_basics.html

[7] D. Raghunandan, "India Plans to Sell Only Electric Cars by 2030." [Online]. Available: https://www.newsclick.in/india-plans-sell-only-electric-cars-2030

[8] J. P. Morgan, "Driving into 2025: The Future of Electric Vehicles." [Online]. Available: https://www.jpmorgan.com/global/research/electric-vehicles

[9] M. J. Coren, "The median electric car in the US is getting cheaper." [Online]. Available: https://qz.com/1695602/the-average-electric-vehicle-is-getting-cheaper-in-the-us/

[10] D. Linden and T. B. Reddy, *Handbook of Batteries 3rd Edition*. New York: McGraw-Hill, 2002.

[11] Y. Nie, C. Y. Chung, and N. Z. Xu, "System State Estimation Considering EV Penetration With Unknown Behavior Using Quasi-Newton Method," *IEEE*

Transactions on Power Systems, vol. 31, no. 6, pp. 4605-4615, 2016, doi: 10.1109/TPWRS.2016.2516593.

[12] N. Z. Xu and C. Y. Chung, "Uncertainties of EV Charging and Effects on Well-Being Analysis of Generating Systems," *IEEE Transactions on Power Systems,* vol. 30, no. 5, pp. 2547-2557, 2015, doi: 10.1109/TPWRS.2014.2362653.

[13] M. Aien, A. Hajebrahimi, and M. Fotuhi-Firuzabad, "A comprehensive review on uncertainty modeling techniques in power system studies," *Renewable and Sustainable Energy Reviews,* vol. 57, pp. 1077-1089, 2016.

[14] Y. V. Makarov, P. V. Etingov, J. Ma, Z. Huang, and K. Subbarao, "Incorporating Uncertainty of Wind Power Generation Forecast Into Power System Operation, Dispatch, and Unit Commitment Procedures," *IEEE Transactions on Sustainable Energy,* vol. 2, no. 4, pp. 433-442, 2011, doi: 10.1109/TSTE.2011.2159254.

[15] J. A. Momoh, *Electric power system applications of optimization*. CRC press, 2017.

[16] H. Holttinen *et al.*, "Methodologies to Determine Operating Reserves Due to Increased Wind Power," *IEEE Transactions on Sustainable Energy,* vol. 3, no. 4, pp. 713-723, 2012, doi: 10.1109/TSTE.2012.2208207.

[17] J. Zhao, C. Wan, Z. Xu, and K. P. Wong, "Spinning Reserve Requirement Optimization Considering Integration of Plug-In Electric Vehicles," *IEEE Transactions on Smart Grid,* vol. 8, no. 4, pp. 2009-2021, 2017, doi: 10.1109/TSG.2016.2597098.

[18] J. Kabouris and F. D. Kanellos, "Impacts of Large-Scale Wind Penetration on Designing and Operation of Electric Power Systems," *IEEE Transactions on Sustainable Energy,* vol. 1, no. 2, pp. 107-114, 2010, doi: 10.1109/TSTE.2010.2050348.

[19] H. Ye and Z. Li, "Robust Security-Constrained Unit Commitment and Dispatch With Recourse Cost Requirement," *IEEE Transactions on Power Systems,* vol. PP, no. 99, pp. 1-10, 2015, doi: 10.1109/TPWRS.2015.2493162.

[20] J. C. Mukherjee and A. Gupta, "A Review of Charge Scheduling of Electric Vehicles in Smart Grid," *IEEE Systems Journal,* vol. 9, no. 4, pp. 1541-1553, 2015, doi: 10.1109/JSYST.2014.2356559.

[21] European Commission. (2017). *Commission Regulation (EU) 2017/2195 of 23 November 2017 establishing a guideline on electricity balancing*.

[22] "Regulatory recommendations for the deployment of flexibility," in "EU SGTF-EG3 Report," Smart Grid Task Force, 2015.

[23] D. Pozo and J. Contreras, "A Chance-Constrained Unit Commitment With an $n-K$ Security Criterion and Significant Wind Generation," *IEEE Transactions on Power Systems,* vol. 28, no. 3, pp. 2842-2851, 2013, doi: 10.1109/TPWRS.2012.2227841.

[24] M. A. Ortega-Vazquez and D. S. Kirschen, "Estimating the Spinning Reserve Requirements in Systems With Significant Wind Power Generation Penetration," *IEEE Transactions on Power Systems,* vol. 24, no. 1, pp. 114-124, 2009, doi: 10.1109/TPWRS.2008.2004745.

[25] A. Papavasiliou, S. S. Oren, and R. P. O. Neill, "Reserve Requirements for Wind Power Integration: A Scenario-Based Stochastic Programming Framework," *IEEE Transactions on Power Systems,* vol. 26, no. 4, pp. 2197-2206, 2011, doi: 10.1109/TPWRS.2011.2121095.

[26] K. Høyland and S. W. Wallace, "Generating scenario trees for multistage decision problems," *Management science,* vol. 47, no. 2, pp. 295-307, 2001.

[27] M. A. Plazas, A. J. Conejo, and F. J. Prieto, "Multimarket optimal bidding for a power producer," *IEEE Transactions on Power Systems,* vol. 20, no. 4, pp. 2041-2050, 2005, doi: 10.1109/TPWRS.2005.856987.

[28] P. M. Esfahani and D. Kuhn, "Data-driven distributionally robust optimization using the Wasserstein metric: Performance guarantees and tractable reformulations," *Mathematical Programming,* vol. 171, no. 1-2, pp. 115-166, 2018.

[29] E. Delage and Y. Ye, "Distributionally robust optimization under moment

uncertainty with application to data-driven problems," *Operations research,* vol. 58, no. 3, pp. 595-612, 2010.

[30] A. Shapiro, *Stochastic programming by Monte Carlo simulation methods*. Humboldt-Universität zu Berlin, Mathematisch-Naturwissenschaftliche Fakultät …, 2000.

[31] E. H. Delage, "Distributionally robust optimization in context of data-driven problems," Stanford University, 2009.

[32] A. Shapiro and T. Homem-de-Mello, "On the rate of convergence of optimal solutions of Monte Carlo approximations of stochastic programs," *SIAM journal on optimization,* vol. 11, no. 1, pp. 70-86, 2000.

[33] Q. P. Zheng, J. Wang, and A. L. Liu, "Stochastic Optimization for Unit Commitment, A Review," *IEEE Transactions on Power Systems,* vol. 30, no. 4, pp. 1913-1924, 2015, doi: 10.1109/TPWRS.2014.2355204.

[34] J. M. Morales, S. Pineda, A. J. Conejo, and M. Carrion, "Scenario Reduction for Futures Market Trading in Electricity Markets," *IEEE Transactions on Power Systems,* vol. 24, no. 2, pp. 878-888, 2009, doi: 10.1109/TPWRS.2009.2016072.

[35] H. Heitsch and W. Römisch, "A note on scenario reduction for two-stage stochastic programs," *Operations Research Letters,* vol. 35, no. 6, pp. 731-738, 2007.

[36] D. Bertsimas and A. Thiele, "A robust optimization approach to inventory theory," *Operations research,* vol. 54, no. 1, pp. 150-168, 2006.

[37] X. Liu and W. Xu, "Economic Load Dispatch Constrained by Wind Power Availability: A Here-and-Now Approach," *IEEE Transactions on Sustainable Energy,* vol. 1, no. 1, pp. 2-9, 2010, doi: 10.1109/TSTE.2010.2044817.

[38] Z. Zhang, Y. Sun, D. W. Gao, J. Lin, and L. Cheng, "A Versatile Probability Distribution Model for Wind Power Forecast Errors and Its Application in Economic Dispatch," *IEEE Transactions on Power Systems,* vol. 28, no. 3, pp. 3114-3125, 2013, doi: 10.1109/TPWRS.2013.2249596.

[39] H. Zhang and P. Li, "Chance Constrained Programming for Optimal Power

Flow Under Uncertainty," *IEEE Transactions on Power Systems,* vol. 26, no. 4, pp. 2417-2424, 2011, doi: 10.1109/TPWRS.2011.2154367.

[40] G. A. Hanasusanto, D. Kuhn, and W. Wiesemann, "A comment on “computational complexity of stochastic programming problems”," *Mathematical Programming,* vol. 159, no. 1-2, pp. 557-569, 2016.

[41] M. Lubin, Y. Dvorkin, and S. Backhaus, "A Robust Approach to Chance Constrained Optimal Power Flow With Renewable Generation," *IEEE Transactions on Power Systems,* vol. 31, no. 5, pp. 3840-3849, 2016, doi: 10.1109/TPWRS.2015.2499753.

[42] D. Bienstock, M. Chertkov, and S. Harnett, "Chance-constrained optimal power flow: Risk-aware network control under uncertainty," *Siam Review,* vol. 56, no. 3, pp. 461-495, 2014.

[43] A. T. Saric and A. M. Stankovic, "An application of interval analysis and optimization to electric energy markets," *IEEE Transactions on Power Systems,* vol. 21, no. 2, pp. 515-523, 2006.

[44] Y. Wang, Q. Xia, and C. Kang, "Unit commitment with volatile node injections by using interval optimization," *IEEE Transactions on Power Systems,* vol. 26, no. 3, pp. 1705-1713, 2011.

[45] L. Wu, M. Shahidehpour, and Z. Li, "Comparison of scenario-based and interval optimization approaches to stochastic SCUC," *IEEE Transactions on Power Systems,* vol. 27, no. 2, pp. 913-921, 2011.

[46] L. El Ghaoui and H. Lebret, "Robust solutions to least-squares problems with uncertain data," *SIAM Journal on matrix analysis and applications,* vol. 18, no. 4, pp. 1035-1064, 1997.

[47] A. Ben-Tal and A. Nemirovski, "Robust solutions of uncertain linear programs," *Operations research letters,* vol. 25, no. 1, pp. 1-13, 1999.

[48] C. Zhao, J. Wang, J. P. Watson, and Y. Guan, "Multi-Stage Robust Unit Commitment Considering Wind and Demand Response Uncertainties," *IEEE Transactions on Power Systems,* vol. 28, no. 3, pp. 2708-2717, 2013, doi:

10.1109/TPWRS.2013.2244231.

[49] D. Bertsimas and M. Sim, "The price of robustness," *Operations research,* vol. 52, no. 1, pp. 35-53, 2004.

[50] D. Bertsimas, D. Pachamanova, and M. Sim, "Robust linear optimization under general norms," *Operations Research Letters,* vol. 32, no. 6, pp. 510-516, 2004.

[51] P. Xiong and C. Singh, "A Distributional Interpretation of Uncertainty Sets in Unit Commitment Under Uncertain Wind Power," *IEEE Transactions on Sustainable Energy,* vol. 10, no. 1, pp. 149-157, 2019, doi: 10.1109/TSTE.2018.2828421.

[52] A. Ben-Tal and A. Nemirovski, "Robust optimization–methodology and applications," *Mathematical Programming,* vol. 92, no. 3, pp. 453-480, 2002.

[53] D. Bertsimas, D. B. Brown, and C. Caramanis, "Theory and applications of robust optimization," *SIAM review,* vol. 53, no. 3, pp. 464-501, 2011.

[54] A. Ben-Tal, L. El Ghaoui, and A. Nemirovski, *Robust optimization*. Princeton University Press, 2009.

[55] V. Gabrel, C. Murat, and A. Thiele, "Recent advances in robust optimization: An overview," *European Journal of Operational Research,* vol. 235, no. 3, pp. 471-483, 2014.

[56] A. Zare, C. Y. Chung, J. Zhan, and S. O. Faried, "A Distributionally Robust Chance-Constrained MILP Model for Multistage Distribution System Planning With Uncertain Renewables and Loads," *IEEE Transactions on Power Systems,* vol. 33, no. 5, pp. 5248-5262, 2018, doi: 10.1109/TPWRS.2018.2792938.

[57] Y. An and B. Zeng, "Exploring the Modeling Capacity of Two-Stage Robust Optimization: Variants of Robust Unit Commitment Model," *IEEE Transactions on Power Systems,* vol. 30, no. 1, pp. 109-122, 2015, doi: 10.1109/TPWRS.2014.2320880.

[58] B. Hu, L. Wu, and M. Marwali, "On the Robust Solution to SCUC With Load and Wind Uncertainty Correlations," *IEEE Transactions on Power Systems,* vol. 29, no. 6, pp. 2952-2964, 2014, doi: 10.1109/TPWRS.2014.2308637.

[59] B. Hu and L. Wu, "Robust SCUC With Multi-Band Nodal Load Uncertainty Set," *IEEE Transactions on Power Systems,* vol. PP, no. 99, pp. 1-1, 2015, doi: 10.1109/TPWRS.2015.2449764.

[60] C. Dai, L. Wu, and H. Wu, "A Multi-Band Uncertainty Set Based Robust SCUC With Spatial and Temporal Budget Constraints," *IEEE Transactions on Power Systems,* vol. 31, no. 6, pp. 4988-5000, 2016, doi: 10.1109/TPWRS.2016.2525009.

[61] P. Xiong and C. Singh, "Distributionally robust optimization for energy and reserve toward a low-carbon electricity market," *Electric Power Systems Research,* vol. 149, pp. 137-145, 2017.

[62] Z. Shi, H. Liang, S. Huang, and V. Dinavahi, "Distributionally Robust Chance-Constrained Energy Management for Islanded Microgrids," *IEEE Transactions on Smart Grid,* vol. 10, no. 2, pp. 2234-2244, 2019, doi: 10.1109/TSG.2018.2792322.

[63] W. Wei, F. Liu, and S. Mei, "Distributionally Robust Co-Optimization of Energy and Reserve Dispatch," *IEEE Transactions on Sustainable Energy,* vol. 7, no. 1, pp. 289-300, 2016, doi: 10.1109/TSTE.2015.2494010.

[64] Y. Chen, W. Wei, F. Liu, and S. Mei, "Distributionally robust hydro-thermal-wind economic dispatch," *Applied Energy,* vol. 173, pp. 511-519, 2016.

[65] Y. Yang and W. Wu, "A Distributionally Robust Optimization Model for Real-Time Power Dispatch in Distribution Networks," *IEEE Transactions on Smart Grid,* vol. 10, no. 4, pp. 3743-3752, 2019, doi: 10.1109/TSG.2018.2834564.

[66] B. Qiaoyan, X. Huanhai, W. Zhen, G. Deqiang, and W. Kit Po, "Distributionally Robust Solution to the Reserve Scheduling Problem With Partial Information of Wind Power," *Power Systems, IEEE Transactions on,* vol. 30, no. 5, pp. 2822-2823, 2015, doi: 10.1109/TPWRS.2014.2364534.

[67] Z. Wang, Q. Bian, H. Xin, and D. Gan, "A Distributionally Robust Co-Ordinated Reserve Scheduling Model Considering CVaR-Based Wind Power Reserve Requirements," *IEEE Transactions on Sustainable Energy,* vol. 7, no. 2, pp.

625-636, 2016, doi: 10.1109/TSTE.2015.2498202.

[68] Y. Zhang, S. Shen, and J. L. Mathieu, "Distributionally Robust Chance-Constrained Optimal Power Flow With Uncertain Renewables and Uncertain Reserves Provided by Loads," *IEEE Transactions on Power Systems,* vol. 32, no. 2, pp. 1378-1388, 2017, doi: 10.1109/TPWRS.2016.2572104.

[69] T. Summers, J. Warrington, M. Morari, and J. Lygeros, "Stochastic optimal power flow based on conditional value at risk and distributional robustness," *International Journal of Electrical Power & Energy Systems,* vol. 72, pp. 116-125, 2015.

[70] J. d. Hoog, T. Alpcan, M. Brazil, D. A. Thomas, and I. Mareels, "Optimal Charging of Electric Vehicles Taking Distribution Network Constraints Into Account," *IEEE Transactions on Power Systems,* vol. 30, no. 1, pp. 365-375, 2015, doi: 10.1109/TPWRS.2014.2318293.

[71] X. Luo and K. W. Chan, "Real-time scheduling of electric vehicles charging in low-voltage residential distribution systems to minimise power losses and improve voltage profile," *IET Generation, Transmission & Distribution,* vol. 8, no. 3, pp. 516-529, 2014, doi: 10.1049/iet-gtd.2013.0256.

[72] S. Xia, S. Q. Bu, X. Luo, K. W. Chan, and X. Lu, "An Autonomous Real-Time Charging Strategy for Plug-In Electric Vehicles to Regulate Frequency of Distribution System With Fluctuating Wind Generation," *IEEE Transactions on Sustainable Energy,* vol. 9, no. 2, pp. 511-524, 2018, doi: 10.1109/TSTE.2017.2746097.

[73] Q. Huang, Q. Jia, and X. Guan, "A Multi-Timescale and Bilevel Coordination Approach for Matching Uncertain Wind Supply With EV Charging Demand," *IEEE Transactions on Automation Science and Engineering,* vol. 14, no. 2, pp. 694-704, 2017, doi: 10.1109/TASE.2016.2585180.

[74] J. Zhao, J. Wang, Z. Xu, C. Wang, C. Wan, and C. Chen, "Distribution Network Electric Vehicle Hosting Capacity Maximization: A Chargeable Region Optimization Model," *IEEE Transactions on Power Systems,* vol. 32, no. 5, pp.

4119-4130, 2017, doi: 10.1109/TPWRS.2017.2652485.

[75] Y. Zheng, Z. Y. Dong, F. J. Luo, K. Meng, J. Qiu, and K. P. Wong, "Optimal Allocation of Energy Storage System for Risk Mitigation of DISCOs With High Renewable Penetrations," *IEEE Transactions on Power Systems,* vol. 29, no. 1, pp. 212-220, 2014, doi: 10.1109/TPWRS.2013.2278850.

[76] T. Soares, R. J. Bessa, P. Pinson, and H. Morais, "Active Distribution Grid Management Based on Robust AC Optimal Power Flow," *IEEE Transactions on Smart Grid,* vol. 9, no. 6, pp. 6229-6241, 2018, doi: 10.1109/TSG.2017.2707065.

[77] S. Xia, S. Bu, C. Wan, X. Lu, K. W. Chan, and B. Zhou, "A Fully Distributed Hierarchical Control Framework for Coordinated Operation of DERs in Active Distribution Power Networks," *IEEE Transactions on Power Systems,* vol. 34, no. 6, pp. 5184-5197, 2019, doi: 10.1109/TPWRS.2018.2870153.

[78] A. Saint-Pierre and P. Mancarella, "Active Distribution System Management: A Dual-Horizon Scheduling Framework for DSO/TSO Interface Under Uncertainty," *IEEE Transactions on Smart Grid,* vol. 8, no. 5, pp. 2186-2197, 2017, doi: 10.1109/TSG.2016.2518084.

[79] Y. K. Renani, M. Ehsan, and M. Shahidehpour, "Optimal Transactive Market Operations With Distribution System Operators," *IEEE Transactions on Smart Grid,* vol. 9, no. 6, pp. 6692-6701, 2018, doi: 10.1109/TSG.2017.2718546.

[80] C. Zhang, Y. Xu, Z. Y. Dong, and J. Ma, "Robust Operation of Microgrids via Two-Stage Coordinated Energy Storage and Direct Load Control," *IEEE Transactions on Power Systems,* vol. 32, no. 4, pp. 2858-2868, 2017, doi: 10.1109/TPWRS.2016.2627583.

[81] A. A. S. Algarni and K. Bhattacharya, "A Generic Operations Framework for Discos in Retail Electricity Markets," *IEEE Transactions on Power Systems,* vol. 24, no. 1, pp. 356-367, 2009, doi: 10.1109/TPWRS.2008.2007001.

[82] A. Safdarian, M. Fotuhi-Firuzabad, and M. Lehtonen, "A Stochastic Framework for Short-Term Operation of a Distribution Company," *IEEE Transactions on*

Power Systems, vol. 28, no. 4, pp. 4712-4721, 2013, doi: 10.1109/TPWRS.2013.2278076.

[83] R. Palma-Behnke, A. J. L. C, L. S. Vargas, and A. Jofre, "A distribution company energy acquisition market model with integration of distributed generation and load curtailment options," *IEEE Transactions on Power Systems,* vol. 20, no. 4, pp. 1718-1727, 2005, doi: 10.1109/TPWRS.2005.857284.

[84] Y. Guo, K. Baker, E. Dall'Anese, Z. Hu, and T. H. Summers, "Data-Based Distributionally Robust Stochastic Optimal Power Flow—Part I: Methodologies," *IEEE Transactions on Power Systems,* vol. 34, no. 2, pp. 1483-1492, 2019, doi: 10.1109/TPWRS.2018.2878385.

[85] C. Duan, W. Fang, L. Jiang, L. Yao, and J. Liu, "Distributionally Robust Chance-Constrained Approximate AC-OPF With Wasserstein Metric," *IEEE Transactions on Power Systems,* vol. 33, no. 5, pp. 4924-4936, 2018, doi: 10.1109/TPWRS.2018.2807623.

[86] C. Wang, R. Gao, W. Wei, M. Shafie-khah, T. Bi, and J. P. S. Catalão, "Risk-Based Distributionally Robust Optimal Gas-Power Flow With Wasserstein Distance," *IEEE Transactions on Power Systems,* vol. 34, no. 3, pp. 2190-2204, 2019, doi: 10.1109/TPWRS.2018.2889942.

[87] Y. Cao, W. Wei, J. Wang, S. Mei, M. Shafie-khah, and J. P. S. Catalao, "Capacity Planning of Energy Hub in Multi-carrier Energy Networks: A Data-driven Robust Stochastic Programming Approach," *IEEE Transactions on Sustainable Energy,* pp. 1-1, 2018, doi: 10.1109/TSTE.2018.2878230.

[88] R. Xie, W. Wei, M. E. Khodayar, J. Wang, and S. Mei, "Planning Fully Renewable Powered Charging Stations on Highways: A Data-Driven Robust Optimization Approach," *IEEE Transactions on Transportation Electrification,* vol. 4, no. 3, pp. 817-830, 2018, doi: 10.1109/TTE.2018.2849222.

[89] Y. Chen, Q. Guo, H. Sun, Z. Li, W. Wu, and Z. Li, "A Distributionally Robust Optimization Model for Unit Commitment Based on Kullback–Leibler Divergence," *IEEE Transactions on Power Systems,* vol. 33, no. 5, pp. 5147-

5160, 2018, doi: 10.1109/TPWRS.2018.2797069.

[90] S. Boyd and L. Vandenberghe, *Convex optimization*. Cambridge university press, 2004.

[91] D. Bertsimas, X. V. Doan, K. Natarajan, and C.-P. Teo, "Models for minimax stochastic linear optimization problems with risk aversion," *Mathematics of Operations Research,* vol. 35, no. 3, pp. 580-602, 2010.

[92] A. Shapiro, "On duality theory of conic linear problems, Miguel A. Goberna and Marco A. Lopez, Eds., Semi-Infinite Programming: Recent Advances," ed: Kluwer Academic Publishers, 2001.

[93] K. Isii, "On sharpness of Tchebycheff-type inequalities," *Annals of the Institute of Statistical Mathematics,* vol. 14, no. 1, pp. 185-197, 1962.

[94] X. Xia and A. Elaiw, "Optimal dynamic economic dispatch of generation: a review," *Electric Power Systems Research,* vol. 80, no. 8, pp. 975-986, 2010.

[95] A. Lorca, X. A. Sun, E. Litvinov, and T. Zheng, "Multistage adaptive robust optimization for the unit commitment problem," *Operations Research,* vol. 64, no. 1, pp. 32-51, 2016.

[96] A. Lorca and X. A. Sun, "Multistage robust unit commitment with dynamic uncertainty sets and energy storage," *IEEE Transactions on Power Systems,* vol. 32, no. 3, pp. 1678-1688, 2017.

[97] J. Warrington, P. Goulart, S. Mariéthoz, and M. Morari, "Policy-based reserves for power systems," *IEEE Transactions on Power Systems,* vol. 28, no. 4, pp. 4427-4437, 2013.

[98] R. A. Jabr, "Adjustable robust OPF with renewable energy sources," *IEEE Transactions on Power Systems,* vol. 28, no. 4, pp. 4742-4751, 2013.

[99] J. Goh and M. Sim, "Distributionally robust optimization and its tractable approximations," *Operations research,* vol. 58, no. 4-part-1, pp. 902-917, 2010.

[100] X. Chen, M. Sim, P. Sun, and J. Zhang, "A linear decision-based approximation approach to stochastic programming," *Operations Research,* vol. 56, no. 2, pp. 344-357, 2008.

[101] D. Bertsimas, E. Litvinov, X. A. Sun, J. Zhao, and T. Zheng, "Adaptive Robust Optimization for the Security Constrained Unit Commitment Problem," *IEEE Transactions on Power Systems,* vol. 28, no. 1, pp. 52-63, 2013, doi: 10.1109/TPWRS.2012.2205021.

[102] M. Shahidehpour and Y. Fu, "Benders decomposition in restructured power systems," *IEEE Techtorial,* 2005.

[103] J. Murphy, "Benders, nested benders and stochastic programming: An intuitive introduction," *arXiv preprint arXiv:1312.3158,* 2013.

[104] J. Gorski, F. Pfeuffer, and K. Klamroth, "Biconvex sets and optimization with biconvex functions: a survey and extensions," *Mathematical Methods of Operations Research,* vol. 66, no. 3, pp. 373-407, 2007.

[105] R. Jiang, J. Wang, and Y. Guan, "Robust Unit Commitment With Wind Power and Pumped Storage Hydro," *IEEE Transactions on Power Systems,* vol. 27, no. 2, pp. 800-810, 2012, doi: 10.1109/TPWRS.2011.2169817.

[106] M. Zugno and A. J. Conejo, "A robust optimization approach to energy and reserve dispatch in electricity markets," *European Journal of Operational Research,* vol. 247, no. 2, pp. 659-671, 2015.

[107] S. I. Vagropoulos, D. K. Kyriazidis, and A. G. Bakirtzis, "Real-Time Charging Management Framework for Electric Vehicle Aggregators in a Market Environment," *IEEE Transactions on Smart Grid,* vol. 7, no. 2, pp. 948-957, 2016, doi: 10.1109/TSG.2015.2421299.

[108] S. Li, M. Brocanelli, W. Zhang, and X. Wang, "Integrated Power Management of Data Centers and Electric Vehicles for Energy and Regulation Market Participation," *IEEE Transactions on Smart Grid,* vol. 5, no. 5, pp. 2283-2294, 2014, doi: 10.1109/TSG.2014.2321519.

[109] N. Holjevac, T. Capuder, N. Zhang, I. Kuzle, and C. Kang, "Corrective receding horizon scheduling of flexible distributed multi-energy microgrids," *Applied Energy,* vol. 207, pp. 176-194, 2017.

[110] W. Yao, J. Zhao, F. Wen, Y. Xue, and G. Ledwich, "A Hierarchical

Decomposition Approach for Coordinated Dispatch of Plug-in Electric Vehicles," *IEEE Transactions on Power Systems,* vol. 28, no. 3, pp. 2768-2778, 2013, doi: 10.1109/TPWRS.2013.2256937.

[111] Z. Xu, W. Su, Z. Hu, Y. Song, and H. Zhang, "A Hierarchical Framework for Coordinated Charging of Plug-In Electric Vehicles in China," *IEEE Transactions on Smart Grid,* vol. 7, no. 1, pp. 428-438, 2016, doi: 10.1109/TSG.2014.2387436.

[112] D. Tang and P. Wang, "Probabilistic Modeling of Nodal Charging Demand Based on Spatial-Temporal Dynamics of Moving Electric Vehicles," *IEEE Transactions on Smart Grid,* vol. 7, no. 2, pp. 627-636, 2016, doi: 10.1109/TSG.2015.2437415.

[113] D. T. Nguyen and L. B. Le, "Optimal Bidding Strategy for Microgrids Considering Renewable Energy and Building Thermal Dynamics," *IEEE Transactions on Smart Grid,* vol. 5, no. 4, pp. 1608-1620, 2014, doi: 10.1109/TSG.2014.2313612.

[114] J. Li, Z. Xu, J. Zhao, and C. Wan, "A Coordinated Dispatch Model for Distribution Network Considering PV Ramp," *IEEE Transactions on Power Systems,* vol. 33, no. 1, pp. 1107-1109, 2018, doi: 10.1109/TPWRS.2017.2735901.

[115] K. Natarajan, M. Sim, and J. Uichanco, "Tractable robust expected utility and risk models for portfolio optimization," *Mathematical Finance,* vol. 20, no. 4, pp. 695-731, 2010.

[116] C. Wang, R. Gao, F. Qiu, J. Wang, and L. Xin, "Risk-Based Distributionally Robust Optimal Power Flow With Dynamic Line Rating," *IEEE Transactions on Power Systems,* vol. 33, no. 6, pp. 6074-6086, 2018, doi: 10.1109/TPWRS.2018.2844356.

[117] Metropolitan Travel Survey Archive [Online] Available: http://www.surveyarchive.org/

[118] B. Venkatesh, R. Ranjan, and H. B. Gooi, "Optimal reconfiguration of radial

distribution systems to maximize loadability," *IEEE Transactions on Power Systems,* vol. 19, no. 1, pp. 260-266, 2004, doi: 10.1109/TPWRS.2003.818739.

[119] I. Pólik and T. Terlaky, "A survey of the S-lemma," *SIAM review,* vol. 49, no. 3, pp. 371-418, 2007.

Appendix

A. Farkas' Lemma [90]

Assume that $\mathbf{A}$ and $\mathbf{b}$ are known. Then, exactly one of $(\mathrm{A}.1)$ and $(\mathrm{A}.2)$ has solutions.

$$\mathbf{A}\boldsymbol{x} = \mathbf{b}, \boldsymbol{x} \geq \mathbf{0} \tag{A.1}$$

$$\mathbf{A}'\boldsymbol{y} \leq \mathbf{0}, \mathbf{b}'\boldsymbol{y} > 0 \tag{A.2}$$

B. S-lemma [119]

Assume that there is a $\boldsymbol{x}$ that satisfies $\boldsymbol{x}'\boldsymbol{Q}_1\boldsymbol{x} + (\boldsymbol{p}_1)'\boldsymbol{x} + r_1 > 0$. Then, if for all $\boldsymbol{x}$, $\boldsymbol{x}'\boldsymbol{Q}_2\boldsymbol{x} + (\boldsymbol{p}_2)'\boldsymbol{x} + r_2 \geq 0$ holds given $\boldsymbol{x}'\boldsymbol{Q}_1\boldsymbol{x} + (\boldsymbol{p}_1)'\boldsymbol{x} + r_1 \geq 0$, there will be a non-negative τ that satisfies $\boldsymbol{x}'\boldsymbol{Q}_2\boldsymbol{x} + (\boldsymbol{p}_2)'\boldsymbol{x} + r_2 \geq \tau(\boldsymbol{x}'\boldsymbol{Q}_1\boldsymbol{x} + (\boldsymbol{p}_1)'\boldsymbol{x} + r_1), \forall \boldsymbol{x}$.

C. Transformation from (3.64) to (3.66)-(3.67)

The ellipsoidal support S_0 given in (3.65) can be rewritten as (C.1) because $\mathbf{M}$ is symmetric. Obviously, for any proper S_0, there will be a $\boldsymbol{\xi}^1$ that satisfies (C.2) or equivalently (C.3). Then, by using S-lemma, (3.64) can be replaced by (C.4)-(C.5). According to the definition of positive semidefinite matrices, (C.4) is equivalent to (3.66). (C.5) is just (3.67).

$$\begin{aligned}
\mathrm{S}_0 &= \{\boldsymbol{\xi}^1 | (\boldsymbol{\xi}^1 - \boldsymbol{\mu}_0)' \cdot \mathbf{M} \cdot (\boldsymbol{\xi}^1 - \boldsymbol{\mu}_0) \leq 1\} \\
&= \{\boldsymbol{\xi}^1 | (\boldsymbol{\xi}^1)' (-\mathbf{M}) \boldsymbol{\xi}^1 + (\boldsymbol{\mu}_0)' \mathbf{M} \boldsymbol{\xi}^1 + (\boldsymbol{\xi}^1)' \mathbf{M} \boldsymbol{\mu}_0 - (\boldsymbol{\mu}_0)' \mathbf{M} \boldsymbol{\mu}_0 + 1 \geq 0\} \\
&= \left\{ \boldsymbol{\xi}^1 \middle| [(\boldsymbol{\xi}^1)' \quad 1] \begin{bmatrix} -\mathbf{M} & \mathbf{M} \cdot \boldsymbol{\mu}_0 \\ (\mathbf{M} \cdot \boldsymbol{\mu}_0)' & -(\boldsymbol{\mu}_0)' \mathbf{M} \boldsymbol{\mu}_0 + 1 \end{bmatrix} \begin{bmatrix} \boldsymbol{\xi}^1 \\ 1 \end{bmatrix} \geq 0 \right\}
\end{aligned} \tag{C.1}$$

$$(\boldsymbol{\xi}^1 - \boldsymbol{\mu}_0)' \cdot \mathbf{M} \cdot (\boldsymbol{\xi}^1 - \boldsymbol{\mu}_0) < 1 \tag{C.2}$$

$$[(\boldsymbol{\xi}^1)' \quad 1] \begin{bmatrix} -\mathbf{M} & \mathbf{M} \cdot \boldsymbol{\mu}_0 \\ (\mathbf{M} \cdot \boldsymbol{\mu}_0)' & -(\boldsymbol{\mu}_0)' \mathbf{M} \boldsymbol{\mu}_0 + 1 \end{bmatrix} \begin{bmatrix} \boldsymbol{\xi}^1 \\ 1 \end{bmatrix} > 0 \tag{C.3}$$

$$[\boldsymbol{\xi}^1 \quad 1]\begin{bmatrix} \boldsymbol{Q}^{\mathrm{d}} & -\boldsymbol{p}^{\mathrm{d}} - \boldsymbol{Q}^{\mathrm{d}}\boldsymbol{\mu}_0 + (\mathbf{F}^1)'\boldsymbol{u}_e/2 \\ \left(-\boldsymbol{p}^{\mathrm{d}} - \boldsymbol{Q}^{\mathrm{d}}\boldsymbol{\mu}_0 + (\mathbf{F}^1)'\boldsymbol{u}_e/2\right)' & r^{\mathrm{d}} + (\mathbf{E}^1 \cdot \boldsymbol{x}^1 - \mathbf{g}^1)'\boldsymbol{u}_e \end{bmatrix}\begin{bmatrix} \boldsymbol{\xi}^1 \\ 1 \end{bmatrix}$$

$$\geq \tau_e \cdot [(\boldsymbol{\xi}^1)' \quad 1]\begin{bmatrix} -\mathbf{M} & \mathbf{M} \cdot \boldsymbol{\mu}_0 \\ (\mathbf{M} \cdot \boldsymbol{\mu}_0)' & -(\boldsymbol{\mu}_0)'\mathbf{M}\boldsymbol{\mu}_0 + 1 \end{bmatrix}\begin{bmatrix} \boldsymbol{\xi}^1 \\ 1 \end{bmatrix}, \forall e \quad \text{(C. 4)}$$

$$\tau_e \geq 0, \forall e \quad \text{(C. 5)}$$